İSTANBUL TECHNICAL UNIVERSITY ★ INSTITUTE OF SCIENCE AND TECHNOLOGY

A DYNAMIC NODE MODEL FOR HIGHWAY NETWORKS

Ph.D. Thesis by

Hilmi Berk ÇELİKOĞLU, M.Sc.

(501022201)

Date of submission : 19 September 2006

Date of defence examination: 14 December 2006

Supervisor (Chairman): Prof. Dr. Ergun GEDİZLİOĞLU

Members of the Examining Committee Prof. Dr. Haluk GERÇEK (İTÜ)

Prof. Dr. Füsun ÜLENGİN (Doğuş Ü.)

Prof. Dr. Nadir YAYLA (İTÜ)

Prof. Dr. Mauro DELL'ORCO (TU Bari)

DECEMBER 2006

İSTANBUL TEKNİK ÜNİVERSİTESİ ★ FEN BİLİMLERİ ENSTİTÜSÜ

KARAYOLU AĞLARI İÇİN DİNAMİK BİR DÜĞÜM NOKTASI MODELİ

DOKTORA TEZİ

Y. Müh. Hilmi Berk ÇELİKOĞLU

(501022201)

Tezin Enstitüye Verildiği Tarih : 19 Eylül 2006

Tezin Savunulduğu Tarih : 14 Aralık 2006

Tez Danışmanı : Prof. Dr. Ergun GEDİZLİOĞLU

Diğer Jüri Üyeleri Prof. Dr. Haluk GERÇEK (İTÜ)

Prof. Dr. Füsun ÜLENGİN (Doğuş Ü.)

Prof. Dr. Nadir YAYLA (İTÜ)

Prof. Dr. Mauro DELL'ORCO (TU Bari)

ARALIK 2006

PREFACE

Prof. Dr. Ergun GEDİZLİOĞLU is gratefully acknowledged for his supervision during my Ph. D study process. I would like to express my solemn thanks for his support, patience, his comments and recommendations during each phase of my personal and academical life within the last four years.

I would like to extend my sincere gratitude to Prof. Dr. Mauro DELL'ORCO for his support and understanding, his outstanding ideas that guided me through the thesis, and his supervision during my study in Technical University of Bari.

Technical University of İstanbul (İTÜ) and the Scientific and Technological Research Council of Turkey (TÜBİTAK) are acknowledged for their financial and constitutional support for the research activities conducted through this study.

I would also like to thank to my colleagues and friends at İTÜ for their help and concern. My special thanks are due to Prof. Dr. Emine AĞAR, for her support and help, Dr. Adem Faik İYİNAM and Ass. Prof. Dr. Şükrüye İYİNAM, for their concern, and Dr. Tanju AKAR and Said Gökhan KARAMAN for their friendship.

The thesis examining committee members, Prof. Dr. Nadir YAYLA, Prof. Dr. Haluk GERÇEK, and Prof. Dr. Füsun ÜLENGİN, are acknowledged for their valuable comments and sharing their precious times.

I am profoundly indebted to my family for always being on my side and supporting me, whole my life. I would like to dedicate this work to my dear father Dr. Haluk ÇELİKOĞLU and my dear mother Gülseren ÇELİKOĞLU, both of whom have always been a great support with their wisdom. My sincere thanks are attributed to my sister Başak ÇELİKOĞLU, for her understanding and continuous assistance. I would like to announce the existence of my inexpressible feelings for my girlfriend Özge MERZALİ, whom made me investigate and believe the infiniteness of love, with her kindest manner and extraordinary personality.

December 2006 Hilmi Berk ÇELİKOĞLU

CONTENTS

ABBREVIATIONS

ATIS	: Advanced Traveller Information Systems
ATMS	: Advanced Traffic Management Systems
CPU	: Central Processing Unit
CTM	: Cell Transmission Model
DL	: Diverging Link
DNM	: Dynamic Node Model
DNL	: Dynamic Network Loading
DTA	: Dynamic Traffic Assignment
DUO	: Dynamic User Optimal
FIFO	: First In First Out
FPP	: Fixed Point Problem
ITS	: Intelligent Transportation Systems
LWR	: Lighthill Whitham Richards
ML	: Merging Link
MP	: Mathematical Programming
NCP	: Non-linear Complementarity Problem
OD	: Origin Destination
PQ	: Point Queue
VIP	: Variational Inequality Problem

LIST OF TABLES

LIST OF FIGURES

LIST OF FREQUENTLY USED SYMBOLS

a : congestion effect parameter;

B(·) : link performance function;

BW : set of merging links;

C : capacity;

d : link length;

D : time-varying demand flow rate;

f(·) : demand flow rate function;

FW : set of diverging links;

G(·) : delay function;

i : index for merging links;

j : index for diverging links;

k : index for nodes;

n : number of vehicles;

N : total number of vehicles that exits from a link;

p : index for paths;

P : set of existing paths;

PQ : point queue;

q : traffic flow;

r : index for diverging links;

s : spacing;

t : index for continuous time;

T : O-D traffic demand horizon;

u : time-varying inflow;

U : cumulative time-varying inflow;

V : speed;

VF : free-flow speed;

y : index for discrete time interval;

w : time-varying outflow;

W : cumulative time-varying outflow;

α : free-flow travel time;

β : parameter of the variable of linear travel time function;

γ : parameter of selected exit link function;

δ : time-varying demand;

Δ : discretisation time interval length;

$\eta(\cdot)$: congestion function;

λ : flow splitting rate;

ρ : minimum over all links of free-flow link travel time;

σ : supply;

τ : link travel time;

ω : instant of time $\leq$ t;

ξ : dummy variable of path-link incidence matrix.

A DYNAMIC NODE MODEL FOR HIGHWAY NETWORKS

SUMMARY

Traffic engineers have been studying the modelling on behaviour of many of the components of a transportation system for years. The research efforts in traffic modelling and traffic assignment have been focused on the modelling of the traffic behaviour in a whole network system. The development of static network models, algorithms and their application in the practice of transportation planning, has achieved remarkable results ‘till eighties. However, even complex and refined static models are not able to capture the time-varying (dynamic) characteristics of traffic, which lead to the development of dynamic models. A large number of dynamic models and solution procedures have been proposed that are usually referred as (within-day) dynamic traffic assignment models in the literature. In order to perform dynamic traffic assignment, it is necessary to solve the dynamic network loading problem that has been indicated as the reproduction of variable link performances given a corresponding origin-destination demand and users' choice model.

So far, the dynamic network loading problem has been studied within a great number of varying models. The variation of model structure is heavily dependant on the assumptions made to obtain a solution for the problem. The main assumption that is made during modelling a dynamic network loading process is on queuing and can be divided into two, which are point-queuing and physical-queuing. Considering the queuing assumption, the models of dynamic network loading can further be classified as link-based and node-based. Despite the existence of an enormous number of link-based models, node-based dynamic network models have been encountered very seldom, which are all set out by physical-queuing assumption.

In this study, an analytical dynamic node model is formulated both to represent flow propagation on highway traffic networks and to be utilized as an integral part of a dynamic network loading process. The proposed node model has an integrate base structured with a mesoscopic link model, set out with an exit link function formulation, and an algorithm written with a set of nodal rules considering the constraints of conservation, capacity, flow splitting and non-negativity. The proposed new dynamic node model in this study is unique in that it encapsulates a mesoscopic approach in node modelling. The uniqueness of the proposed model is also valid for the node modelling with point-queuing assumption.

The proposed mesoscopic link model component is developed by considering the over-saturation phenomenon. This model is set out with link exit function formulation, discretisation on time dimension, defining capacity constraint rules for

over-saturated states and uniformly accelerated speed assumption, which allows a realistic representation of outflow dynamics. The validity of the link model component is sought by running the model using theoretical input data to simulate over-saturation condition on a single link. Following, the configuration for multiple links structure is coded to be integrated to node modelling. The time-varying inflows that enter to multiple merging links simultaneously are input to the mesoscopic link model. The outflows that exit from these merging links are computed regarding the link and flow characteristics. Then outflows of the merging links are input to a node as inflows. These conflicting flows are processed within the node component with predefined splitting rates and characteristics of the diverging links, and then the nodal exiting flows are computed. The node model problem is formulated as to maximize the total flow passing through the node subject to the constraints of conservation, capacity, flow splitting and non-negativity. The optimization problem is solved by simulation within the modelling horizon. Simulation process of the proposed model lasted as the inflows to merging links are wholly discharged from the entire node structure.

The main difference of the proposed dynamic node model in comparison to other models of different approaches is that it satisfies capacity constraints regarding to splitting rules and consequently holds first-in-first-out rule.

The integrated model structure provided more realistic results in representing outflow dynamics. It is seen that the outflows of the link model component existed respecting to capacity constraints and the diagrams of these outflows seemed alike the sinusoidal inflow curves under the set node configuration. Despite the flows requiring to enter the diverging links are above over-saturation rates, the capacity restraint is respected. The results show that the model appears realistic in the representation of point-queuing process and diverging link flow dynamics, and is quite easy to calculate.

KARAYOLU AĞLARI İÇİN DİNAMİK BİR DÜĞÜM NOKTASI MODELİ

ÖZET

Trafik mühendisleri, ulaştırma sisteminin pek çok bileşeninin davranışını yıllardır modellemeye çalışmaktadır. Trafik modellemesi ve trafik atamasında araştırmalar, tüm bir ağ sisteminin davranışını modelleme üzerinde yoğunlaşmıştır. Statik ağ modelleri ile algoritmaları ve bunların ulaştırma planlamasına uygulama çalışmaları ile 80'li yıllara kadar önemli sonuçlar elde edilmiştir. Fakat, en gelişmiş statik modellerle bile trafiğin zamana-bağımlı (dinamik) özellikleri ifade edilememiştir. Bu eksiklik, dinamik modellerin geliştirilmesine neden olmuştur. Dolayısıyla, genellikle (gün-içi) dinamik trafik ataması modelleri denilen çok sayıda dinamik model ve çözüm yöntemi önerilmiştir. Bir dinamik trafik ataması yapabilmek için öncelikle, verilen talep ve kullanıcı özellikleri ile değişken bağ başarımının ifade edildiği dinamik ağ yükleme probleminin çözülmesi gerekir.

Günümüzde dinamik ağ yükleme problemi üzerinde çok sayıda farklı modeller kullanılmaktadır. Model yapısındaki farklılaşma, ağırlıklı olarak, çözüm elde etmek için yapılan varsayımlara bağlıdır. Bir dinamik ağ yükleme sürecini modellemede yapılan en temel varsayım kuyruklanma varsayımıdır. Kuyruklanma; fiziksel kuyruklanma ve nokta kuyruklanma olarak ikiye ayrılır. Kuyruklanma varsayımı da dikkate alınarak, modeller ayrıca bağ temelli ve düğüm noktası temelli olarak gruplandırılır. Geçmişte çalışılan çok fazla sayıda bağ temelli model olmasına karşın, tümü fiziksel kuyruklanma varsayımı ile oluşturulmuş çok az sayıda düğüm noktası temelli modelin var olduğu söylenebilir.

Bu çalışmada; karayolu trafik ağlarında akım yayılımı modellemesi yapan ve dinamik ağ yüklemesi sürecine tümleştirilebilen çözümlemeli bir düğüm noktası modeli önerilmiştir. Önerilen tümleşik modelin; bağ çıkış fonksiyonu ile oluşturulmuş karma-boyut bağ modeli ve korunum, kapasite, akım dağılımı ve negatif olmama kısıtları ile yazılan düğüm noktası kurallarıyla tümleşik bir yapısı vardır. Bu çalışma kapsamında önerilen yeni dinamik düğüm noktası modeli, karma-boyut yaklaşımı temel alınarak oluşturulan tek düğüm noktası modelidir. Ayrıca model, nokta kuyruk varsayımıyla oluşturulan bir düğüm noktası modeli olması açısından da tektir.

Önerilen karma-boyut (mesoscopic) bağ modeli, aşırı-doygun akım durumu irdelenerek geliştirilmiştir. Bu model; başarım fonksiyonu olarak bağ çıkış fonksiyonu kullanan, çözüm için zaman boyutunda ayrıklaştırma gerektiren, aşırı-doygun durumlar için kapasite kısıtı içeren ve taşıt hareketini düzgün ivmelendirerek gerçekçi akım dinamikleri temsiline olanak sağlayan bir benzetim modelidir. Bağ

modeli bileşeninin geçerlilik sınaması öncelikle aşırı-doygun kuramsal verinin tek bir bağ üzerinde denenmesi ile yapılmıştır. Daha sonra, düğüm noktası yapısında tümleşik olarak kullanılması için çoklu bağ varlığında çalışacak kod yazılmıştır. Katılan bağlara giren dinamik akım hacmi, karma-boyut bağ modeline girdi oluşturmuştur. Katılan bağlardan çıkan akım hacmi, bağ ve akım özelliklerine göre hesaplanmıştır. Daha sonra, katılan bağların çıktı akım hacimleri, düğüm noktasına giren hacim olarak atanmıştır. Çatışan bu akımlar; önceden belirlenmiş dağılım oranları ve ayrılan bağ özellikleri varlığında düğüm noktası bileşeninde işlenerek ayrılan bağlara giren akım hacimleri belirlenmiştir. Düğüm noktası problemi; korunum, kapasite, akım dağılımı ve negatif olmama kısıtlarına göre düğüm noktasını geçen akım hacmini enbüyükleyecek şekilde yazılmıştır. Eniyileme problemi, modelleme süreci içerisinde benzetim yolu ile çözülmüştür. Önerilen modelin benzetimi, katılan tüm bağlardaki akım temizlenene dek sürmüştür.

Önerilen dinamik düğüm noktası modelinin, farklı yaklaşımlara göre oluşturulan diğer modellere göre en temel farklılığı, dağılım kuralları ile kapasite kısıtını sağlaması ve dolayısıyla ilk-giren-ilk-çıkar düzenine uymasıdır.

Tümleşik model yapısı, akım dinamiklerini gerçekçi biçimde temsil etmiştir. Bağ modeli bileşeni ile hesaplanan çıktı akımlarının kapasite kısıtına ve kuramsal eğrilere uyduğu görülmüştür. Düğüm noktasında ayrılan bağlara var olan talep aşırı-doygun olmasına karşın kapasite kısıtına uyulduğu görülmüştür. Sonuçlar, modelin nokta kuyruk sürecini ve ayrılan bağ akım dinamiklerini gerçekçi biçimde benzettiğini ve hesap yönteminin kolay olduğunu göstermektedir.

1. INTRODUCTION

Traffic engineers have been studying the modelling on behaviour of many of the components of a transportation system for years. The research efforts in traffic modelling and traffic assignment have been focused on the modelling of the traffic behaviour in a whole network system. Since the seminal contribution of Wardrop [1], the development of static network models, algorithms and their application in the practice of transportation planning, has achieved remarkable results. However, even complex and refined static models are not able to capture the time-varying characteristics of traffic, which lead to the development of dynamic models. A large number of dynamic models and solution procedures have been proposed that are usually referred as (within-day) dynamic traffic assignment models in the literature. These models can be used both to evaluate traffic flows and to simulate the effects of regulation strategies on users' behaviour. In order to perform dynamic traffic assignment, it is necessary to solve the dynamic network loading problem that has been indicated as the reproduction of variable link performances given a corresponding origin-destination demand and users' choice model.

So far, the dynamic network loading problem has been studied within a great number of varying models. The variation of model structure is heavily dependant on the assumptions made to obtain a solution for the problem and can be classified as link-based and node-based. Despite the existence of an enormous number of link-based models, node-based dynamic network models have been encountered very seldom.

In this study, an analytical dynamic node model is formulated both to represent flow propagation on highway traffic networks and to be utilized as an integral part of a dynamic network loading process. The proposed node model also has an integrate base structured with a mesoscopic link model and node flow rules. The solution to the proposed model is obtained by simulation.

The following section gives a brief description on the dynamic traffic assignment. The third section explains the dynamic network loading concept with a general

problem formulation and dynamic network loading models by classification. The fourth section traces the link-based and the node-based modelling approaches. The formulation and the solution of the proposed dynamic node model are explained in details with numerical examples in the fifth section. The utilization of the proposed dynamic node model in a dynamic network loading process is handled in the sixth section with a numerical application. The last section concludes the study with findings, discussion and the possible future extensions.

2. DYNAMIC TRAFFIC ASSIGNMENT

Dynamic traffic assignment (DTA) is to determine the network traffic pattern in time-varying environment as a result of dynamic demand and supply interaction. DTA has significant differences than static assignment. The inclusion of the temporal dimension in DTA can represent real traffic much better in terms of capturing route and departure time choices, hence, traffic dynamics representation is carried out in more details.

DTA models have a wide range of applicability in both real-time traffic control and management and off-line network planning and policy evaluations. These models are in fact the fundamental components in developing intelligent transportation systems (ITS) technologies such as advanced traveller information systems (ATIS) and advanced traffic management systems (ATMS). DTA models can be utilized for predicting the flow patterns to optimize signals at junctions, to yield the shoulder to emergency vehicles, and impose time-varying tolls for congestion management in ATMS. Moreover, DTA models can be used to determine the optimal route and departure time to provide within ATIS anticipatory traffic information for travellers, based on predicted traffic flow patterns. For traffic planning purpose, DTA models can be used instead of static models to evaluate more accurately infrastructure improvements, congestion management, environmental pollution and so on.

Since the proposed model throughout this thesis is a flow propagation model and deals with flows at node level, the explanations given in the following sections are independent of DTA scheme.

2.1. Components of Dynamic Traffic Assignment

DTA consists of two components, which are a travel choice principle and a traffic flow modelling component as shown in Figure 2.1.

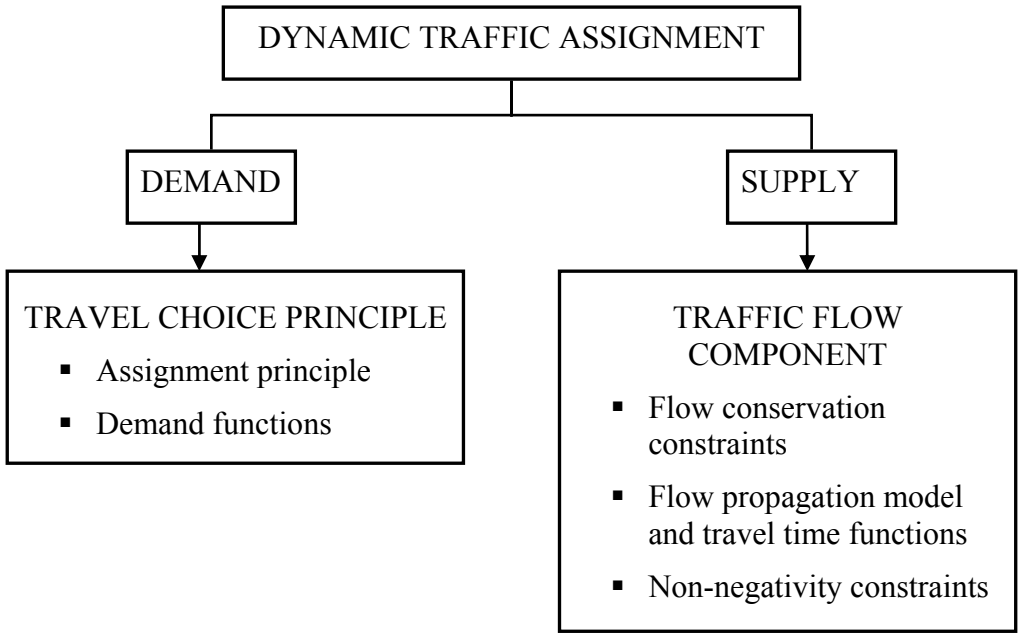

Figure 2.1: Components of Dynamic Traffic Assignment

The decision of travellers on whether travelling or not, and if so, how to select routes, departure times, modes and destinations are modelled by the travel choice principle in presence of an assignment principle and a demand function. The traffic flow modelling component models the flow propagation throughout a network and hence regulates the network performance in terms of travel time with respect to flow conservation constraints, flow propagation model, travel cost functions, and non-negativity constraints.

2.1.1. Travel Choice Principle

The most commonly used assignment principles in DTA are generally:

1- Minimising disutility or user cost or travel;

2- Minimising perceived disutility; and,

3- Minimising average user cost.

The most commonly adopted travel choice principle in DTA studies is a dynamic extension of Wardrop's first principle [1], called the dynamic user optimal (DUO) principle [2]. This principle assumes that travellers make their route and departure time choices to minimise their travelling costs, such as travel time. Most of the existing networks planning procedures are developed under this assumption. The

travel choice principle can mathematically be formulated as: the nonlinear complemantarity problem (NCP), the variational inequality problem (VIP), and fixed-point problem (FPP), by assuming that route travel time is a function of route flows or implicitly defined in the solution set of these problems. The existence and uniqueness of solutions to these problems are strictly defined in the literature [3-5].

Relationship between travel cost and demand can be determined by demand functions. The demand is elastic if it is a function of travel cost, and fixed otherwise.

2.1.2. Traffic Flow Modelling Component

The traffic-flow component can be modelled as a set of side constraints on the solution set or as a unique mapping of route flows. Representing traffic dynamics as side constraints explicitly is cumbersome and makes the solution difficult to be obtained efficiently [6]. Proposing traffic flow modelling component as a unique mapping of route flows, opens up a new way to analyze DTA problems. The outputs of this mapping are route travel times, which can be computed as a function of route flows.

DTA has the flow conservation constraints to ensure that the demand does not disappear or the total demand is smaller than the total route flows. Non-negativity is a typical constraint in traffic assignment to restrict flows. Unlike static assignment models, DTA contains a flow propagation or a dynamic network loading model integrated to a travel cost function to propagate flows on a network. The travel cost function represents the relationship between travel time and generalized cost.

The current trend on traffic flow propagation modelling, including the proposed new flow propagation model throughout this thesis, has been capturing the actual traffic dynamics such as First-in-first-out (FIFO) requirement, causality, and queue spillback. FIFO at link level means that users entering the link earlier will leave prior to others and has been studied in many works [7-10]. Causality is that the speed and the travel time of a vehicle on a link is affected by the speed of vehicles ahead but not by the vehicles behind [7, 10, 11]. Queue spillback is the spilling of the end of queue backwards in the network and has been modelled in many studies [12-17]. These models can generate unrealistic traffic propagation, such as instantaneous flow propagation, which means that traffic propagation speed is faster than the free-flow speed. Other traffic models avoid this drawback.

The above mentioned traffic models develop the properties of DTA problems, and the resultant route choice decisions, which in turn affect the algorithmic development, the network design and the predictions of network performances.

A detailed explanation on dynamic network loading models is given in section 3.2.

2.2. Dynamic Traffic Assignment Problem

In terms of the dynamic problem structure, compared with static traffic assignment, DTA contains one more component, the dynamic network loading (DNL) model. The inclusion of this component makes the resultant formulation more complex and the solutions more difficult.

The mathematical formulations of DTA problems, based on the dynamic extensions of Wardrop's principles [1], can be studied by having a classification according to the following criteria:

1- Whether travellers have only route choices or have both route and departure time choices;

2- Whether demands are fixed or elastic;

3- Whether travellers have complete information about the network (whether the assignment is deterministic or stochastic) or not; and,

4- Whether the problem considers multiple traveller classes or not.

In this study, a dynamic node model is proposed by derivation from a DNL model that can be utilized in DTA, assuming a single class user formulation and varying demand existence. The adopted DNL problem formulation is explained in sections 3.2.1 and 3.2.2. Since DTA is a more general frame and is upstream DNL, the problem formulation of DTA is skipped here. Only the approaches to DTA are summarized in the following.

2.3. General Frameworks for Dynamic Traffic Assignment Problem

An analytical formulation of a DTA model is generally obtained with the following approaches:

1- Mathematical programming (MP) [18-23],

2- Optimal control theory [24-28],

3- Variational inequality problem (VIP) [2, 11, 29, 30],

4- Nonlinear complementarity problem (NCP) [5, 31],

5- Fixed-point problem (FPP) [32-34].

The MP approach and the optimal control theory approach for DTA were introduced in 1978 and 1989 respectively, by Merchant and Nemhauser [18,19] and Friesz et al. [24]. After the introduction of the VIP approach to DTA by Friesz et al. [11], significant studies have been carried out with this approach. The NCP and FPP approaches have not been attractive in the past although Nagurney [3], Patriksson [35], Florian and Hearn [36], and other researchers pointed out the equivalence conditions among VIP, NCP, and FPP [3, 35, 36].

The past DTA literature can be reviewed by classifying the various approaches into four broad methodological groups: mathematical programming, optimal control, variational inequality, and simulation. A comprehensive review on DTA formulations based on these groups and approaches are given in the studies by Tong and Wong [37] and Peeta and Ziliaskopoulos [38].

3. TRAFFIC FLOW MODELLING AND DYNAMIC NETWORK LOADING

3.1. Traffic Flow Modelling

Researchers from engineering, mathematics, operations research, and physics have proposed numerous traffic flow models with various modelling approaches since 1950. Almost each decade was dominated by a certain modelling approach [39]. In the fifties, the propagation of shockwaves was described by fluid-dynamic models for kinematic waves. The investigations in the sixties concentrated on microscopic car-following models. During the seventies gas kinetic models for spatio-temporal change of speed distribution were studied. The simulation of macroscopic fluid-dynamic models was begun to be encountered frequently in the eighties. The nineties were dominated by real-time hybrid simulation models having various structures to model traffic flow and by the systematic investigations of the dynamic solutions of the models developed in the previous 50 years.

The traffic flow models, that are utilized in dynamic network loading (DNL), are classified into macroscopic, mesoscopic, and microscopic models based on modelling approach. Each traffic flow model has its own application area. None of them are false or correct but models from a certain approach fit somehow the objectives of application [40].

The microscopic traffic flow models describe the dynamics of individual vehicles and their interactions, such as follow-the-leader and cellular automata models.

The macroscopic traffic flow models, having sufficient similarities to make the hydrodynamic theory useful in describing traffic dynamics [41], describe the collective vehicle dynamics in terms of aggregate variables; density, flow, and speed (e.g. fluid-dynamic models).

The mesoscopic traffic flow models describe the microscopic vehicle dynamics as a function of aggregate link performances.

A DNL process has to be settled either based on a fundamental traffic flow model or utilizing the properties of a traffic flow model.

Theories relating to the description of continuous vehicular traffic are defined upon the variables such as flow (q), density (k), and speed (v). Due to the relationship q=k·v, it can be said that only two of these variables are independent. The first fluid dynamic theory describing the traffic flow was by Lighthill and Whitham, and by Richards [42, 43], which is hereafter referred as the LWR theory. The underlying hypothesis of this theory is that flow is strictly a function of density q=Q(k), which is equivalent to say that speed is strictly a function of density: v=V(k). So, the fundamental conservation law of fluid dynamics can be written in terms of a continuity equation as given in (3.1):

$$\frac{dk}{dt} + \frac{d\left(kV(k)\right)}{dx} = 0 \qquad \textbf{(3.1)}$$

or alternatively as:

$$\frac{dk}{dt} + C(k)\frac{dk}{dx} = 0 \qquad \textbf{(3.2)}$$

where; “x” is the number of vehicle on the link and C(k)=dQ(k)/dk.

The theory states that slight changes in flow are propagated upstream along kinematic waves, whose velocity (relative to the road) is given by c=C(k) (e.g. the slope of flow-density curve). The model is solved by determining the function k(x, t), given the appropriate boundary conditions. Solution can either be had by using graphical techniques [42] or numerically [12, 44].

Different variations of this model can be characterized by speed-density relationship v=V(k), or equivalently, c=C(k). To be realistic, C(k) should be monotonically decreasing, or at least non-increasing, with increasing density. The pioneer proposition of the LWR model utilized a well-known relationship between speed and density, which is proposed by Greenshields [45] as given in (3.3):

$$v = v^{max}\left(1 - \frac{k}{k^{max}}\right) \qquad \textbf{(3.3)}$$

where, “v^{max}” is the maximum speed and “k^{max}” is the maximum (jamming) density of the traffic. The complete model can be obtained by substituting (3.3) into (3.1) as given in (3.4):

$$\frac{dk}{dt} + \left(v^{max}\right)\frac{dk}{dx} - \left(\frac{v^{max}}{k^{max}}\right)\frac{dk^2}{dx} = 0 \qquad \textbf{(3.4)}$$

Considering the hydrodynamic analogy given with (3.1), (3.2), and (3.4), the DNL models should respect the conservation principle derived from continuity equations. These models perform the representation of traffic flow motion as fluids.

3.2. Dynamic Network Loading

A DNL model provides a mapping from the time-dependent path demand flows to the time-dependent link variables of flow, density, and speed. This modelling approach is an integral component of the DTA problem. Many different methods to the DNL problem have been developed in the past. These methods are distinguished primarily by the way they represent traffic flow, continuous or discrete. Solutions for these models are generally encountered as time discretisation, where the state of the network is determined over short time intervals of constant length. With the application of DNL models, the DTA problem is solved iteratively. An initial set of time-dependent paths is chosen, the DNL model is run, and the path choices for the next iteration are adjusted as a function of the path travel times obtained [46]. Another approach to DTA is based on a feedback mechanism within a single iteration of the DNL model. This approach, also a feature of some traffic simulation software, uses current network conditions as an input to the path choices at origins.

Discrete-flow DNL models can further be decomposed by the representation of space dimension that may also be either continuous or discrete (a detailed classification of DNL models are given in section 3.2.4). Discrete-flow models based on car-following logic are defined on continuous space [47, 48], while the ones based on cellular-automata approach use a discrete notation of space [49]. All solution methods for discrete-flow models in the literature are discrete-time approaches, with the exception of direct applications of queuing methodology to modelling traffic flow.

Continuous-flow DNL models are generally either defined over the entire length of a link, or on link segments. It can be said that link-based (analytical) models generally belong to discrete-flow DNL case, while the macroscopic models belong to continuous-flow DNL case. Link-based models are inspired by the solution of static

traffic assignment problem, and are based on a performance function formulation, which can be a travel time function or a link exit function (a detailed explanation of link-based model formulation is given in section 4.2).

3.2.1. Dynamic Network Loading Problem

The problem of DNL is used in analytical approaches to DTA models. Given path flow rate and link performance functions, the DNL problem consists of determining time-dependent network flow conditions, such as link travel times, total number of vehicles on links, and link inflow and outflow rates. The accurate way to utilize a DNL approach is to formulate the DNL problem as a continuous-time system of nonlinear equations expressing link dynamics, flow conservation, flow propagation, and boundary constraints. Solutions to continuous-time DNL problem is sought by designing a discrete-time version of the model with the help of appropriate solution algorithms. These algorithms find a discrete-time solution that approximates the continuous-time solution.

Although the DNL problem has been recognized at the conceptual level as an important component in dynamic models of traffic flow [11, 50, 51], it was not until recently that this problem was explicitly studied as a central problem in analytical approaches to the DTA problem. Numerous analytical DTA models, implicitly or explicitly, contain various formulations to the DNL problem [2, 18, 19, 52-58].

Researches, in which analytical models for the DNL problem are applied, explicitly proposed and analyzed in the studies of Friesz et al. [11], Wu et al. [50], and Xu et al. [51]. The model of Friesz et al. is formulated as a system of equations expressing link dynamics, flow conservation, flow propagation, and boundary constraints [11]. In the analysis of their model, they assumed linear link travel time functions. The model of Wu et al. extends that of Friesz et al. by considering nonlinear link travel time functions [50]. Xu et al. further studied the model of Wu et al. [51].

The DNL problem can be formulated as a system of equations. A general description of this model is given in the following.

3.2.2. Dynamic Network Loading Model Formulation

3.2.2.1. Notations

The physical traffic network can be represented by a conceptual directed network, $\Omega = (N, I)$, where "N" is the set of nodes and "I" is the set of directed links. In the following, the index "r" denotes an origin node, the index "s" denotes a destination node, and the index "p" denotes a path between origin-destination (O-D) pair (r, s). The subset of paths between O-D pair (r, s) is denoted by "P_{rs}". The variables are grouped at path, link, link-path, and time base as given in the following.

Path Variables

$f_p^{rs}(t)$ = departure flow rate on path "p" for O-D pair (r, s) at time "t".

Link Variables

$U^i(t)$ = cumulative entrance flow (inflow) on link "i" during interval [0, t];

$W^i(t)$ = cumulative exit flow (outflow) on link "i" during interval [0, t];

$N^i(t)$ = number of vehicles (load) on link "i" at time "t";

$B^i(\cdot)$= performance function of link "i", where the argument is number of vehicles on link "i";

$\tau^i(t)$ = travel time over link "i" for flows entering link "i" at time "t" ($\tau^i(t) = B^i[N^i(t)]$).

Link-Path Flow Variables

(i, p) = a link-path pair;

(r, s) = O-D pair of path "p";

$u_p^{i,rs}(t)$ = entrance flow (inflow) rate at time "t";

$w_p^{i,rs}(t)$ = exit flow (outflow) rate at time "t";

$U_p^{i,rs}(t)$ = cumulative entrance (inflow) flow at time "t";

$W_p^{i,rs}(t)$ = cumulative exit flow (outflow) at time "t"; and

$N_p^{i,rs}(t)$ = partial flow on link load induced by flow on path "p" at time "t".

Time Variables

t = index for continuous time;

[0,T] = O-D traffic demand period;

$[0,T_\infty]$ = analysis period-interval of time from instant when flows enter network to least instant when all flows exit network;

ρ = minimum over all links of free-flow link travel time;

$\Delta = \rho / M$, where "M" is a user-defined positive integer; and

y = index for time interval $[(y-1)\Delta, y\Delta]$.

3.2.2.2. Definitions

The two definitions used to formulate the DNL model considering FIFO, are given in the following.

Definition 1

FIFO 1: A link is said to verify the FIFO property if and only if the following inequality is verified:

$$\forall(t_1,t_2)\in[0,T] \quad \text{if} \quad t_1 \le t_2 \quad \text{then} \quad t_1 + \tau^i(t_1) \le t_2 + \tau^i(t_2) \qquad \textbf{(3.5)}$$

This is equal to saying that, no overtaking happens.

Definition 2

FIFO 2: A link is said to verify the strict FIFO property if and only if the following inequality is verified:

$$\forall(t_1,t_2)\in[0,T] \quad \text{if} \quad t_1 < t_2 \quad \text{then} \quad t_1 + \tau^i(t_1) < t_2 + \tau^i(t_2) \qquad \textbf{(3.6)}$$

In transportation networks, this can be translated into the property that a flow entering a link, cannot catch a flow that entered earlier.

3.2.2.3. Link Dynamic Equations

The link dynamic equations express the relationship between the flow variables of a link (see Figure 3.1), which are given by (3.7).

$$\frac{dN_p^{i,rs}(t)}{dt} = u_p^{i,rs}(t) - w_p^{i,rs}(t), \quad \forall (r,s), \forall p \in P_{rs}, \forall i \in p \qquad \textbf{(3.7)}$$

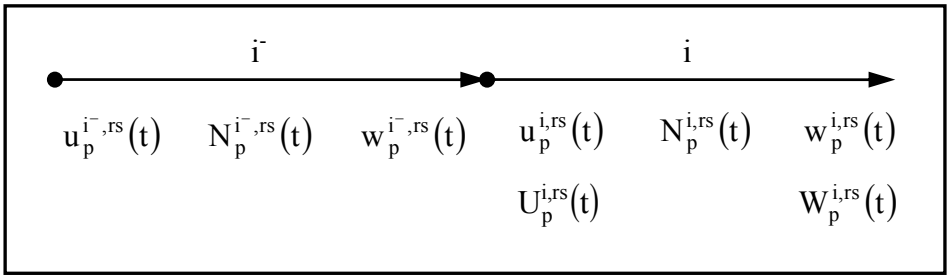

Figure 3.1: Flow Variables

3.2.2.4. Flow Conservation Equations

The flow conservation equations for the nodes where trips originate are given in (3.8), where "i" is the first link of path "p".

$$u_p^{i,rs}(t) = f_p^{rs}(t), \quad \forall (r,s), \forall p \in P_{rs} \qquad \textbf{(3.8)}$$

The flow conservation equations between two consecutive links, "i^-" and "i", on path $p \in P_{rs}$ can be expressed as given in (3.9), where "i" is after "i^-" (see Figure 3.1).

$$u_p^{i,rs}(t) = w_p^{i^-,rs}(t) \qquad \textbf{(3.9)}$$

3.2.2.5. Flow Propagation Equations

Flow propagation equations are used to describe the flow progression over time. A flow entering link "i" at time "t" exits the link at time $t+\tau^i(t)$. Therefore, by time "t", the cumulative outflow of link "i" should be equal to the integral of all inflow rates, which would have entered link "i" at an earlier time "ω" and exited link "i" by time "t". This relationship is given by (3.10), where "ψ" is $[\omega: \omega+\tau^i(\omega) \le t]$.

$$W_p^{i,rs}(t) = \int_{\omega \in \psi} u_p^{i,rs}(\omega) d\omega, \quad \forall (r,s), \forall p \in P_{rs}, \forall i \in p \qquad \textbf{(3.10)}$$

For it is assumed that the network is empty at t = 0, the boundary conditions given in (3.11) are required.

$$U_p^{i,rs}(0)=0 \quad W_p^{i,rs}(0)=0 \quad N_p^{i,rs}(0)=0, \quad \forall(r,s), \forall p \in P_{rs}, \forall i \in p \qquad \textbf{(3.11)}$$

3.2.2.6. Summary of Dynamic Network Loading Model Formulation

In summary, the continuous-time DNL problem is formulated by the system of equations (3.7)-(3.11). In this system of equations, the known variables are departure flow rates $f_p^{rs}(t)$ and link performance functions $B^i(\cdot)$. Link travel times $\tau^i(t)$ are obtained from link performance models with the definitional constraint given by (3.12).

$$\tau^i(t)=B^i\left(N^i(t)\right) \qquad \textbf{(3.12)}$$

A link performance function can be either a travel time function or a link exit function.

The unknown variables are $u_p^{i,rs}(t)$, $w_p^{i,rs}(t)$, $U_p^{i,rs}(t)$, $W_p^{i,rs}(t)$, and $N_p^{i,rs}(t)$. After these unknown variables are determined, link loads $N^i(t)$ can be computed as given in (3.13).

$$N^i(t)=\sum_{rs\in p}\sum_{p\in P_{rs}} N_p^{i,rs}(t) \qquad \textbf{(3.13)}$$

3.2.3. Solution to Dynamic Network Loading Problem

To construct a solution to the DNL model formulated in the preceding section, the following two assumptions are made:

- Link travel times are bounded from below by a positive number, and

- The travel time of a link depends only on the current or past traffic conditions on the link.

Since, (i) a link has a minimum length and the travel speed is finite, and (ii) the travel time for a user entering the link usually depends only on the number of vehicles that entered the link earlier, the above given two assumptions are realistic.

3.2.3.1. Solution Procedure

"ρ" denotes the minimum link travel time of all links. The entire analysis period [0, T_∞] can be divided into intervals of length "ρ". These intervals are numbered 0, 1, 2,

. . . . The m^{th} interval corresponds to $[m\cdot\rho, (m + 1)\rho]$. A solution to the model can be constructed by induction on these intervals in a chronological order.

For $m = 0$ and $t \in [0, \rho]$, because $\tau^i(t) \geq \rho$, there is no exit flow. Therefore, $\forall i \in I$, $W_p^{i,rs}(t) = w_p^{i,rs}(t) = 0$.

The inflow rate $u_p^{i,rs}(t)$ can be determined with flow conservation equation (3.8) and $U_p^{i,rs}(t)$ can be computed as given in (3.14).

$$U_p^{i,rs}(t) = \int_0^t u_{ip}^{rs}(t)dt, \quad \forall(r,s), \forall p \in P_{rs}, \forall i \in p \qquad \textbf{(3.14)}$$

After $U_p^{i,rs}(t)$ and $W_p^{i,rs}(t)$ are determined, $N_p^{i,rs}(t)$ can be computed as given in (3.15).

$$N_p^{i,rs}(t) = U_p^{i,rs}(t) - W_p^{i,rs}(t), \quad \forall(r,s), \forall p \in P_{rs}, \forall i \in p \qquad \textbf{(3.15)}$$

Therefore, for $m = 0$, a solution of all unknown variables can be found. For $m > 0$, it is assumed that a solution of all unknown variables exists for each "m" intervals. A solution of all unknown variables can be found for interval $m + 1$. For interval $m + 1$ and $t \in [(m + 1)\rho, (m + 2)\rho]$, the exit flows for all links can be computed by using the flow propagation equations as given in (3.10).

Because $\tau^i(t) \geq \rho$, "ω" must be less than $(m + 1)\rho$. By the induction assumption, $u_p^{i,rs}(\omega)$ is known for all $\omega < (m + 1)\rho$. Therefore, $W_p^{i,rs}(t)$ and $w_p^{i,rs}(t)$ can be determined for all $i \in I$. By using the flow conservation equations and link dynamics equations, $u_p^{i,rs}(t)$, $U_p^{i,rs}(t)$, and $N_p^{i,rs}(t)$ can be determined. Therefore, a solution of all unknown variables can be found for interval $m + 1$.

A solution of all unknown variables exists for every interval "m" by induction. This procedure indicates the way to construct a solution to the DNL model and can be used in the development of an exact solution algorithm [59].

The solution algorithms sought for DNL problem should find a discrete-time solution that approximates the continuous-time solution. The discrete-time solutions can be obtained by dividing continuous time into small intervals with a length that is at least equal to the minimum free-flow travel time over all links. In the following,

explanations on the discretisation of continuous time and discrete DNL model are given.

3.2.3.2. Discretisation of Continuous Time

An important consideration in discretisation of time is the determination of interval length. In general, a smaller interval length gives more accurate results because a discrete model will approach a continuous model as interval length goes to zero. However, for the same analysis period, the number of intervals will increase when the interval length decreases. For the computational burden increases with the number of intervals, more intervals result in loss of computational efficiency. Therefore, in determining the interval length, a trade-off may need to be made between accuracy and efficiency.

The following method is used to discretise the continuous time into small intervals. Interval length "Δ" is chosen as $\Delta = \rho / M$, where M is a positive integer.

After the continuous time period is divided into small intervals of length "Δ", each interval is indexed by an integer "y", numbered from y = 0, 1, 2, …. Index "y" represents the y^{th} interval $[y \cdot \Delta, (y + 1)\Delta]$.

3.2.3.3. Discrete Dynamic Network Loading Model

A typical discrete DNL model can be derived based on the continuous model given by equations (3.7)-(3.11). For each interval "y", it can be assumed that the flow rate functions are constant within that interval and the cumulative flow variables are piecewise linear, for example as given in (3.16).

$$u_p^{i,rs}(t) = u_p^{i,rs}(y \cdot \Delta), \quad \forall t \in [y \cdot \Delta, (y+1)\Delta] \tag{3.16}$$

Therefore, the discrete DNL model can be formulated as follows:

Link dynamics equations

$$N_p^{i,rs}(y \cdot \Delta) = U_p^{i,rs}(y \cdot \Delta) - W_p^{i,rs}(y \cdot \Delta), \quad \forall y, \forall (r,s), \forall p \in P_{rs}, \forall i \in p \tag{3.17}$$

Flow conservation equations

$$u_p^{i,rs}(y\cdot\Delta)=\begin{cases} f_p^{i,rs}(y\cdot\Delta) & \text{if} \quad \text{i is first link on path p} \\ w_p^{i^-,rs}(y\cdot\Delta) & \text{if} \quad \text{i is after } i^- \end{cases}, \quad \forall y,\forall(r,s),\forall p\in P_{rs} \quad \textbf{(3.18)}$$

Flow propagation equations

$$W_p^{i,rs}(y\cdot\Delta)=\sum_{j\in\left|l:\,0\le l\Delta+\tau^i(l\Delta)\le(y-1)\Delta\right|} u_p^{i,rs}(j\cdot\Delta)\Delta, \quad \forall y,\forall(r,s),\forall p\in P_{rs} \qquad \textbf{(3.19)}$$

Boundary (or initial) conditions

$$U_p^{i,rs}(0)=0 \;\; W_p^{i,rs}(0)=0 \;\; N_p^{i,rs}(0)=0, \quad \forall(r,s),\forall p\in P_{rs},\forall i\in p \qquad \textbf{(3.20)}$$

$u_p^{i,rs}(y\cdot\Delta)$ is needed in flow propagation equations. The solution value of this variable can be determined from flow conservation equations. If link "i" is not the first link on a path, $u_p^{i,rs}(y\cdot\Delta)$ is determined by the exit flow rate $w_p^{i-,rs}(y\cdot\Delta)$ of the preceding link.

The cumulative inflow $U_p^{i,rs}(y\cdot\Delta)$ is needed to compute $N_p^{i,rs}(y\cdot\Delta)$ in link dynamics equations, as given in (3.21).

$$U_p^{i,rs}(y\cdot\Delta)=\sum_{j=0}^{y} u_p^{i,rs}(j\cdot\Delta)\Delta \qquad \textbf{(3.21)}$$

On the basis of the discrete model formulated in this section, DNL solution algorithms can be developed.

3.2.4. Dynamic Network Loading Model Classifications

The classification of DNL models has been varying due to variations in both the theoretical structure and the applicability of these models since they were first used. At the beginning, the classification was being done into two: macroscopic models, treating traffic flow as a hydrodynamic flow, and microscopic models, studying the dynamics on individual vehicles dimension. Mesoscopic modelling with the assumption of packet approach has then become a class of DNL. The need for a better representation of traffic dynamics and the reproduction of traffic flow motion on the network have been the main reasons for both seeking the solutions and the

more specific classifications of DNL models. The variation in classification is due to the reasons including the discretisation dimension and size of discretisation slice, and queuing assumption. Therefore, an exact definition on the categorization of DNL models can not be done due to existences given below.

- Some approaches adopt a mixed modelling method.
- Similar approaches have different assumptions.

In this section, the classification of DNL models is handled upon discretisation scheme and queuing assumption.

3.2.4.1. Classification upon Discretisation Scheme

A great number of different DNL approaches have been presented and, due to the continuous spread among the conceivable network traffic simulation models, many others are conceived every year. In the following, a classification based on the discretisation adopted by several models is proposed. Moreover, it is hard to state that all the same requirements are respected by a group of similar models. According to time, space, and demand discretisation, it is possible to represent models in a three-dimensional space where the "x", "y", and "z" axes represent time, space, and demand respectively (Figure 3.2) [60].

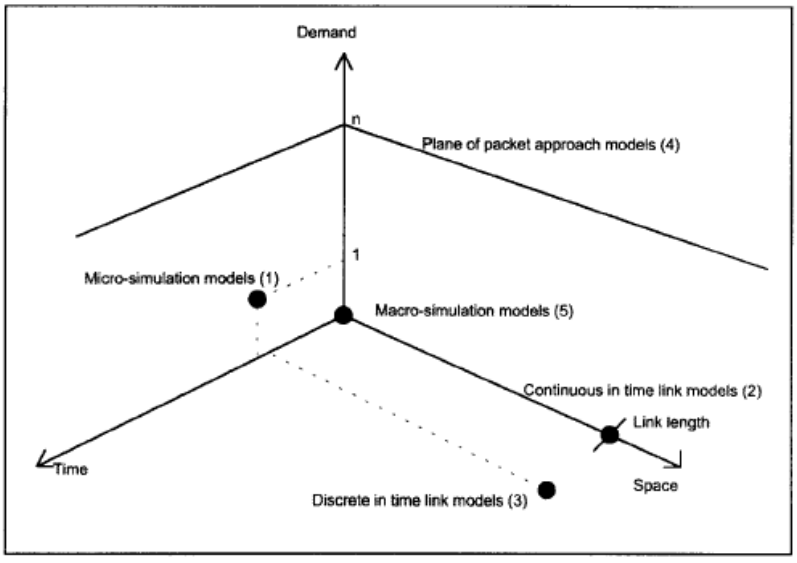

Figure 3.2: Three-dimensional representation of network traffic models according to time, space, and demand discretisation [60].

The following main modelling approaches can be identified by considering the discretisation dimension:

- microsimulation models,
- continuous time link models,
- discrete time link models,
- models following a packet approach, and
- macrosimulation models (continuous in time and space models).

Microsimulation models are based on the simulation of the movements of single users/vehicles. This simulation is indicated in reproducing some specific traffic situations, such as intersection, parking facilities, overtaking, lane changing or for the evaluation of control strategies dependent on individual driver behaviour. There are too many studies that have involved microscopic simulation approach in the literature including (???) [61-64]. Also, several simulation packages (CORSIM, HUTSIM, INTEGRATION, NETSIM, SIMNET, SIMIR, etc.) have been developed and most are particularly useful for special aspects of traffic flow within microscopic approach. Some mixed models have been proposed, based on a microscopic or quasi-microscopic simulation, obtaining macroscopic link characteristics such as speed and density [65]. A detailed literature review can be found in the study by Helbing [39].

Many authors, including Friesz et al. [24], Wie et al. [25], Boyce et al. [67], Fernandez and De Cea [68] and Adamo et al. [69], have proposed formulations of continuous time link models that are based on a space discretisation which divides up the path of the users into links together forming the network. Link FIFO concept has been handled in a number of studies with continuous time link models [7, 50, 51, 58, 70]. Some of these continuous models have been numerically solved with a time discretisation and so can be related to concepts originated in the discrete time link model proposed by Merchant and Nemhauser [18, 19] and later studied in some other models [21, 71, 72]. Models not requiring spatial discretisation and so called link-based models can be subdivided into whole link models and wave models, since they are being proposed within a macroscopic approach.

Whole link models do not take into account the propagation of flow states along a link, since the performances are assumed to depend on a space-average variable, such as density [73]. This leads to a poor representation of travel times that gets worse as the link length increases [74]. But these models allow adopting any fundamental diagram of traffic flow, and are widely used in DTA applications due to

their simplicity [11, 37]. Wave models, based on the simplified kinematic wave theory of LWR, implicitly consider the propagation of flow along a link, determining link performances as a function of the traffic conditions encountered while travelling throughout the link. These models, better representing the bottlenecks, are appropriate in studying queue formation considering the capacity constraint, free-flow and queuing speed [75, 76]. Regarding to the examples given above, we can say that a portion of discrete time link models are proposed by macroscopic and the rest are proposed by mesoscopic approach.

In packet approach methods, users/vehicles are grouped together to form packets that can be moved along the network so to realize a discretisation of demand of each OD pair. It is possible to distinguish between a point packet approach [77-79] in which a group of users is concentrated into a single point and a continuous packet approach [80-83], where the users are supposed to be uniformly distributed in time or space along the packet. There are also studies that can not be grouped into mesoscopic classes given above [46, 65, 84]. Heuristic generalization of within-day static methods [85, 86] can also be grouped into mesoscopic modelling approach.

Continuous in time and space models (or macroscopic models) are more advanced models those are based on continuous traffic simulation such as Lighthill and Whitham's model [42] or Payne's model [87]. In macroscopic DNL models, vehicles are modelled with piecewise continuous functions of density and flow, in space-time, analogous to fluid flow. The mathematical theory behind these models is based on temporal, one-dimensional fluid dynamics and formulated with a system of differential equations in time and space dimension, which requires the application of finite difference methods for solution [12, 13, 44, 88]. The kinematic wave theory was proposed by Lighthill and Whitham, and Richards [42, 43] regarding to conservation principle and with the assumption of an equilibrium speed-density relationship. The macroscopic LWR approach failed to describe more complex traffic flow states because of having an unrealistic assumption of adopting the equilibrium speed instantaneously. Inequilibrium state models are developed by including the continuity equation and an equation representing the acceleration behaviour [89-91]. With integrating the use of flow-density relationship, these models provide realistic results in the presence of a computational burden. The simplest macroscopic traffic models are based on the concept that vehicle traffic at a

given point in space-time is affected only by local traffic within a neighbourhood of that point [12, 13]. The fundamental relationship of flow-density, is set by empirical measurements on flow and density [45]. Many models of this type have been developed for freeway network simulation [26, 87]. The cell transmission models of Daganzo [12, 13] originate from the model of Lighthill and Whitham [42].

3.2.4.2. Classification upon Queuing Assumption

DNL models in DTA have been proposed with adopting a queuing assumption, which are point-queuing and physical queuing. Models set out with point-queuing assumption can not capture queue spillback while the ones with the other assumption can. Because of the capability of capturing queue spillback, the physical-queuing assumption is more realistic compared with the other one.

Capturing queue spillback in traffic flow modelling affects the nature of the DTA problem substantially [14]. It is because the location of the tail of a queue is an important factor in determining the shortest routes at each instant of time in DTA problems with physical queues. Kuwahara and Akamatsu proved that the resulting route choice pattern obtained by a DTA model with physical-queuing assumption can significantly differ from the model with point-queuing assumption [16].

Capturing the effects of physical-queues in traffic flow adds difficulties in obtaining an ideal DUO solution of DTA problems in a general network. Moreover, capturing the effects of physical-queues in traffic flow not only alters the resultant route choice pattern and causes difficulties in obtaining solutions, but also changes the properties of DTA problems and affects the algorithmic development, transport network design, and the predictions of network performances [6, 30, 31]. Therefore, it is essential to determine the most appropriate approach for flow propagation modelling on a network by considering the main differences between these two assumptions.

Based on the properties of point-queuing, we can derive the followings:

- Queues have no physical lengths.
- The storage capacity of each link can be ignored and all links can contain as many vehicles as loaded.
- Queues can not propagate backward over links due to the second deduction.

- The outflow rate of a link only depends on its own link flow, because its downstream links always have enough storage capacities.

Since queues can not pass over a junction horizontally, point queues are also named as vertical queues. Point-queuing assumption is generally appropriate in the situation when link lengths are long, the storage capacities are sufficient, and the demands are low enough.

Since the physical-queuing assumption considers the lengths of vehicles, the storage capacities of links can not be ignored. Therefore, a queue with a physical length is called a physical-queue. When a physical queue occupies the whole link, it passes over the junction and hence it is also named as horizontal queue. Making a physical-queue assumption is appropriate when the links are short, the demand for them is high, and spillback occurrence is frequent.

In this study, the link model component of the proposed DNM is set out with the assumption of point-queuing. So, the given examples to link models in section 4.2.1 are all selected for point-queue approach.

4. FLOW PROPAGATION MODELS

4.1. Properties of Flow Propagation Models

These models use a hydrodynamic analogy for the representation of traffic flow as mentioned in section 3.1. The flow q(t) through an "S" section of a road can be given as in equations (4.1).

$$q(t) = \lim_{\Delta t \to 0} \frac{\text{number of vehicles passed through S during} [t, t+\Delta t]}{\Delta t} \qquad \textbf{(4.1a)}$$

$$q(t) = \lim_{\Delta t \to 0} \frac{\Delta n}{\Delta t} \qquad \textbf{(4.1b)}$$

Considering the hydrodynamic analogy, these models should respect the conservation principle derived from continuity equations (explained in details in section 3.1.1) as given in (4.2). Differentiating (4.2) with respect to "t" gives (4.3), where (ω + travel time at ω instant) ≤ t and u(t), w(t) and n(t) are all continuous functions of time "t".

$$n(t) = \int_0^t (u(\omega) - w(\omega)) d\omega \qquad \textbf{(4.2)}$$

$$\frac{dn(t)}{dt} = u(t) - w(t) \qquad \textbf{(4.3)}$$

The continuity equation given in (4.3) is implicitly valid in every link model. Equation (4.4a), used to calculate the difference on number of vehicles on a link at time (t+1), and equation (4.4b), used to calculate the number of vehicles on a link at time (t+1), can be written by discretising equation (4.3):

$$\Delta n(t+1) = (u(t) - w(t)) \cdot \Delta t \qquad \textbf{(4.4a)}$$

$$n(t+1) = n(t) + (u(t) - w(t)) \cdot \Delta t \qquad \textbf{(4.4b)}$$

where “t” denotes the individual time interval (t = 0, 1, 2, ..., T); n(t) is the number of vehicles on the link within the interval “t”; u(t) is the flow entering the link in the period “t”, and w(t) is the exiting flow.

A full satisfactory dynamic link loading model should satisfy the following requirements as a DNL method should do.

- FIFO rule respect: The users’ travelling should be consistently simulated ensuring that no overtaking can occur between two users who have entered a link at different times, while still moving on the link. Carey first described the necessity of respecting the FIFO rule [53], which has been imposed in some models with a set of additional constraints [92]. In general, the models presented in the literature do not hold FIFO rule, hence the problem of inconsistencies between flow propagation and link travel time occur.
- Flow propagation and speed consistency: Flow propagation through a network should be consistent with the speed of the flow. So, no propagation must be allowed at a higher speed than free-flow speed.

Respect of link models to FIFO rule is explained in details peculiar to varying formulations in the travel time function and the exit link function subsections.

4.2. Modelling Approaches on Flow Propagation Models

Flow propagation models necessitate the solution of a system of differential equations, based on Eq. (4.3), by means of two different performance functions:

- exit link function formulation; and,

- travel time function formulation.

There are also models, which are set out by a mixed approach that adopts both of the above mentioned functions.

4.2.1. Link Exit Function Formulation

Exit flow “w” is assumed to depend on the number of vehicles, “n”, on the link, regardless of their position, as given in (4.5).

$$w = W(n) \qquad \textbf{(4.5)}$$

Since W(n) represents a physical term, this function is assumed to be independent from time in the former study of Merchant and Nemhauser [18]. In this study, it is noted that this function, used to determine the number of vehicles, can be selected arbitrarily.

Merchant and Nemhauser (M-N) required the link exit function to satisfy the inequality condition given in (4.6), considering a very high value for the maximum number of vehicles n_{max} [18].

$$0 \le W(n) \le n_{max} \quad \textbf{(4.6)}$$

Upon this approach, the outflow "w" at time "t" on a link or link segment is a non-decreasing function of the total number of vehicles on the whole link or on the link segment respectively, as given in (4.7).

$$w^i(t) = W\left(n^i(t)\right) \quad \textbf{(4.7)}$$

Here, W(·) is a function, which is non-negative, continuous, non-decreasing and bounded by n(t).

The total number of vehicles on link (or link segment) "i" at time "t" can be determined from the inflow $u^i(t)$ and outflow $w^i(t)$, as given in (4.8).

$$\frac{\partial n^i(t)}{\partial t} = u^i(t) - w^i(t) \quad \textbf{(4.8)}$$

By finite difference approximation, (4.9) is obtained substituting Eq. (4.7) into Eq. (4.4b).

$$n^i(t+\Delta t) - n^i(t) = \left(u^i(t) - W^i(t)\right) \cdot \Delta t \quad \textbf{(4.9)}$$

The left hand side of (4.9) is the rate of change on the number of vehicles on link "i" at time "t", which is equal to the difference between the corresponding inflow and outflow.

If there is a series of links without merges and diverges, the inflow of a link "i" is equal to the outflow of a link "i⁻", the upstream of link "i", as given in (4.10).

$$u^i(t) = w^{i^-}(t) \quad \textbf{(4.10)}$$

Therefore, when the case is network assignment for the first link of a path, the link flow rates are equal to the corresponding path flow rates, as given in (4.11).

$$u^i(t) = f_p^{rs}(t) \qquad \textbf{(4.11)}$$

Here, $f_p^{rs}(t)$ is the path flow departing at time "t" and travelling between "rs" O-D pair.

Equations (4.7)-(4.11) provide the basic principle of modelling traffic flow on a series of straight (untraversed) links.

Given the initial number of vehicles $n^i(1)$ and the inflows of the first links (which are the path flows) at any time, the time-varying traffic on a series of links without any merges and diverges can be computed sequentially over time, with the algorithm given below.

1. Calculate the outflow $w^i(t)$ on each link dependent to $n^i(t)$ with the Eq. (4.7).
2. Determine the inflow $u^i(t)$ of each link with equations (4.10) and (4.11).
3. Calculate the number of vehicles $n^i(t+\Delta t)$ with Eq. (4.9).
4. Consider the next time interval until end of the modelling horizon.

In order to extend the above given algorithm to a general network with multiple O-D pairs, one more extension is required. The inflows, the outflows and the number of vehicles on a link are disaggregated by path "p" so as to direct traffic at diverges and merges in a general network with multiple O-D pairs. The relationships between aggregated and disaggregated variables are given in (4.12) and (4.13).

$$u^i(t) = \sum_p \xi_p^i \cdot u_p^i(t) \qquad \textbf{(4.12)}$$

$$n^i(t) = \sum_p \xi_p^i \cdot n_p^i(t) \qquad \textbf{(4.13)}$$

Here, $\xi_p{}^i$ is equal to 1 if link "i" is on path "p", and zero otherwise. The disaggregated outflow and the flow conservation for disaggregated variables can be calculated as given in (4.14) and (4.15) respectively.

$$w_p^i(t) = \frac{n_p^i(t)}{n^i(t)} \cdot W^i\left(n^i(t)\right) \qquad \textbf{(4.14)}$$

$$n_p^i(t+\Delta t) - n_p^i(t) = \left(u_p^i(t) - w_p^i(t)\right) \cdot \Delta t \qquad \textbf{(4.15)}$$

The path flow concept given with (4.10) and (4.11) can be applied in a network scheme as given in (4.16).

$$u_p^i(t) = \begin{cases} w_p^{i^-}(t), & \text{if } i^- \text{ is the preceeding link along route p} \\ f_p^{rs}(t), & \text{if i is the first link of route p} \end{cases} \qquad \textbf{(4.16)}$$

The following algorithm summarizes the determination of flows and number of vehicles on all links under exit function approach when a network is considered.

1. Set t = 1.
2. Determine the total number of vehicles of each link based on $n^i_p(t)$ with Eq. (4.13).
3. Calculate the aggregated outflow $w^i(t)$ of each link with (4.7).
4. Calculate the outflow $w^i_p(t)$ with (4.14).
5. Obtain inflow $u^i_p(t)$ with (4.16).
6. Determine $n^i_p(t+\Delta t)$ with (4.15).
7. If t = T, where T is the last time interval of the modelling horizon, stop. Otherwise set t = t+1 and go to Step 2.

Once all the inflows and outflows are determined, the link travel times can then be calculated as explained in section 4.2.2 by following (4.17).

$$u_p^i(t) = w_p^i\left(t + \tau_p^i(t)\right) \qquad \textbf{(4.17)}$$

This method can be adopted in other network loading approaches.

In this subsection, the basic theoretical structure of flow propagation modelling, set out with point-queuing assumption and exit link formulation, is explained. When modelling of the link component of the proposed DNM in this study is considered to

be done by a DNL approach, it is right to conclude that the links are modelled with the system of differential equations as given in (4.18).

$$\text{General formulation in link exit function models} \begin{cases} \dfrac{dn(t)}{dt} = u(t) - w(t) \\ w = W(n) \end{cases} \quad \textbf{(4.18)}$$

This approach was first adopted in M-N model [18] and was then improved by a number of researchers including Ho [20], Carey [21, 93, 94], Carey and Srinivasan [95], Friesz et al. [24], Lasdon [96], Lam and Huang [27], Wie [97], Wie et al. [71, 98, 99], Wie and Tobin [100], Yang and Huang [28], and others.

The exit flow function approach has been criticized by researchers due to its limitations. The first deficiency is the violation of FIFO requirement [58, 74, 99, 101] unless entry times are carefully checked in determining outflows. The second deficiency is that exit flow models can lead to flow propagations inconsistent with travel time and speed. Adisson and Heydecker [102] showed that the dynamic response of the changes in inflows is slower even than wave models. Moreover, they showed that it can cause the instantaneous propagation of traffic leading to zero travel times for some travellers while others have infinite travel times. The third deficiency is that exit flow functions can lead to the violation of casuality [33]. Astarita showed that an increase in inflow rate can result in a decrease in outflow rate when a concave and differentiable exit flow function is adopted [58]. The last deficiency is the difficulty in specifying an appropriate exit flow function [101].

The link model that is set out as an integral part of the proposed DNM throughout this thesis is proposed to tackle with the above mentioned deficiencies of the exit link functions.

4.2.2. Travel Time Function Formulation

The main difference between this approach and the exit flow function approach is that the former starts computation with a travel time function and requires the outflow to be defined from the inflows and link travel times, while the other starts with an exit flow function and requires the link travel time to be defined from the inflows and the outflows. This is equal to saying that the former calculates link travel

times before exit flows where the latter provides a computation vice versa and the former employs predefined link travel time functions to calculate exit flows where the latter is dependent on the predefined exit flow functions to determine exit flows. If the links are sufficiently short, and if time is appropriately discretised, or if congestion tends to be in the form of queues, then the travel time function based models give a more accurate consistent approximation to link flow behaviour [103, 104]. This is explored in many works for a widely used model introduced by Merchant and Nemhauser [18, 19].

In link travel time formulation, travel time of a user arriving the entrance of a link at time "t" is introduced as $\tau(t)$. Since the traffic flow is continuous and is resembled as a fluid, the user is treated just as a particle of this fluid. Each of the users arriving the entrance of a link have their own travelling time "τ", which is the exact time to traverse a link. As the propagation of flows through a link is described by the relationships between control variables at each point in time, the travel time $\tau(t)$ for traffic entering a link at time "t" can be expressed as given in Eq. (4.19), which is derived by following Ran et al. [55].

$$\tau(t) = T(u(t), n(t), w(t)) \qquad \textbf{(4.19)}$$

Most of the travel time formulations proposed in the literature are special cases of the form given in (4.19). Five types of separable, differentiable, positive and increasing travel time function forms have been widely adopted in the literature.

4.2.2.1. Type 1

The travel time $\tau^i(t)$ on link "i" is defined as a function of some or all of its control variables. The former model considering this type of function with all of the control variables was proposed in the work by Ran et al. as given in (4.20) [55].

$$\tau^i(t) = T_1^i\left(n^i(t), u^i(t)\right) + T_2^i\left(n^i(t), w^i(t)\right) \qquad \textbf{(4.20)}$$

Here, T_1^i is labelled as the "instantaneous flow-dependent running time" and T_2^i as the "instantaneous queuing delay". Both T_1^i and T_2^i are assumed to be non-negative and increasing functions of their variables "n", "u" and "n", "w". These functions have been taken to be separable in some of the studies including Ran et al [55], Boyce et al. [105] and the others. Therefore, by applying separability the formulation

given with (4.20) can be written in term given with (4.21), where α^i is the free-flow travel time.

$$\tau^i(t) = \alpha^i + f^i\left(u^i(t)\right) + g^i\left(w^i(t)\right) + h^i\left(n^i(t)\right) \quad \textbf{(4.21)}$$

4.2.2.2. Type 2

In this type, the travel time $\tau^i(t)$ is a function of its link occupancy (number of vehicles on the link) $n^i(t)$ and inflow $u^i(t)$ as given in (4.22).

$$\tau^i(t) = T^i\left(u^i(t),\, n^i(t)\right) \quad \textbf{(4.22)}$$

This type of functions are adopted in the works by Ran et al. [106], Chen and Hsueh [29, 107], Wie et al. [5], and the others. It is proven that this type of travel functions violate FIFO rule [74].

4.2.2.3. Type 3

If the travel time $\tau^i(t)$ is only a function of its link occupancy $n^i(t)$ as given in (4.23).

$$\tau^i(t) = T^i\left(n^i(t)\right) \quad \textbf{(4.23)}$$

This function is a special case of the first one and was adopted by Friesz et al. [11], Astarita [7, 58], Wu et al. [50], Xu et al. [51], Zhu and Marcotte [108], Carey and McCartney [109], Rubio-Arandaz et al. [110], and others.

In this study, one of the models compared with the proposed model is formulated with this type of travel time function.

4.2.2.4. Type 4

Travel time $\tau^i(t)$ is a function of the number of vehicles in the queue $n^{qi}(t - t')$ in this type (see Eq. (4.24)), where "t′" is a positive constant. This formulation is a special class of functions given by (4.23) and explained in the third type.

$$\tau^i(t) = \alpha^i + \frac{n^{qi}\left(t + \alpha^i\right)}{s^i} \quad \textbf{(4.24)}$$

Here, s^i is the maximum exit rate and α^i is the free-flow travel time. This type of function assumes that each link is made up of two segments: a running and a queuing

segment. The running segment has a constant travel time α^i and no queuing. The queuing segment is downstream and followed by the running segment. It has a bottleneck with no spatial dimension comprised of a point queue. Since the entry time of the vehicle to the queuing segment is later than that to the running segment by β^i, the travel time at t depends on the queue $t+\alpha^i$. Function in (4.24) is adopted by Bernstein et al. [111], Kuwahara and Akamatsu [112, 113], Huang and Lam [9], and the others.

4.2.2.5. Type 5

In the last type, travel time $\tau^i(t)$ is assumed to be a function of the density $k^i(t)$ as given in (4.25).

$$\tau^i(t) = T^i\left(k^i(t)\right) \qquad \textbf{(4.25)}$$

This function is also a special case of the class given in third type and was employed in the studies by Jayakrishnan et al. [114], Ran et al. [115], and the others.

After choosing a travel time function and adding this to the series of equations to model flow propagation, one relation is left to compute the outflows. This relation can be derived as given in the following.

Since it is assumed that traffic enters and leaves only at the beginning and end of the link, conservation implies the traffic volume as in (4.26).

$$n(t) = \int_0^t \left(u(\omega) - w(\omega)\right)d\omega \qquad \textbf{(4.26)}$$

Further, consider that traffic which enters the link at time "t" leaves at time $t+\tau(t)$, where $\tau(t)$ is the travel time. If FIFO and conservation hold, the number of vehicles that enter the link by time "t" must equal the number that have left by time $t+\tau(t)$, as given in (4.27):

$$\int_{-\infty}^{t} u(\omega)d\omega = \int_{-\infty}^{t+\tau(t)} w(\omega)d\omega \qquad \textbf{(4.27)}$$

where, [ω: ω+τ(ω) ≤ t]. Differentiating (4.27) with respect to "t" and rearranging the resultant term gives (4.28), which is the final component of a travel time function based flow propagation model and computes the outflows.

$$w(t+\tau(t)) = \frac{u(t)}{1+\frac{d\tau(t)}{dt}} \qquad \textbf{(4.28)}$$

The most widely used travel time formulation of Friesz et al. [11] violates FIFO. But with a set of additional constraints [92] and piecewise travel time functions [58] models respecting FIFO has been set out. One of the models that is selected for comparison within this study is set out on the travel time formulation of of Friesz et al. [11]. Comparison is given in details in section 5.1.2.

The first models presented based on travel time function [11, 50, 55] can be considered as an implicit formulation of the problem.

General formulation in travel time function formulation models is given in (4.29).

$$\left.\begin{aligned} \frac{dn(t)}{dt} &= u(t) - w(t) \\ \tau(t) &= T(n(t)) \\ w(t+\tau(t)) &= \frac{u(t)}{1+\frac{d\tau(t)}{dt}} \end{aligned}\right\} \qquad \textbf{(4.29)}$$

4.2.3. Mixed Approach

In the works by Friesz et al. [24], Lam and Huang [27], Yang and Huang [28], and others, a mixed approach of exit link function and travel time function was employed. In this approach, the outflows are determined dependent to exit flow functions but travel times are determined separately by travel time functions. So, the outflows and travel times calculated under this approach are not consistent, opposing to the previous two approaches [116, 117]. Moreover, this approach does not guarantee FIFO and the conservation of the number of vehicles [58].

The procedure to determine the outflows under this approach is the same as the one for the exit link function approach. Link travel times are estimated by the travel time

functions using the link occupancies determined by the algorithm given in section 4.2.1. Route travel times are then calculated.

5. PROPOSED DYNAMIC NODE MODEL

Intersection modelling of traffic networks is mainly based on the signalization scheme. Dynamic models for signalized intersections are studied in the literature [118, 119] and out of the scope of this study, since the structured model in this study is proposed for flow propagation modelling at unsignalized intersections. Node models for unsignalized intersections can be grouped dependant on the queuing assumption. A few number of studies have been carried out considering physical queuing, including Daganzo [13], Adamo et al. [69], Kuwahara and Akamatsu [16], and Rubio-Ardanaz et al. [110]. Recently, an effort to model flow propagation at unsignalized intersections by point queue assumption has been made in works by Dell'Orco et al. [120], Celikoglu [121], and Celikoglu et al. [122] by the proposition of a dynamic node model (DNM). The following section describes a new DNM derived from the current model proposition.

5.1. Link Model Component

In this section, the dynamic link loading problem is handled by considering traffic flow relationships. A link exit formulation is proposed assuming the existence of a valid relationship between speed and density. The link model is then set out by a mesoscopic approach with respect to flow conservation principle and capacity constraint. The proposed link model provides iterative computation for the solution of the problem.

Mesoscopic models, explained in details in section 3, assume that vehicles are either grouped in discrete packets or spread within continuous packets. A frequently used mesoscopic approach is to group vehicles together into packets and each packet is treated as a single vehicle [123]. The packets are arranged in order of their entry time and the travel time is calculated, assuming that packets experience junction delays as a function of current flow on the link. Vehicles entering or leaving the link are respectively added or subtracted in the appropriate time intervals to produce new flow estimates.

Flow propagation is generally studied with discrete packets when the mesoscopic approach is adopted. The link model proposed in this study is developed by both considering the over-saturation phenomenon and improving the computational efficiency on a previously proposed link model [66, 124]. This model is set out with link exit function formulation, discretisation on time dimension, defining capacity constraint rules for over-saturated states and uniformly accelerated speed assumption, which allows a realistic representation of outflow dynamics. Model has an iterative structure, which converges to a target performance with the coded algorithm.

5.1.1. Assumptions

Within the proposed mesoscopic model a discrete packet is made up of a "pile" of vehicles, all located at the head of the packet: if the head of a packet occupies a link during interval [t, t+Δt], all vehicles belonging to that packet are assumed to occupy the same link. With these hypotheses, the difficulties of continuous packet models are avoided, but at the cost of a high level of simplification that could influence external consistency, which is the capacity of the model to represent the phenomenon correctly. Since the vehicles are all located at the head of the packet, and move all together, in this study they are assumed to be of the same class.

The speed has been assumed equal for all packets running on link “I” at the same time “t” ($\partial V/\partial s = 0$) and acceleration is constant and common for all vehicles on the link in the reference period. Therefore, with the assumptions that:

- the vehicles of each packet are all located at the head of the packet;
- the speed is equal for all packets on the link;
- the movement of vehicles is uniformly accelerated;

a relation between speed and density exists and is valid.

5.1.2. Theoretical Basis of Link Model Component

Let “P” be the set of feasible paths on the network; the set of vehicles, leaving in the same interval “ω” and following the same path “p” ($p \in P$) is called a “packet” (ω, p). Movement of vehicles is studied for discrete time intervals [t-Δt, t], [t, t+Δt]; in these reference periods, speed can be assumed to be accelerated uniformly. The speed of a

generic packet (ω, p) is generally both a function of the space "s" (and thus of the entry time on the link, $t_{\omega,p}$) and of the time t: V = V(s, t), where s = s(t, $t_{\omega,p}$). In the literature simplified approaches are applied: the speed is assigned to each packet on entering the link and does not change over time ($\partial V/\partial t = 0$), or is assumed equal for all packets running at the same time t on the link ($\partial V/\partial s = 0$).

Additionally, consider a generic link in which:

- $m_{\omega,p}$ is the total number of vehicles belonging to packet (ω,p);
- $a^i(t)$ is the acceleration during the interval [t, t+Δt] constant and common, in the reference period, for all vehicles on link "I";
- $n^i_{\omega,p}(t)$ is the number of vehicles in packet (ω,p) on link "i" at time "t";
- $s^i_{\omega,p}(t)$ is the position on link "i" of the head of the packet (ω,p) at time "t". The value of $s^i_{\omega,p}(t)$ is zero if packet (ω,p) is not on the link;
- $n^i(t)$ is the total number of vehicles on link "i" at time "t",
- $k^i(t)$ is the density on link "i" at time "t";
- $N^i(t)$ is the number of vehicles in exiting flow from link "i" at time "t",
- $\overline{N^i(t)}$ is the number of vehicles that exceeds the capacity and can not exit from link "i" at time "t",
- d^i is the length of link "i",
- $V^i(t)$ is the speed at time "t" on link "i", common to all vehicles on the link,
- $w^i(t)$ is the exiting flow from link "i" at time "t".

Speed is a function of average density $k^i(t)$: $V^i(t) = V(k^i(t))$, where $k^i(t) = n^i(t)/d^i$. So, the total number of vehicles on a link can be calculated with (5.1).

$$n^i(t) = \sum_{p \in P} \sum_{\omega \le t} n^i_{\omega,p}(t) \qquad \textbf{(5.1)}$$

With the assumptions given in section 5.1.1 and relying on to the existence of a valid relationship between speed and density, the variables $V^i(t)$, $n_{\omega,p}{}^i(t)$, and $s_{\omega,p}{}^i(t)$ can be derived from relationships given in (5.2), (5.3), (5.4) and (5.5).

$$s^i_{\omega,p}(t) = s\left(V^i(t-\Delta t),\ V^i(t),\ s^i_{\omega,p}(t-\Delta t)\right) \quad \textbf{(5.2)}$$

$$n^i_{\omega,p}(t) = n\left(s^i_{\omega,p}(t),\ s^i_{\omega+1,p}(t)\right) \quad \textbf{(5.3)}$$

$$N^i(t) = N\left(\overline{N^i(t-\Delta t)},\ n^i(t)\right) \quad \textbf{(5.4)}$$

$$V^i(t) = V\left(N^i(t)\right) \quad \textbf{(5.5)}$$

Here, $n^i_{\omega,p}(t) = 0$ when $\omega > t$; and "s", "n" and "V" are continuous functions.

The outflow at time "t" on link "i", $w^i(t)$, is also obtained as a function of $N^i(t)$, as given in (5.6).

$$w^i(t) = w\left(N^i(t)\right) \quad \textbf{(5.6)}$$

The speed can be assumed equal for all vehicles on the link, or assigned to each packet at the entry time. In the first case, since it would be $V^i(t) = V(N^i(t))$, the speed of each packet would also depend on the vehicle number behind the packet itself. However, the influence of this assumption on the model is lower as Δt approaches zero ($\Delta t \to 0$). It is worth noting that all existing mesoscopic models suffer from this drawback, since aggregate performances are used. Because of this approximation, the model based on the relationships given by (5.3) changes to (5.7) ($n^i_{\omega,p}(t)$ is only a function of $s^i_{\omega,p}(t)$ and can only have two values).

$$n^i_{\omega,p}(t) = \begin{cases} 0, & \text{if} \quad s^i_{\omega,p}(t) = 0 \\ m_{\omega,p}, & \text{if} \quad s^i_{\omega,p}(t) > 0 \end{cases} \quad \textbf{(5.7)}$$

The latter expressions of the model are given with (5.8)-(5.13).

$$s^i_{\omega,p}(t+\Delta t) = s\left(V^i(t),\ V^i(t+\Delta t),\ s^i_{\omega,p}(t)\right) \quad \textbf{(5.8)}$$

$$n^i_{\omega,p}(t+\Delta t) = \begin{cases} 0, & \text{if} \quad s^i_{\omega,p}(t+\Delta t) = 0 \\ m_{\omega,p}, & \text{if} \quad s^i_{\omega,p}(t+\Delta t) > 0 \end{cases} \quad \textbf{(5.9)}$$

$$n^i(t+\Delta t) = \sum_{p \in P} \sum_{\omega \le t} n^i_{\omega,p}(t+\Delta t) \quad \textbf{(5.10)}$$

$$N^i(t+\Delta t) = N\left(\overline{N^i(t)},\ n^i(t+\Delta t)\right) \quad \textbf{(5.11)}$$

$$V^i(t+\Delta t) = V\left(N^i(t+\Delta t)\right) \quad \textbf{(5.12)}$$

$$w^i(t+\Delta t) = w\left(N^i(t+\Delta t)\right) \tag{5.13}$$

Depending on the physical assumptions, the values of speed and space variables can be calculated as in Eq. (5.14) and Eq. (5.15).

$$V^i(t+\Delta t) = V^i(t) + \left(a^i(t)\cdot\Delta t\right) \tag{5.14}$$

$$s^i_{\omega,p}(t+\Delta t) = s^i_{\omega,p}(t) + V^i(t)\cdot\Delta t + \frac{1}{2}\cdot a^i(t)\cdot\Delta t^2 \tag{5.15}$$

The model given with Eqs. (5.8)-(5.13) is a fixed-point problem with respect to the variable $V^i(t+\Delta t)$, which can be resolved by the Method of Successive Averages [4]. The speed $V^i(t+\Delta t)$ is at first calculated through (5.14). Then, applying the model (Eqs. (5.8)-(5.13)), the speed value is calculated by successive iterations as given in (5.16), where $V_y^i(t+\Delta t)$ is the value of speed $V^i(t+\Delta t)$ at iteration "y".

$$V^i_{y+1}(t+\Delta t) = \left(\frac{1}{y}\cdot V\left(N\left(n\left(s\left(V^i_y(t+\Delta t)\right)\right)\right)\right)\right) + \left(\frac{(y-1)}{y}\cdot\left(V^i_y(t+\Delta t)\right)\right) \tag{5.16}$$

The iteration stops when the difference between two consecutive speed values is not greater than a fixed threshold. Then, the current value of acceleration is calculated as in (5.17) and used as input in successive calculations.

$$a^i(t+\Delta t) = \frac{\left(V^i(t+\Delta t) - V^i(t)\right)}{\Delta t} \tag{5.17}$$

The capacity constraint for the exiting flows requires a comparison between the calculated outflow and the capacity of the link. The number of exiting vehicles from a link is updated, prior to speed calculation given by (5.12) and (5.16), with the relation given by (5.18) in the iterative process of the model:

$$N^i(t+\Delta t) = \begin{cases} \overline{N^i(t)} + n^i(t+\Delta t) & \text{if} \quad \overline{N^i(t)} + n^i(t+\Delta t) \le C^i\cdot\Delta t \\ C^i\cdot\Delta t & \text{if} \quad \overline{N^i(t)} + n^i(t+\Delta t) > C^i\cdot\Delta t \end{cases} \tag{5.18}$$

where C^i denotes the assigned capacity of the link "i".

Figure 5.1 shows the flowchart of the algorithm for a sample generic packet.

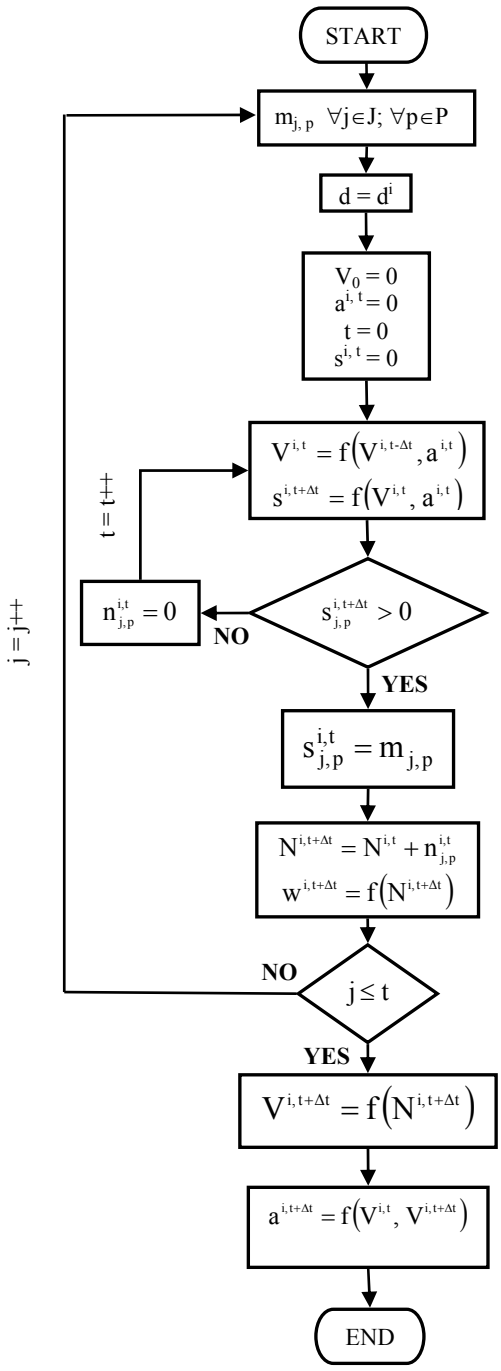

Figure 5.1: Flowchart of Proposed Algorithm for a Sample Generic Packet

The equations (5.8) to (5.15) trace explicitly the movement of vehicles, while the constraint given through (5.18) expresses the link performance in an aggregate way. The proposed model is then definitely a mesoscopic one, according to definitions mentioned in section 3.2.4.

5.1.3. Validity of Link Model

The proposed link model, set out with the series of equations given through (5.8)-(5.17), is now ready to simulate the flow propagation on a link. But first, the validity of the model is explored with the help of a single peak sinusoidal inflow data. Then the model is run with real data and its resulting performance is evaluated in comparison to models of Merchant and Nemhauser [18], Friesz et al. [11], and CONTRAM [125].

5.1.3.1. Validity and Simulation with Theoretical Data

Pre-trials of the investigated algorithm were carried out on a link 4 km long and having a capacity of 4400 veh/h. To test the efficiency of the proposed model in tackling over-saturation states, the maximum inflow was assigned as 6120 veh/h. Time was discretised into one second intervals. In over-saturation conditions, the queue spillback for the link under examination was simulated assuming the existence in the initial node of a buffer area, for the temporary storage of vehicles exceeding the maximum density. Therefore, in this case constraints on the density were not assigned on purpose. Furthermore, to avoid circulation blockage, a creeping speed of 10 km/h was assumed when the density exceeded the maximum.

In under-saturation conditions, the Greenshields [45] speed-density relationship (5.19) is applied to compute speed value, $V^i(t)$, of each packet by substituting the value of free flow speed on link "i", VF^i, given by (5.20), and the average density $k^i(t) = N^i(t)/d^i$; k^i_{max} is the maximum density on the link "i". The resulting equation is (5.21).

$$V^i(t) = VF^i\left(1 - \frac{k^i(t)}{k_{max}}\right) \qquad \textbf{(5.19)}$$

$$VF^i = 4 \cdot \frac{C^i}{k^i_{max}} \qquad \textbf{(5.20)}$$

$$V^i(t) = 4 \cdot \frac{C^i}{k^i_{max}} \cdot \left(1 - \frac{N^i(t)}{d^i \cdot k_{max}}\right) \qquad \textbf{(5.21)}$$

The resulting outflow diagrams are represented and compared in Figure 5.2 and Figure 5.3 with the results obtained using some existing macroscopic and

mesoscopic models. As for macroscopic simulation, two space-discrete models were considered: one, with an exit link formulation [18, 19], even though this model suffers from the drawbacks already described; and another one, with a travel time formulation [11]. In the first case, equations (4.7) and (4.9) were used to calculate the number of vehicles on the link. We've chosen the exit link function W(n) according to the authors' assumptions: W(n) should be a non-decreasing, continuous, concave function with respect to (4.6) [18, 19]. Therefore, a suitable function is given in (5.22) (see Appendix A for a detailed explanation on the selected arbitrary function).

$$W(n) = \frac{k^i_{max} d^i}{3} \cdot \left(1 - e^{-\frac{n}{\frac{k^i_{max} \cdot d^i}{3}}} \right) \qquad \textbf{(5.22)}$$

In the second case, equation (4.25) was used to calculate the travel time on the link, assuming the following linear formulation for $T(n^i(t))$ given in (5.23).

$$\tau^i(t) = \alpha + \beta\left(n^i(t)\right) = \frac{d^i}{VF^i} + \frac{d^i}{VF^i \cdot n^i_{max}}\left(n^i(t)\right), \ \alpha = \frac{d^i}{VF^i}, \ \beta = \frac{d^i}{VF^i \cdot n^i_{max}} > 0 \qquad \textbf{(5.23)}$$

In both cases, d^i, k^i_{max}, n^i_{max}, and VF^i were respectively the length of the link "i", the maximum density, the maximum number of vehicles, and the free-flow speed on the link "i", as denoted above. Then, it was possible to calculate the value of exiting units.

As for mesoscopic models, we considered the CONTRAM model, and used the educational package [125]. All these models were tested on the same link and with the same characteristics.

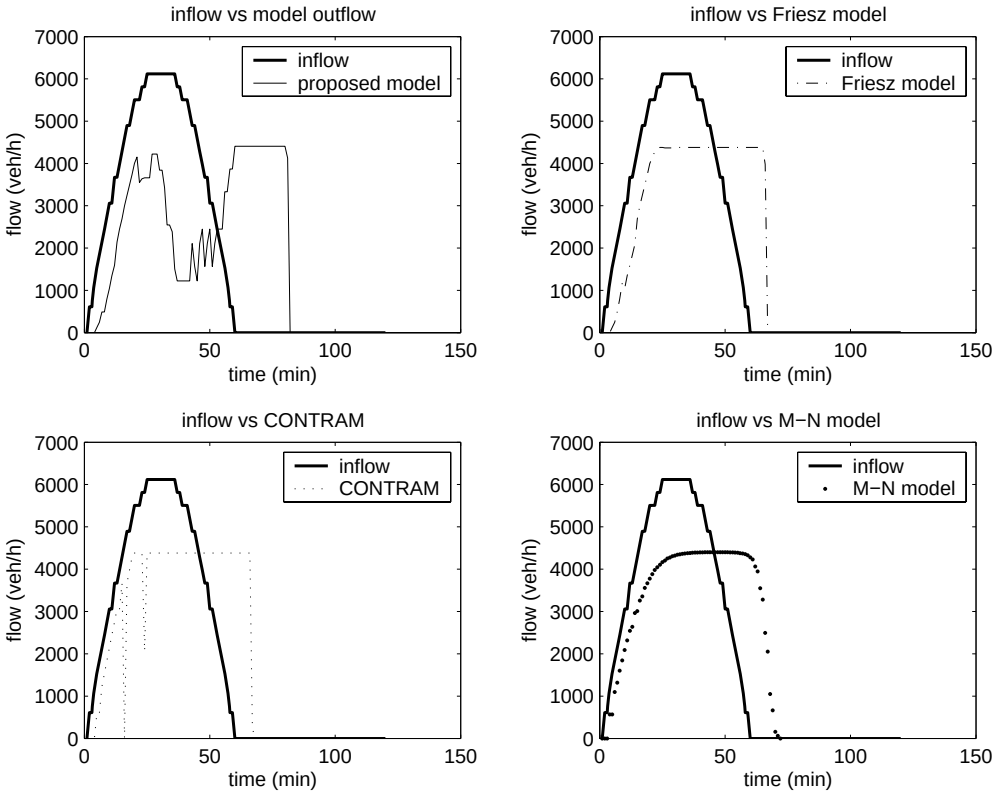

Figure 5.2: Separate Comparison of Theoretical Inflow and Outflow Diagrams in Over-saturation Condition

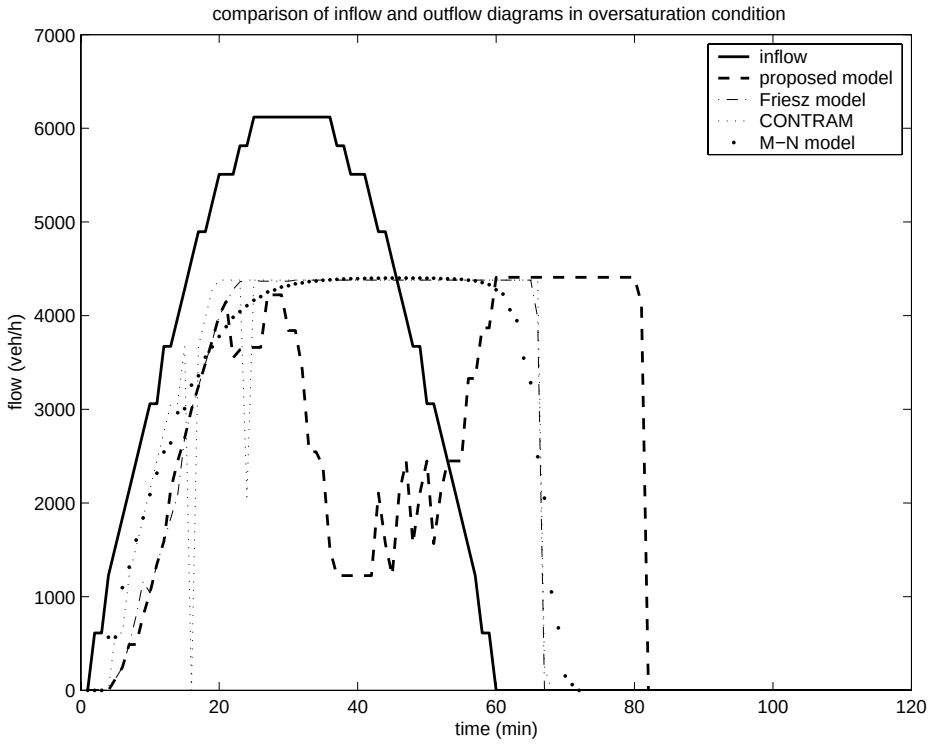

Figure 5.3: Overall Comparison of Theoretical Inflow and Outflow Diagrams in Over-saturation Condition

Simulation for the proposed model with theoretical data required a longer simulation time than the other models, due to lower level of outflow reached in over-saturation conditions. In fact, from Figure 5.3 it can be seen that after 21 minutes the outflow calculated through the proposed model reaches the saturation, and then decreases rapidly to around 1200 veh/h, while the outflow calculated through other models remains at the capacity value. This different behaviour of the proposed model seems intuitively more correct, due to effects of congestion, and has been captured by considering acceleration. The relationships between traffic flow characteristics were plotted in order to evaluate the behaviour and the robustness of the simulated models. Two fundamental diagrams of traffic flow, flow-density and speed-flow, have been plotted in Figure 5.4 and Figure 5.5 respectively, to show the closeness to the theoretical curve of the compared models and their deviations from it.

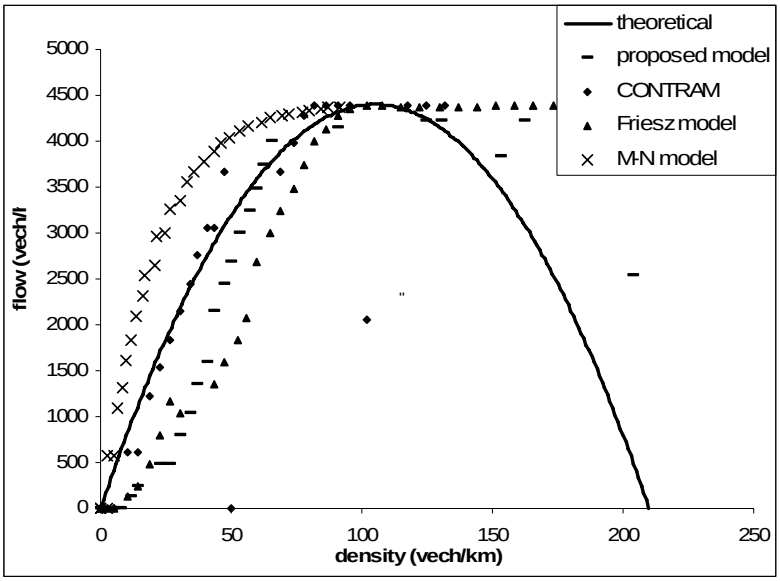

Figure 5.4: Flow-density Diagrams (theoretical data)

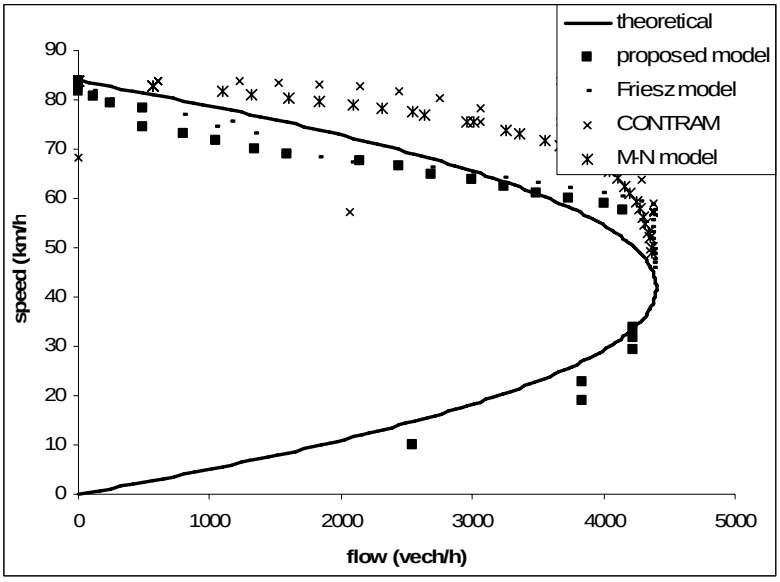

Figure 5.5: Flow-speed Diagrams (theoretical data)

From Figure 5.4 and Figure 5.5, it can clearly be seen that the proposed model seems to be able to tackle over-saturation phenomena by responding to saturation state. The values generated in this condition prove the model's capacity constraint, robustness, and proper processing. The model is then ready to run with the assignment of real data.

5.1.3.2. Validity and Simulation with Real Data

The proposed algorithm was applied to simulate the flow propagation along a section of the Bosporus Bridge in Istanbul (Türkiye), considering the traffic volumes at the entrances and exit of the bridge on the Anatolian side, and the start point of a tidal flow lane and the bridge exit on the European side (data is collected by Ass. Prof. Dr. İsmail Şahin) [126]. The bridge has 3 lanes, which are all 4 km, in each direction, plus an additional tidal lane. The selected link has a capacity of 8700 veh/h, and a maximum density of 600 veh/km. Figure 5.6 reproduces a schematic section of the bridge [126].

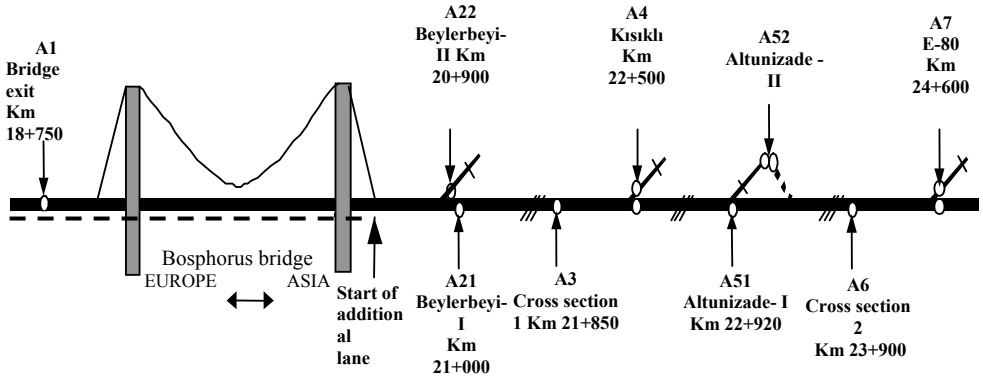

Figure 5.6: Schematic Representation of the Bosporus Bridge [126]

Some statistical performance criteria were calculated for the outcomes of the simulations to measure the closeness of both the proposed algorithm and the previously mentioned models to the field data. The criteria chosen in this case were the root mean square percent error (RMSPE), and the coefficient of determination (R^2) (see Appendix B for the mathematical expressions of RMSPE and R^2). A comparison of the proposed model to referred existing models was carried out at the same time.

Comparisons of resultant outflows with the actual outflow are represented by diagrams in Figure 5.7 and Figure 5.8.

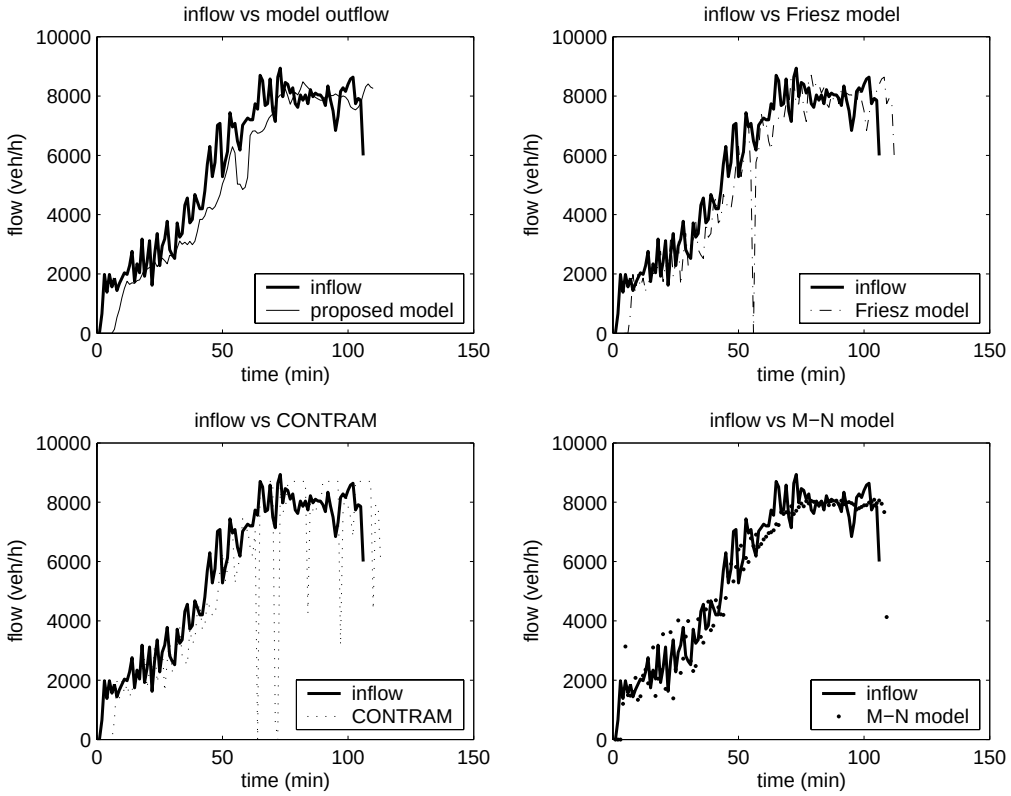

Figure 5.7: Separate Comparisons of Actual Outflow and Resultant Outflow Diagrams

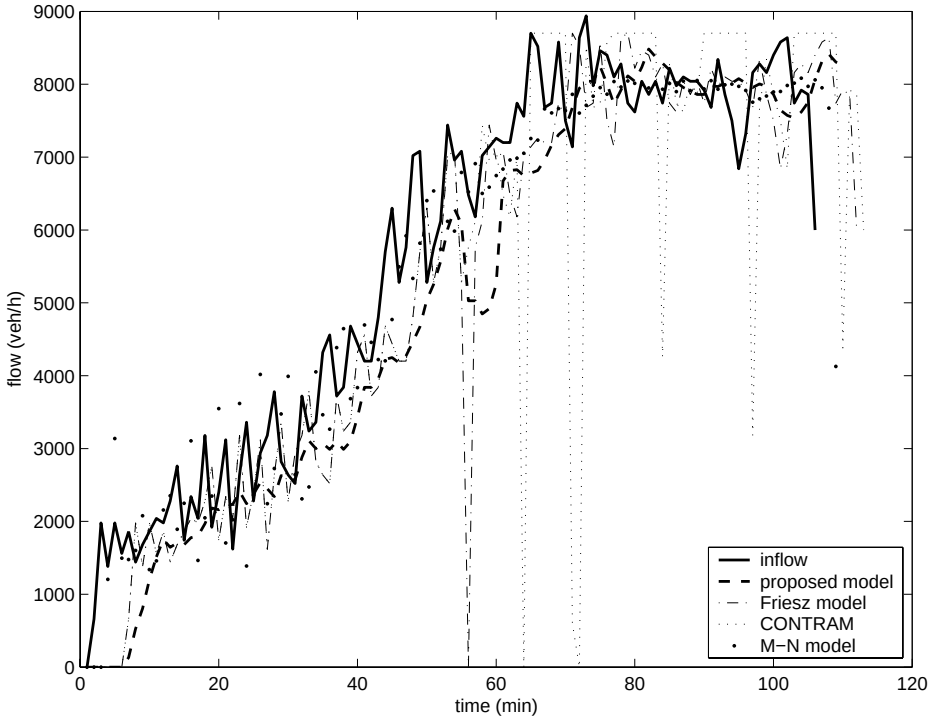

Figure 5.8: Comparison of Actual Outflow and Resultant Outflow Diagrams

The closeness of the outcomes, obtained from the models compared and corresponding to actual outflow observations, was evaluated in terms of two selected statistical performance criteria and the simulation time shown in Table 5.1.

Table 5.1: Selected Performance Criteria Values on Models

	coefficient of determination	RMSPE* (%)	simulation time (min)
Proposed model	0.921	27.510	110
Merchant - Nemhauser model	0.951	18.838	109
Friesz model	0.869	28.203	112
CONTRAM	0.716	32.199	113

* Root Mean Square Percent Error

The proposed model had quite satisfactory performance in terms of statistics, especially in comparison to the Friesz and CONTRAM models. Only the Merchant-Nemhauser model shows better performances in under-saturation conditions but, among other ones, also this model fails to tackle over-saturation conditions, as shown in figures 5.3, 5.4, and 5.5.

The flow-density and speed-flow diagrams have been plotted in Figure 5.9 and Figure 5.10 respectively to present the performances of the considered models with respect to a theoretical base.

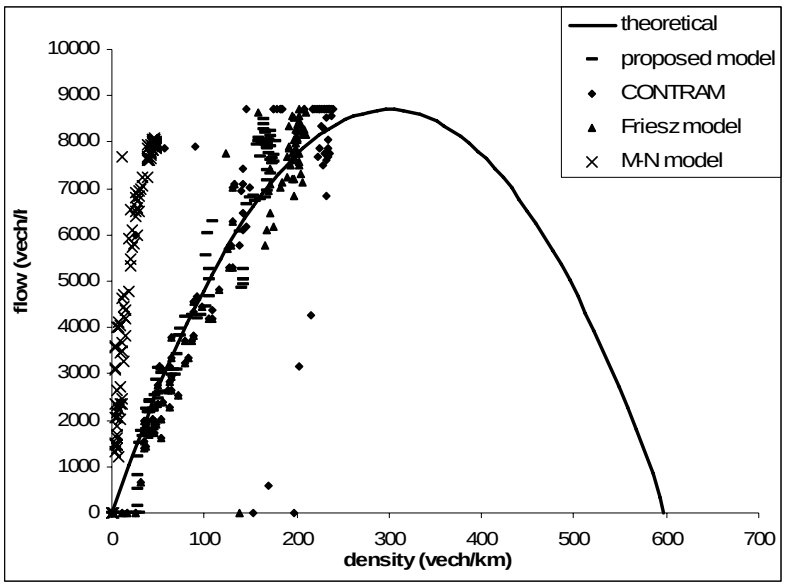

Figure 5.9: Flow-density Diagrams with Real Data

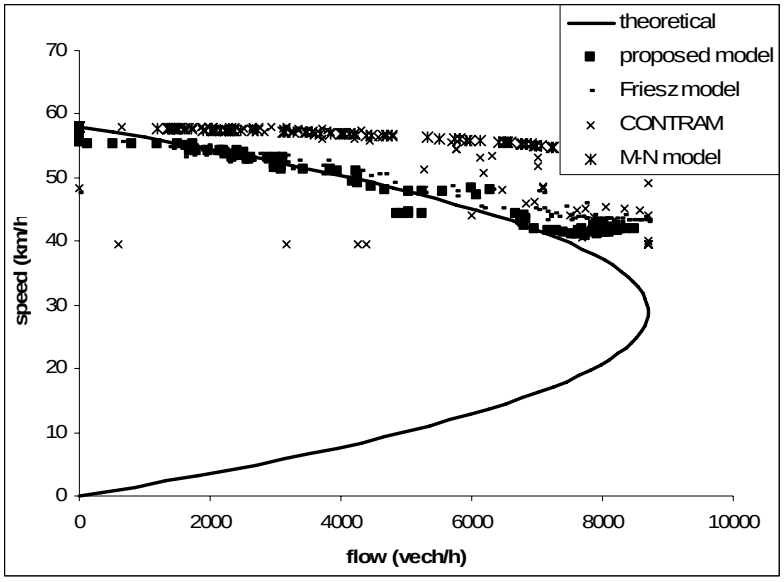

Figure 5.10: Flow-speed Diagrams with Real Data

The behaviour of the capacity constraint model was evaluated with a number of critical terms from the simulations. The maximum outflow and the minimum speed, computed during the model runs, also allow the calculation of the maximum available density. These values, as well as the rate of capacity used (q_{MAX}/C), are given in Table 5.2. The acceleration behaviours depicted after simulations with real data are presented in Fig 5.11. The maximum, minimum and the average values of acceleration behaviour simulated with different models are presented in Table 5.3.

Table 5.2: Critical Values of Flow Characteristics Calculated with Real Data

	maximum outflow $\mathbf{q_{MAX}}$ (veh/h)	minimum speed $\mathbf{V_{MIN}}$ (km/h)	maximum density $\mathbf{q_{MAX}/V_{MIN}}$ (veh/km)	$\mathbf{q_{MAX}/C}$	travel time (min)
Proposed model	8484	40.90	207	0.98	110
Merchant-Nemhauser model	8085	53.30	152	0.93	109
Friesz model	8700	42.94	203	1.00	112
CONTRAM	8700	39.50	221	1.00	113

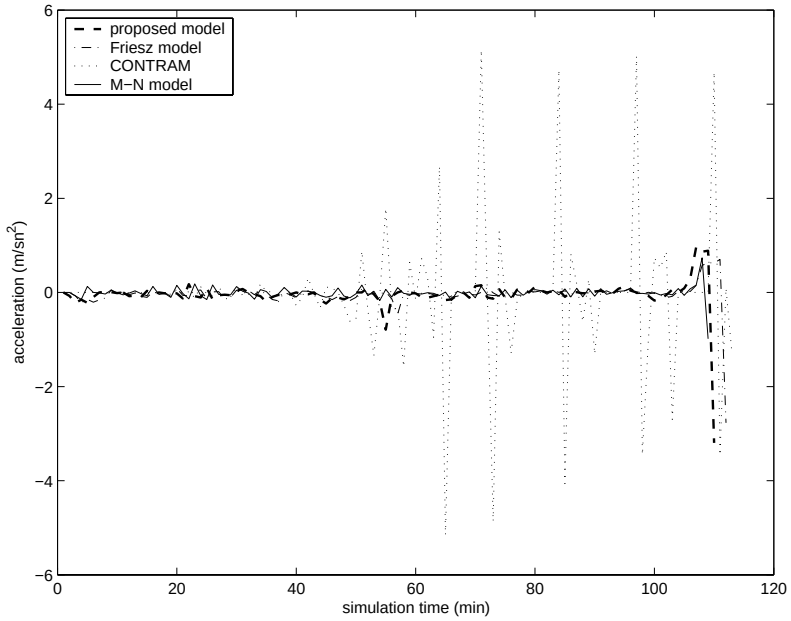

Figure 5.11: Comparison of Calculated Acceleration (real data)

Table 5.3: Critical Acceleration and Deceleration Values Computed with Real Data

	acceleration (m/sec^2)			deceleration (m/sec^2)		
	max	min	avg	max	min	avg
Proposed model	0.967	0.001	0.149	3.196	0.013	0.156
Merchant - Nemhauser model	0.735	0.001	0.087	0.984	0.008	0.074
Friesz model	0.702	0.004	0.098	2.770	0.004	0.116
CONTRAM	5.153	0.001	0.934	5.153	0.001	0.788

Referring to Figure 5.11 and Table 5.3, it's clear that the acceleration behaviour encountered after CONTRAM runs is not realistic since the maximum values experienced more than 5.00m/sec^2.

Simulation results imply that the proposed model performed somewhat better than CONTRAM and Friesz models in determining link outflows (Figure 5.7 and Table 5.1). The Merchant - Nemhauser model had the highest minimum speed (53 km/h) and the lowest maximum density, while the proposed model, since the link capacity is reached during the simulation, returned some speed values equal to the assigned creeping speed (10 km/h). From Figure 5.8 and Figure 5.12 it can be clearly seen that the proposed model is the only one capable both to fit the real data and to reach the creeping speed in case of over-saturation. Thus, it can be stated that the proposed algorithm could return accurate outputs even in congested conditions. Considering the critical values of traffic flow characteristics (Table 5.2), the performances of the

proposed model are of the same level, if not somewhat better, than the other existing models. The speed curves obtained after model runs with real data are presented in Figure 5.13.

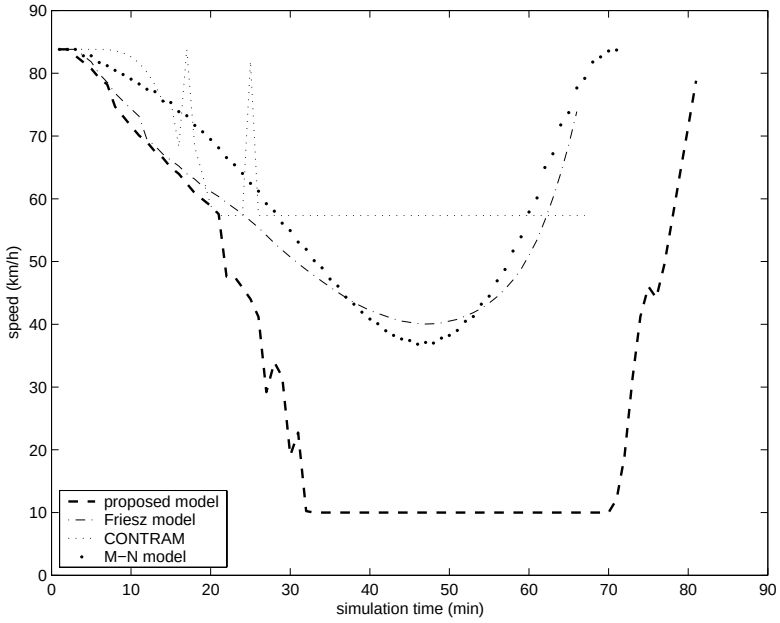

Figure 5.12: Comparison of Calculated Speed (theoretical data)

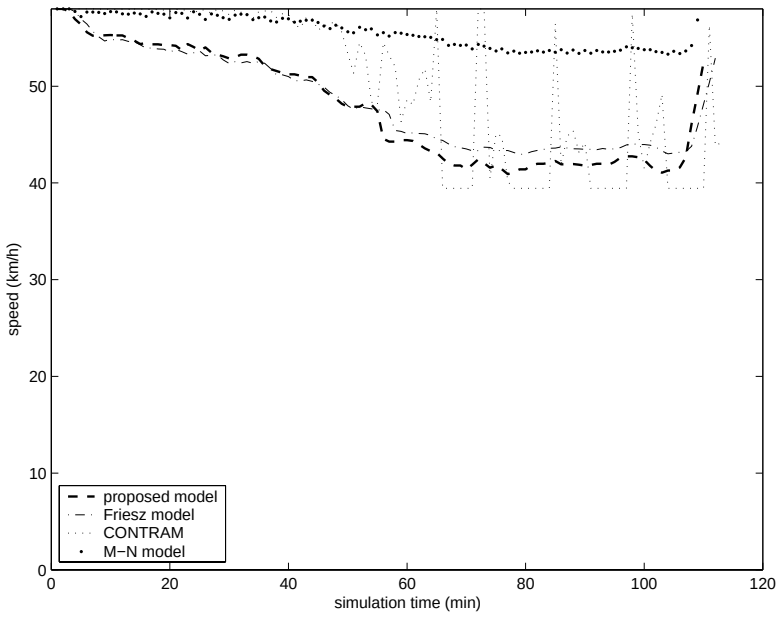

Figure 5.13: Comparison of Calculated Speed (real data)

Since the proposed link model explicitly considers acceleration behaviour, the travel times obtained in over-saturation condition (Figure 5.14) are higher in comparison to

Friesz and M-N models, which demonstrate the simulation ability of model's real life.

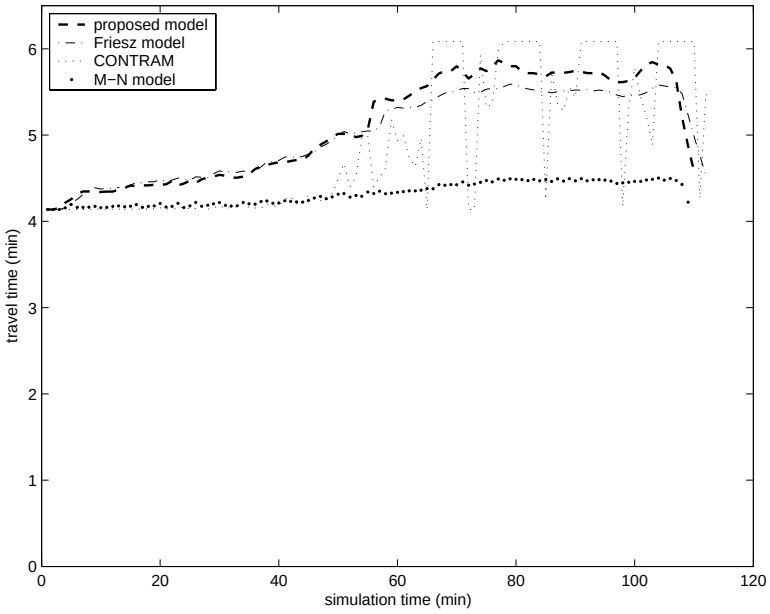

Figure 5.14: Comparison of Travel Times (real data)

5.2. Node Component

Simulation of traffic demand on a network initially requires the determination of merging and diverging flows at a node. During structuring the DNM by node rule definitions, it is assumed that there are nodes at both at the beginning and at the end of the links. This is equal to saying that a link begins where another ends (Figure 5.15). In this section, the node component is set out for a single node to seek the appropriate and accurate integrate model structure for modelling flow propagation.

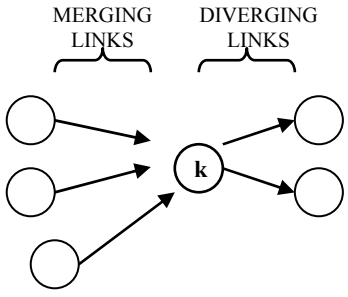

Figure 5.15: A Sample Highway Node

5.2.1. Basic Notations for Node Component

The variables, with their notations, of the node algorithm coded for the proposed DNM are given below.

- FW_k : The set of links that are diverging from a node "k".
- BW_k : The set of links that are merging to a node "k".
- i : A link included in the set of merging links to node "k" ($i \in BW_k$).
- r : A link included in the set of diverging links from node "k" ($r \in FW_k$).
- $w^{ik}(t)$: The exiting flow from link "i" that enters node "k" at time "t" ($i \in BW_k$).
- $u^{kr}(t)$: The total flow entering to link "r" at time "t", which exits from node "k" at time "t" ($r \in FW_k$).
- $w^{ikr}(t)$: The partial flow requiring to enter link "r" at time "t", which exits from link "i" at time "t" ($i \in BW_k$ ve $r \in FW_k$).
- $\delta^{ik}(t)$: The total demand that is present from link "i" at time "t" ($i \in BW_k$ and $r \in FW_k$).
- $\delta^{ikr}(t)$: The partial demand that is present from link "i" to link "r" at time "t" ($i \in BW_k$ and $r \in FW_k$).
- $u^{ikr}(t)$: The partial flow entering link "r" at time "t", which exits from link "i" at time "t" ($i \in BW_k$ and $r \in FW_k$).
- $\sigma^{kr}(t)$: The total supply (capacity) of link "r" at time "t" ($i \in BW_k$ and $r \in FW_k$).
- $\sigma^{ikr}(t)$: The partial supply of link "r" allocated to link "i" at time "t" ($i \in BW_k$ and $r \in FW_k$).
- C^r : The capacity of link "r" ($r \in FW_k$).
- $PQ^r(t)$: The total number of vehicles that are stored in the point-queue at the entrance of link "r" at time "t" ($r \in FW_k$).
- $f^r(t)$: The congestion value that exists due to the capacity constraint and present point-queue on link "r" at time "t" ($r \in FW_k$).

- $G^r(t)$: The delay that occurs due to the capacity constraint and present point-queue on link "r" at time "t" ($r \in FW_k$).
- λ^{ir} : The partial flow splitting rate from a merging link "i" to a diverging link "r" ($i \in BW_k$ and $r \in FW_k$).

5.2.2. Node Component Rules and Constraints

The node rules component of the presented DNM contains another set of constraints considering the flow conservation principle, diverging link capacities and splitting rates at a node in addition to the present constraints previously defined for the link model component. The main difference of the proposed DNM in comparison to other models is that it respects capacity constraints regarding to splitting rules and consequently holds FIFO rule. As previously defined in section 5.1, for a point-queuing assumption is made for the whole integrated model structure, the delays calculated in the presence of these vertical queues are considered instead of the physical queues. A point-queue (PQ) at the entrance of a diverging link is present only if one of the events given below exists:

- If the total flow requiring to enter a diverging link exceeds this link's capacity;
- If there is any amount of exceeding flow obtained by the computation for the previous time interval, depending on to time discretisation to have a solution for the formulation.

Delays due to flow states on each diverging link have been calculated with the conical delay function proposed by Spiess [127]. The calculated delays are assumed to be solely dependent to the diverging link capacities. It is assumed that there becomes no delay as a result of flow conflicting. So, the partial flows exiting from merging links are considered to traverse junction area without any loss. This assumption is consistent, since the sample junction is unsignalized and therefore no specific control action is sought. Moreover, the relative increase or decrease on total delays calculated as (Delay due to flow conflict)+(Delay due to flow condition) do not have significant deviations in comparison to the case that delays due to flow conflict are not considered. The partial splitting rates from merging links to diverging ones are assumed to be known while coding the algorithm for DNM. This is

extended to known path flows in the sample network model application, given in section 7.1.

In this section, the nodal splitting rules and constraints are introduced. Note that since the sample node is a single one and, hence, there is no path flow, the flow rates $u^{ikr}(t)$ and $w^{ikr}(t)$ are equal to the partial supply and demand rates, respectively as given in (5.24) and (5.25). The first constraint is the non-negativity of the partial flow entering link "r" at time "t", which exits from link "i" at time "t" and the partial flow requiring to enter link "r" at time "t", which exits from link "i" at time "t".

$$\sigma^{ikr}(t) = u^{ikr}(t) \geq 0, \quad \forall i \in BW_k \text{ and } \forall r \in FW_k \tag{5.24}$$

$$\delta^{ikr}(t) = w^{ikr}(t) \geq 0, \quad \forall i \in BW_k \text{ and } \forall r \in FW_k \tag{5.25}$$

A constraint derived from diverging link capacity is that the total flow attempting to enter link "r" at time "t" (also given in (5.26)) can be equal at most to the capacity of link "r", as given in (5.27).

$$u^{kr}(t) = \sum_{i \in BW_k} w^{ikr}(t) \quad \forall i \in BW_k \text{ and } \forall r \in FW_k \tag{5.26}$$

$$u^{kr}(t) \leq C^r \qquad \forall r \in FW_k \tag{5.27}$$

Regarding to flow conservation principle, the total flow attempting to enter all diverging links at time "t" can be at most equal to the amount of total flows exiting from the whole merging links at time "t". This inequality constraint given with (5.28) turns out to an equality constraint when the finite modelling time horizon is considered.

$$\sum_{r \in FW_k} u^{kr}(t) \leq \sum_{i \in BW_k} w^{ik}(t) \tag{5.28}$$

Respecting to capacity constraint and above mentioned delay assumption, the total flow attempting to enter all diverging links can be determined from (5.29).

$$\sum_{r \in FW_k} u^{kr}(t) = \begin{cases} \sum_{i \in BW_k} w^{ik}(t), & \text{if} \quad \sum_{i \in BW_k} w^{ik}(t) \leq \sum_{r \in FW_k} C^r \\ \sum_{r \in FW_k} C^r, & \text{if} \quad \sum_{i \in BW_k} w^{ik}(t) > \sum_{r \in FW_k} C^r \end{cases} \tag{5.29}$$

When the whole process to model the node is considered as the modelling horizon [0, T_∞], the inequality constraint given with (5.28) turns out to an equality constraint to hold, as given in (5.30).

$$\sum_{t=0}^{T}\sum_{r\in FW_k} u^{kr}(t) = \sum_{t=0}^{T}\sum_{i\in BW_k} w^{ik}(t) \qquad t\in[0,T] \tag{5.30}$$

Respecting to the point-queuing assumption that is made both in link model and for node rules, the amount of the flow that can not enter a diverging link due to capacity constraint is stored virtually in the vertical plane dimension at the entrance of this link. The length of a possible PQ at the entrance of a diverging link is equal to the total number of vehicles that can not enter the link. This PQ can be determined by assuming that there is no initial queue when t=0, as given in (5.31).

$$PQ^r(t) = \begin{cases} 0, & \text{if } (t=0) \vee \left(u^{kr}(t) + \dfrac{PQ^r(t-\Delta t)}{\Delta t} \le C^r \right) \\ \left(u^{kr}(t) - C^r\right)\cdot\Delta t + PQ^r(t-\Delta t), & \text{if } u^{kr}(t) + \dfrac{PQ^r(t-\Delta t)}{\Delta t} > C^r \end{cases} \tag{5.31}$$

Delays that occur due to capacity constraint have been represented with varying types of flow-rate delay functions proposed and applied in the past [128]. These functions G(·) are usually expressed as the product of the free-flow time, the minimum time to traverse a link "r", by a normalized congestion function f(η), as given in Eq. (5.32) [129]:

$$G^r\left(\eta^r(t)\right) = t^r{}_{free-flow}\cdot f\left(\eta^r(t)\right) \tag{5.32}$$

where, the argument of delay function $G^r(\cdot)$ of a link "r" is the ratio flow-volume/capacity $\eta^r(\cdot)$ on link "r" (see Appendix C for a detailed explanation on the delay functions). Dependent on the vertical queuing process, the volume is considered as inflow $u^{kr}(t)$ requiring to enter a diverging link in our case. The conical congestion function used in this study to model delays on diverging links has the desired properties of a delay function (see Appendix C for a detailed explanation on the conical delay function) and have the form given in (5.33), which is proposed by Spiess [127]:

$$f\left(\frac{u^{kr}(t)}{C^r}\right) = 2 + \sqrt{a^2\left(1-\frac{u^{kr}(t)}{C^r}\right)^2 + b^2} - a\left(1-\frac{u^{kr}(t)}{C^r}\right) - b \qquad \textbf{(5.33)}$$

where, "b" is given as b=(2a-1)/(2a-2). Parameter "a" is any number larger than 1 and defines how sudden the congestion effects change when the capacity is reached. So a unique and constant value, 2, is selected for the computation of all diverging link dynamics to have a comparison on the same base.

Considering the necessity of PQ assumption made in the proposed DNM, delay due to capacity constraint at a diverging link entrance at time "t" is represented by the congestion value $f^r(t)$ as given in (5.34).

$$f^r(t) = \begin{cases} 0, & \text{if } PQ^r(t) = 0 \\ f\left(\eta^r(t)\right), & \text{if } PQ^r(t) > 0 \end{cases} \quad \forall r \in FW_k \text{ and } t \in [0, T] \qquad \textbf{(5.34)}$$

$f^r(t)$ is the congestion value and delay at time "t" can be calculated by multiplying this value with free-flow travel time as given in (5.32).

There are two kinds of splitting factors that can be used in system dynamics, which are path based and link based. Path based splitting is given as ratio of the destination based flow on a link out of a node and the total flow from the same node to the same destination. Link based split factor input takes the ratio of the flow into a link "r" from a node "k" and the total flow from the same node. Since the path based split factors are considered in the network assignment context, the link based split rates are appropriate in modelling a single node and are used in the node modelling section of this study.

Since it is impossible to channelise the users that will exit from a merging link $i \in BW_k$ and will require to enter a diverging link $r \in FW_k$ to another diverging link, the splitting factors are processed as constants. These split factors are calculated assuming that we have information on the currently transferred flow volumes between BW_k and FW_k link sets. The splitting rate λ^{ir} for a flow that is split from a merging link "i" to a diverging link "r" is calculated as given in (5.35). The constraint associated with this splitting factor inputs considering the conservation principle is given by (5.36). Considering (5.36), it is seen that the FIFO rule holds.

$$\lambda^{ir} = \frac{\sigma^{ikr}(t)}{\delta^{ik}(t)}, \qquad \lambda^{ir} \geq 0 \tag{5.35}$$

$$\sum_{r \in FW_k} \lambda^{ir} = 1 \tag{5.36}$$

When the capacity constraint on diverging links is considered, the relations given with (5.35) and (5.36) change and λ^{ir} is calculated for two different conditions, under-saturation and over-saturation, as given in (5.37).

$$\lambda^{ir} = \begin{cases} \dfrac{\sigma^{ikr}(t)}{\delta^{ik}(t)}, \text{if } u^{kr}(t) = \sum\limits_{i \in BW_k} w^{ikr}(t) \leq C^r \\ \dfrac{C^r}{\delta^{ik}(t)}, \text{if } u^{kr}(t) = \sum\limits_{i \in BW_k} w^{ikr}(t) > C^r \end{cases} \quad \forall i \in BW_k,\ \forall r \in FW_k \text{ and } \lambda^{ir} \geq 0 \tag{5.37}$$

Constraint given in (5.36) is valid if the total flow entering to a diverging link does not exceed the capacity of this link. Otherwise, constraint given in (5.38) should hold.

$$\sum_{r \in FW_k} \lambda^{ir} \leq 1 \tag{5.38}$$

5.3. Integrated Structure of Proposed Dynamic Node Model

The whole structure of the model is obtained by integrating the link model component, whose theoretical basis is given in section 5.1.1, to the node component, examined in section 5.2.2, to set out a DNM that can be utilized in DNL studies. Before the integration, the link model, performance evaluation of which is had for a single link, is updated to provide outflow computation when multiple links are considered. Then, the theoretical basis for node component is set out. The entire process beginning with dynamic inflow initialization to merging links and ending with dynamic outflow computation is coded in the purpose of evaluating the validation and the applicability of the proposed DNM.

The proposed model is set out to model flow propagation through a node by considering an objective function. The objective is maximizing the total flow passing through the node (given in (5.39)) subject to the constraints given in the previous section; (5.24), (5.25), (5.27), (5.28), (5.29), (5.30), (5.37) and (5.38).

$$\max\left\{\sum_{t\in T}\sum_{i\in BW_k}\sum_{r\in FW_k} u^{ikr}(t)\right\} \quad \textbf{(5.39)}$$

The modelling is done with adding the constraints on the objective function to node component as well as the splitting rates, queuings, delays and conservation rules. The flow propagation is modelled within the newly proposed simulation process, respecting to (5.30) in the modelling horizon.

5.4. Validity of Dynamic Node Model

In this section, the performance of the proposed DNM is evaluated within the predefined node rules and dynamic traffic flow loadings. The validity of the DNM is evaluated on a sample node with the configuration of four varying flow conditions and link characteristics.

5.4.1. Sample Node Configurations

The sample node structure is set out with four merging and three diverging links. The performance of the proposed DNM is explored under four different node configurations that are set up to simulate over-saturation condition. For the proposed model is set out to model flow propagation at a single node, the flow splitting factors are assumed to be known with the information on path flows. Therefore, these factors (Table 5.4) are assumed to be constant and same for all of the sample node configurations in under-saturation condition. In over-saturation condition, the factors are updated upon the allowable flow rates regarding to capacity constraints.

Table 5.4: Splitting Factors for Sample Node Configurations

	DL1	DL2	DL3
ML1	0.5	0.25	0.25
ML2	0.4	0.3	0.3
ML3	0.2	0.3	0.5
ML4	0.6	0.2	0.2

5.4.1.1. First Configuration

The link and the flow characteristics of the first sample configuration are given in Table 5.5.

Table 5.5: Link and Flow Characteristics of First Configuration

	ML1	ML2	ML3	ML4
Length (km)	4	6	8	7
Capacity (veh/h)	3000	4000	5000	3500
Maximum flow rate (veh/h)	3600	5040	6120	4320
Maximum density (veh/km)	180	200	220	190
Creeping speed (km/h)	12	10	8	11
Free-flow speed (km/h)	67	80	91	74

The time-varying inflows $u^i(t)$ to merging links are generated theoretically to fit single-peak sinusoidal curve as shown in Figure 5.16. Relationships between the dynamic loadings of merging links are given with (5.40).

$$u^1(t) = \frac{u^2(t)}{1.4} = \frac{u^3(t)}{1.7} = \frac{u^4(t)}{1.2} \qquad \textbf{(5.40)}$$

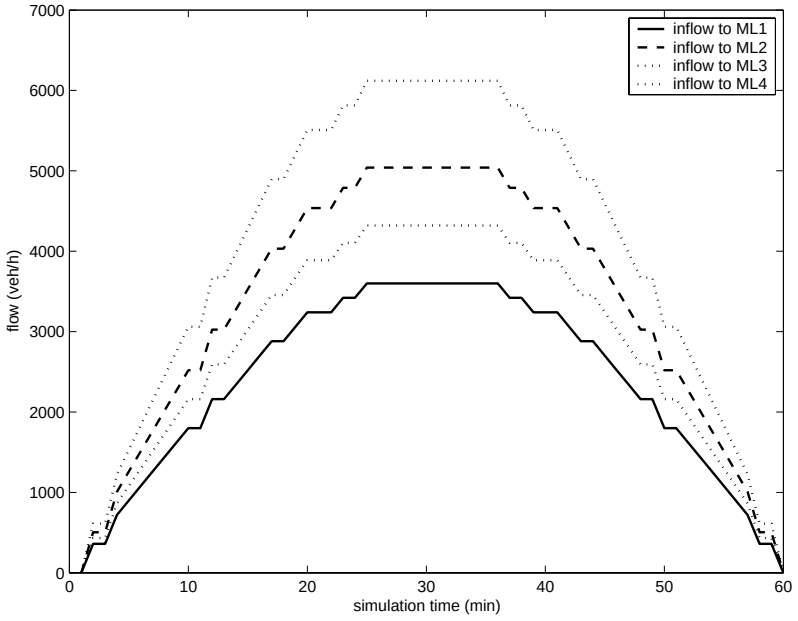

Figure 5.16: Time-varying Traffic Loaded to Merging Links within First Configuration

The simulation times needed to discharge the dynamic loadings completely from merging links are given in Table 5.6.

Table 5.6: Times Needed for Link Model Component Simulations within First Configuration

	ML1	ML2	ML3	ML4
Simulation time (min)	68	85	69	71
CPU time (sec)	0.156	0.14	0.063	0.078

The time-varying outflows $w^i(t)$ computed by the link model component of the proposed DNM are plotted with the corresponding inflows as shown in Figure 5.17.

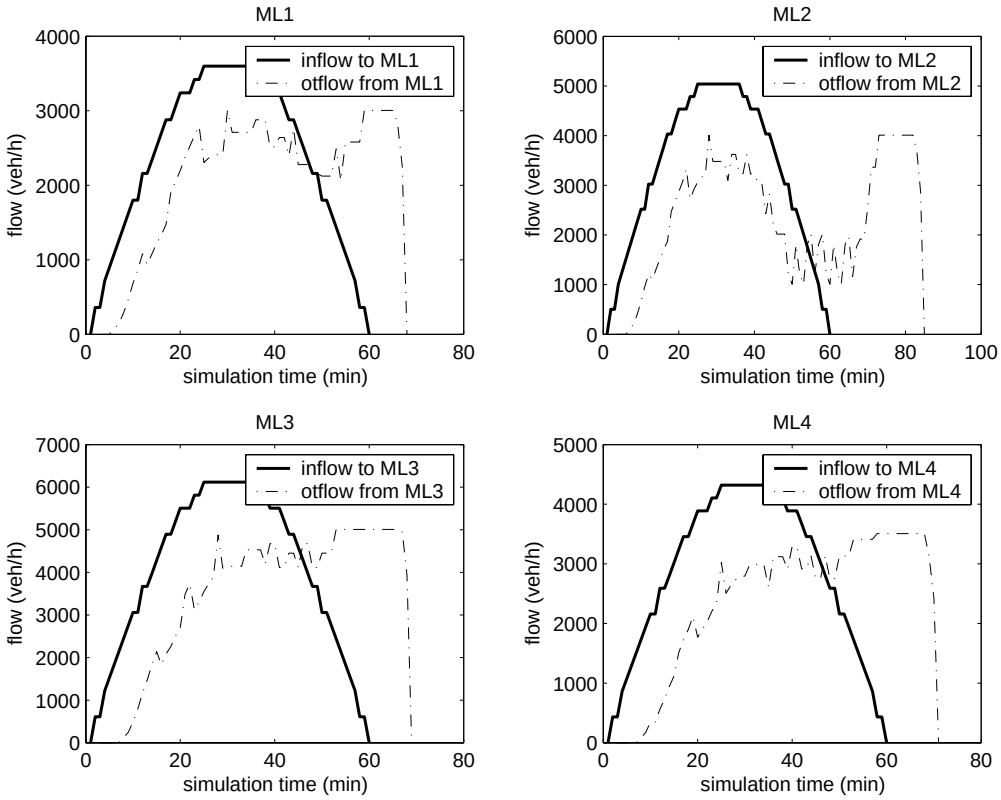

Figure 5.17: Outflows, Computed with Link Model Component, with Corresponding Inflows within First Configuration

The inflows $u^r(t)$ that are entering to diverging links computed with DNM runs are shown in Figure 5.18.

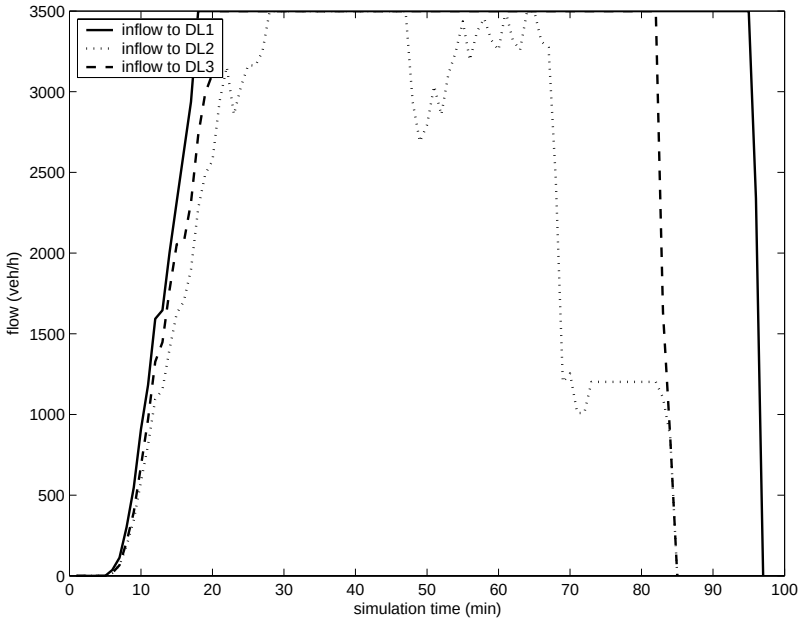

Figure 5.18: Inflows to Diverging Links Computed with DNM within First Configuration

Some critical values, capacity C^r and maximum inflow rate attempting to enter w^{kr}_{max}, and simulation times of diverging links are given in Table 5.7.

Table 5.7: Critical Values and Required Simulation Times on Diverging Links in First Configuration

	DL1	DL2	DL3
Capacity (veh/h)	3500	3500	3500
w^{kr}_{max} (veh/h)	7632	5112	6336
Simulation time (min)	97	85	85

The point-queues, $PQ^r(t)$, formed at the entrance of diverging links are shown in Figure 5.19.

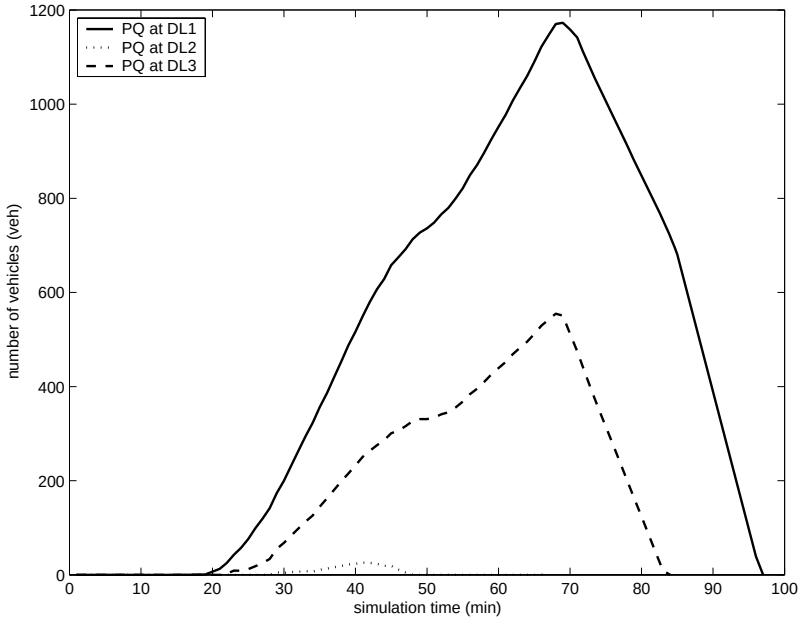

Figure 5.19: Point-queues at Entrance of Diverging Links in First Configuration

The delays on diverging links $G^r(t)$, occurring due to capacity constraints, are shown in Figure 5.20. Since the free-flow time is constant, the congestion values calculated with the conical congestion function (see Eq. (5.33) and (5.34) in section 5.2.2) are considered to represent delays.

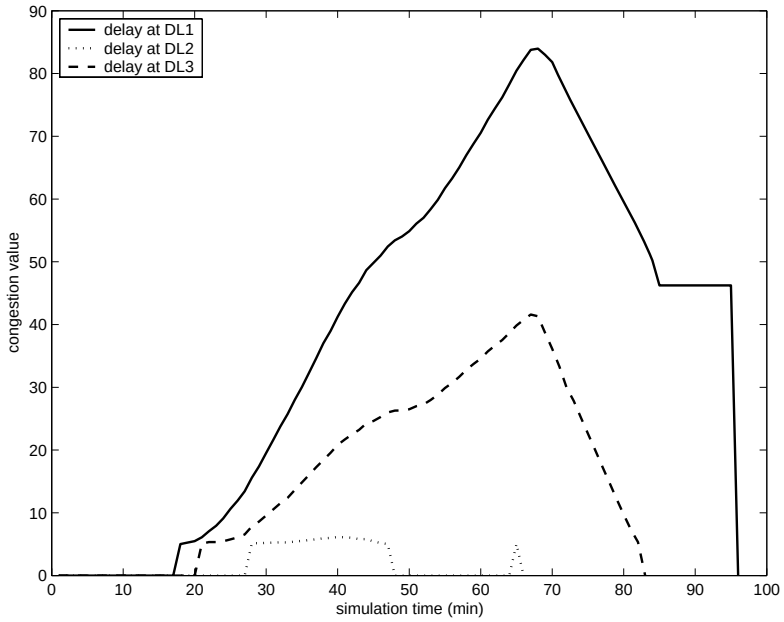

Figure 5.20: Delays on Diverging Links in First Configuration

5.4.1.2. Second Configuration

The link and the flow characteristics of the second sample configuration are given in Table 5.8.

Table 5.8: Link and Flow Characteristics of Second Configuration

	ML1	ML2	ML3	ML4
Length (km)	4	4	4	4
Capacity (veh/h)	3000	4900	6000	4000
Maximum flow rate (veh/h)	3600	5040	6120	4320
Maximum density (veh/km)	180	210	240	195
Creeping speed (km/h)	12	10	8	11
Free-flow speed (km/h)	67	93	100	82

The time-varying inflows $u^i(t)$ to merging links, generated theoretically to fit single-peak sinusoidal curve, are same as loaded for the first configuration and previously shown in Figure 5.16.

The simulation times needed to discharge the dynamic loadings completely from merging links are given in Table 5.9.

Table 5.9: Times Needed for Link Model Component Simulations within Second Configuration

	ML1	ML2	ML3	ML4
Simulation time (min)	68	63	63	64
CPU time (sec)	0.094	0.062	0.063	0.031

The time-varying outflows $w^i(t)$ computed by the link model component of the proposed DNM are plotted with the corresponding inflows as shown in Figure 5.21.

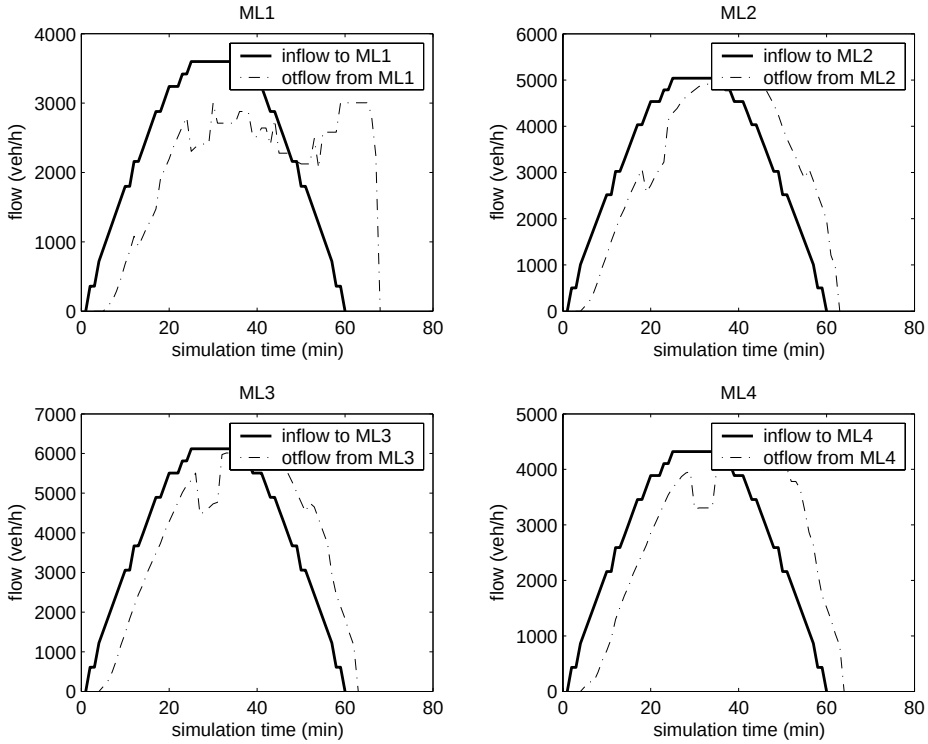

Figure 5.21: Outflows, Computed with Link Model Component, with Corresponding Inflows within Second Configuration

The inflows $u^r(t)$ that are entering to diverging links computed with DNM runs are shown in Figure 5.22.

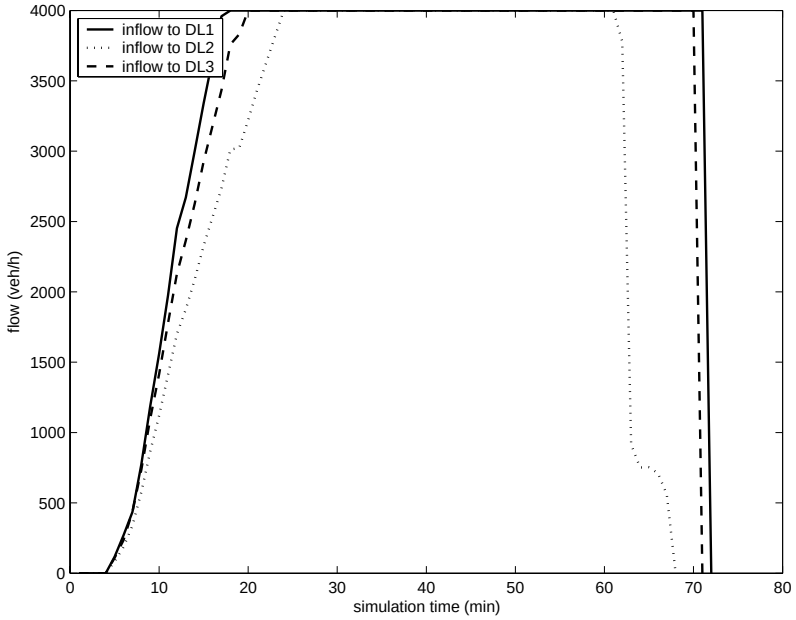

Figure 5.22: Inflows to Diverging Links Computed with DNM within Second Configuration

Some critical values, capacity C^r and maximum inflow rate attempting to enter w^{kr}_{max}, and simulation times of diverging links are given in Table 5.10.

Table 5.10: Critical Values and Required Simulation Times on Diverging Links in Second Configuration

	DL1	DL2	DL3
Capacity (veh/h)	4000	4000	4000
w^{kr}_{max} (veh/h)	7632	5112	6336
Simulation time (min)	72	68	71

The point-queues, $PQ^r(t)$, formed at the entrance of diverging links are shown in Figure 5.23.

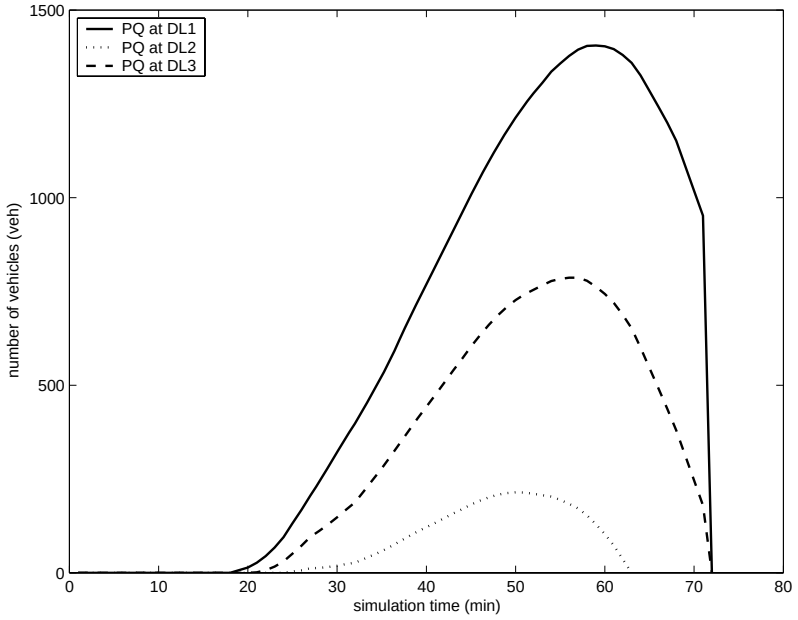

Figure 5.23: Point-queues at Entrance of Diverging Links in Second Configuration

The delays on diverging links $G^r(t)$, occurring due to capacity constraints, are shown in Figure 5.24. As done before, the congestion values are considered to represent delays.

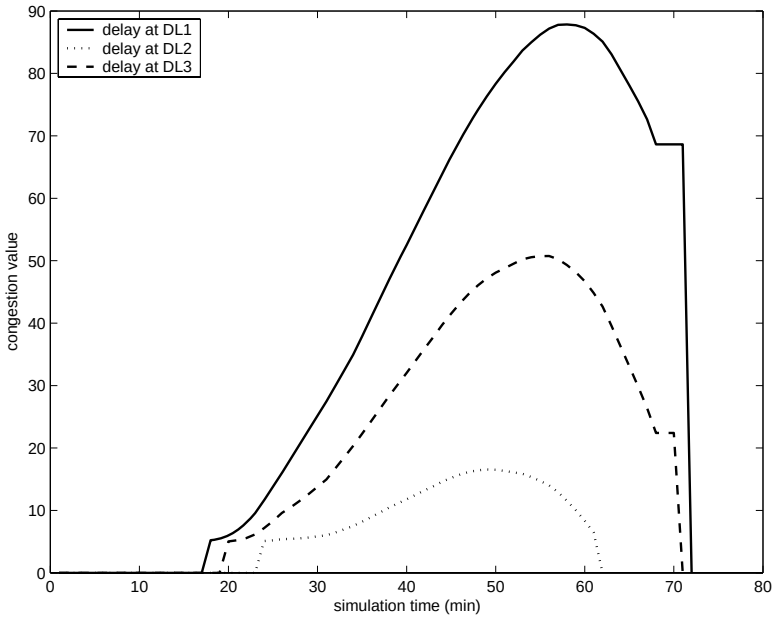

Figure 5.24: Delays on Diverging Links in Second Configuration

5.4.1.3. Third Configuration

The link and the flow characteristics of the third sample configuration are given in Table 5.11.

Table 5.11: Link and Flow Characteristics of Third Configuration

	ML1	ML2	ML3	ML4
Length (km)	5	5	5	5
Capacity (veh/h)	3000	4000	5000	3500
Maximum flow rate (veh/h)	3600	3960	4140	4320
Maximum density (veh/km)	180	189	191	195
Creeping speed (km/h)	12	11.5	11.25	11
Free-flow speed (km/h)	67	85	105	72

The time-varying inflows $u^i(t)$ to merging links are generated theoretically to fit single-peak sinusoidal curve as shown in Figure 5.25. Relationships between the dynamic loadings of merging links are given with (5.41).

$$u^1(t) = \frac{u^2(t)}{1.1} = \frac{u^3(t)}{1.15} = \frac{u^4(t)}{1.2} \qquad \textbf{(5.41)}$$

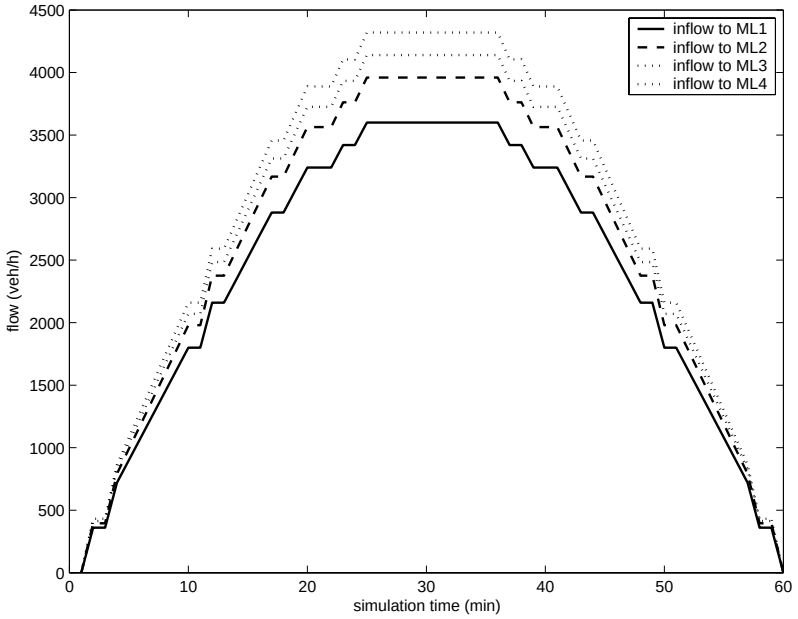

Figure 5.25: Time-varying Traffic Loaded to Merging Links within Third Configuration

The simulation times needed to discharge the dynamic loadings completely from merging links are given in Table 5.12.

Table 5.12: Times Needed for Link Model Component Simulations within Third Configuration

	ML1	ML2	ML3	ML4
Simulation time (min)	67	64	63	76
CPU time (sec)	0.094	0.016	0.031	0.078

The time-varying outflows $w^i(t)$ computed by the link model component of the proposed DNM are plotted with the corresponding inflows as shown in Figure 5.26.

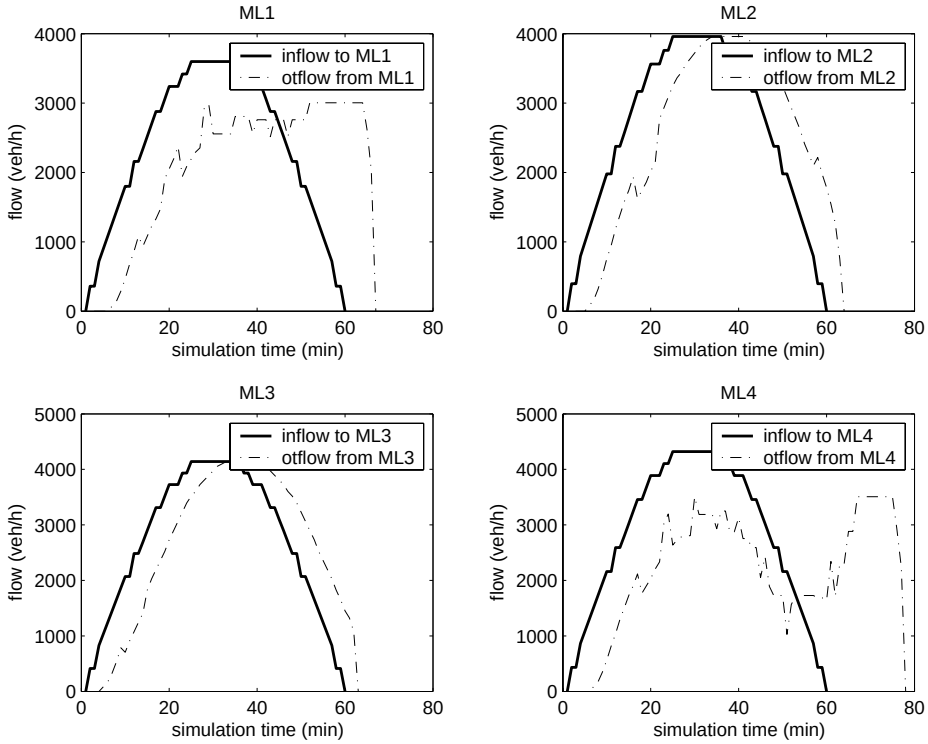

Figure 5.26: Outflows, Computed with Link Model Component, with Corresponding Inflows within Third Configuration

The inflows $u^r(t)$ that are entering to diverging links computed with DNM runs are shown in Figure 5.27.

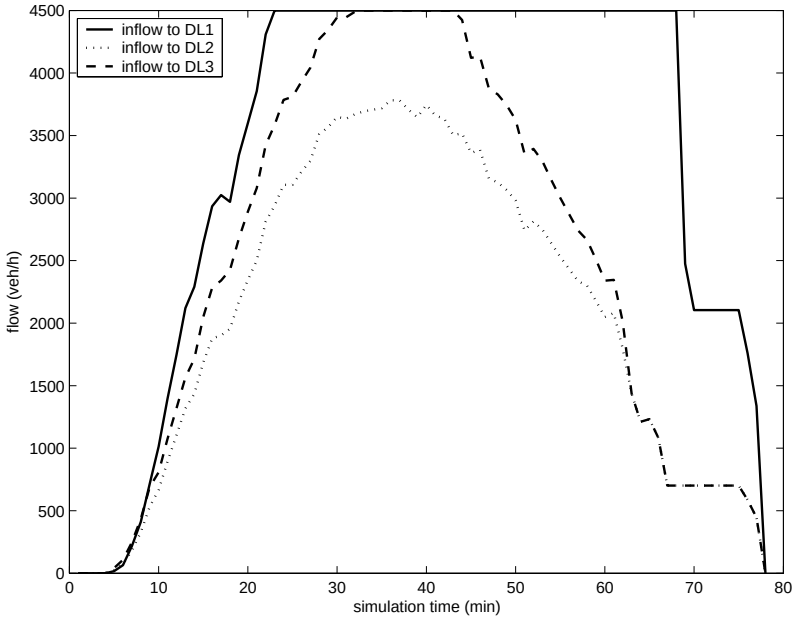

Figure 5.27: Inflows to Diverging Links Computed with DNM within Third Configuration

Some critical values, capacity C^r and maximum inflow rate attempting to enter w^{kr}_{max}, and simulation times of diverging links are given in Table 5.13.

Table 5.13: Critical Values and Required Simulation Times on Diverging Links in Third Configuration

	DL1	DL2	DL3
Capacity (veh/h)	4500	4500	4500
w^{kr}_{max} (veh/h)	6804	4194	5022
Simulation time (min)	78	78	78

The point-queues, $PQ^r(t)$, formed at the entrance of diverging links are shown in Figure 5.28.

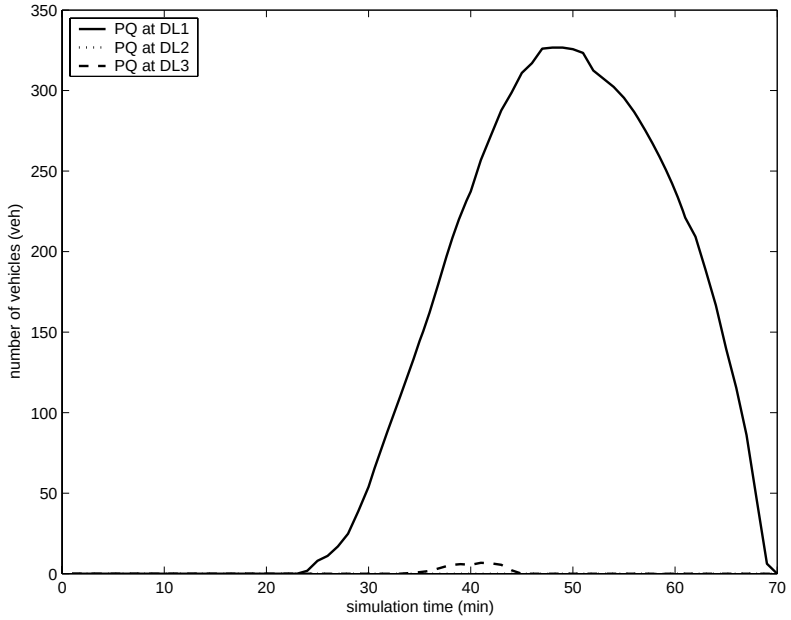

Figure 5.28: Point-queues at Entrance of Diverging Links in Third Configuration

The delays on diverging links $G^r(t)$, occurring due to capacity constraints, are shown in Figure 5.29. As done before, the congestion values are considered to represent delays.

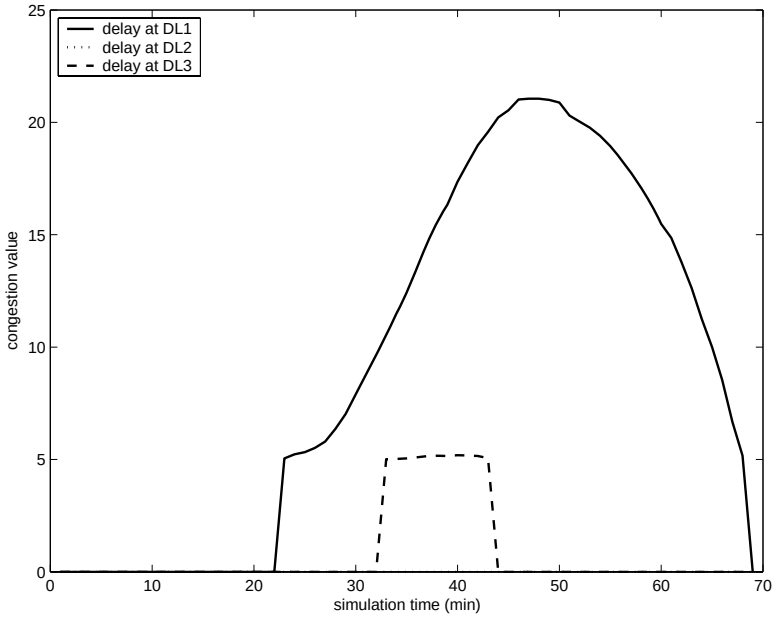

Figure 5.29: Delays on Diverging Links in Third Configuration

5.4.1.4. Fourth Configuration

The link and the flow characteristics of the first sample configuration are given in Table 5.14.

Table 5.14: Link and Flow Characteristics of Fourth Configuration

	ML1	ML2	ML3	ML4
Length (km)	5	5	5	5
Capacity (veh/h)	3600	3600	3600	3600
Maximum flow rate (veh/h)	3600	3600	3600	3600
Maximum density (veh/km)	180	180	180	180
Creeping speed (km/h)	12	12	12	12
Free-flow speed (km/h)	80	80	80	80

The time-varying inflows $u^i(t)$ to merging links are generated theoretically to fit single-peak sinusoidal curve as shown in Figure 5.30. Both the merging link characteristics (Table 5.14) and the loaded dynamic inflows patterns (see Eq. 5.42) are same for the fourth configuration.

$$u^1(t) = u^2(t) = u^3(t) = u^4(t) \qquad \textbf{(5.42)}$$

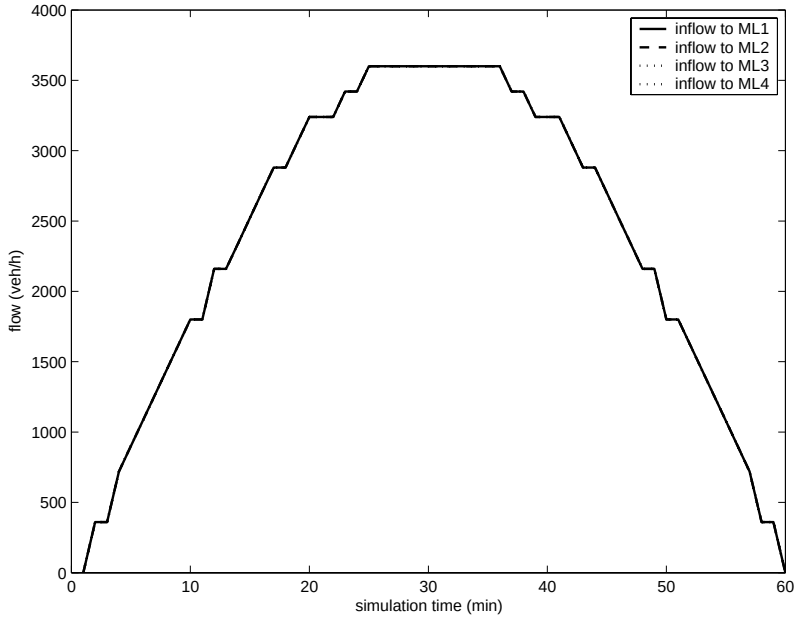

Figure 5.30: Time-varying Traffic Loaded to Merging Links within Fourth Configuration

The simulation times needed to discharge the dynamic loadings completely from merging links are given in Table 5.15.

Table 5.15: Times Needed for Link Model Component Simulations within Fourth Configuration

	ML1	ML2	ML3	ML4
Simulation time (min)	64	64	64	64
CPU time (sec)	0.047	0.031	0.031	0.047

The time-varying outflows $w^i(t)$ computed by the link model component of the proposed DNM are plotted with the corresponding inflows as shown in Figure 5.31.

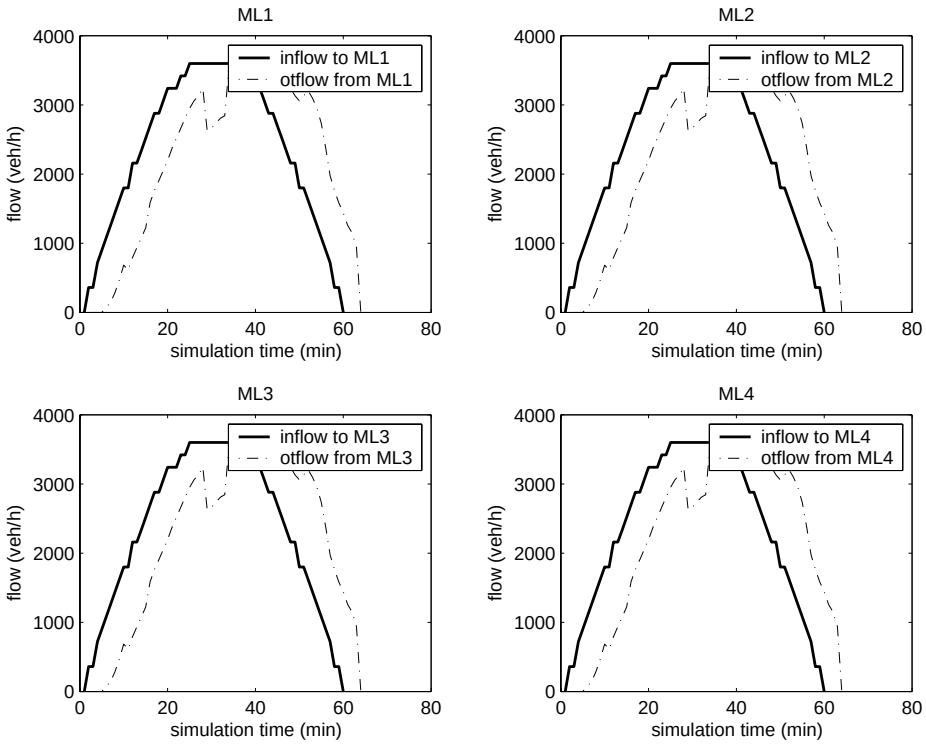

Figure 5.31: Outflows, Computed with Link Model Component, with Corresponding Inflows within Fourth Configuration

The inflows $u^r(t)$ that are entering to diverging links computed with DNM runs are shown in Figure 5.32.

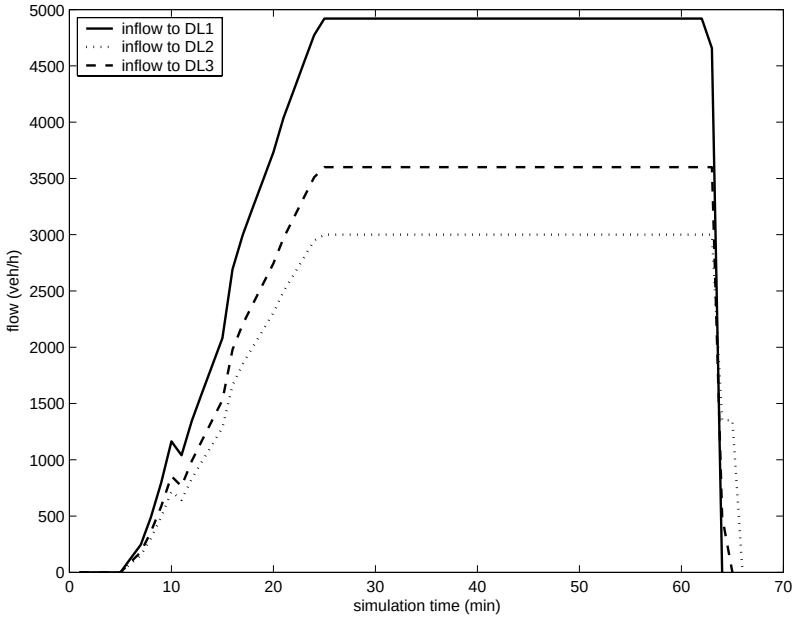

Figure 5.32: Inflows to Diverging Links Computed with DNM within Fourth Configuration

Some critical values, capacity C^r and maximum inflow rate attempting to enter w^{kr}_{max}, and simulation times of diverging links are given in Table 5.16.

Table 5.16: Critical Values and Required Simulation Times on Diverging Links in Fourth Configuration

	DL1	DL2	DL3
Capacity (veh/h)	4900	3000	3600
w^{kr}_{max} (veh/h)	6120	3780	4500
Simulation time (min)	64	66	65

The point-queues, $PQ^r(t)$, formed at the entrance of diverging links are shown in Figure 5.33.

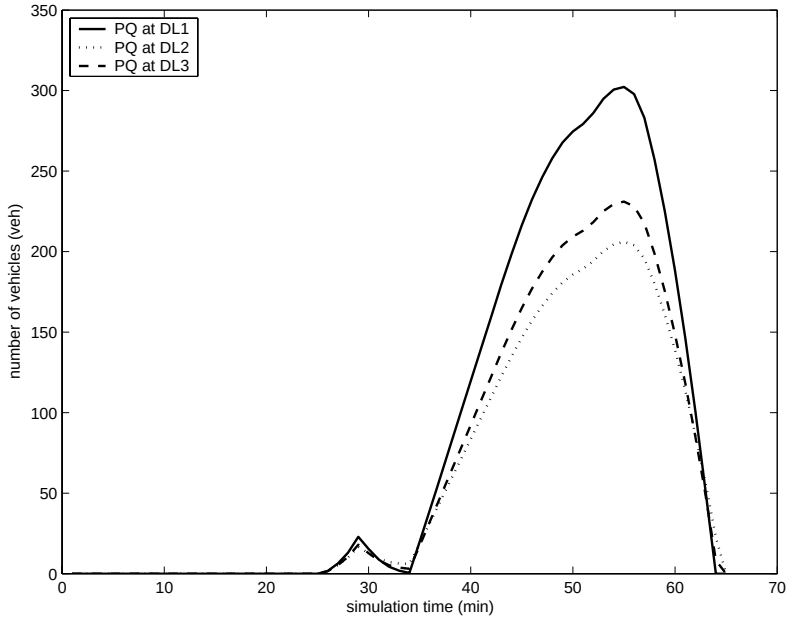

Figure 5.33: Point-queues at Entrance of Diverging Links in Fourth Configuration

The delays on diverging links $G^r(t)$, occurring due to capacity constraints, are shown in Figure 5.34. As done before, the congestion values are considered to represent delays.

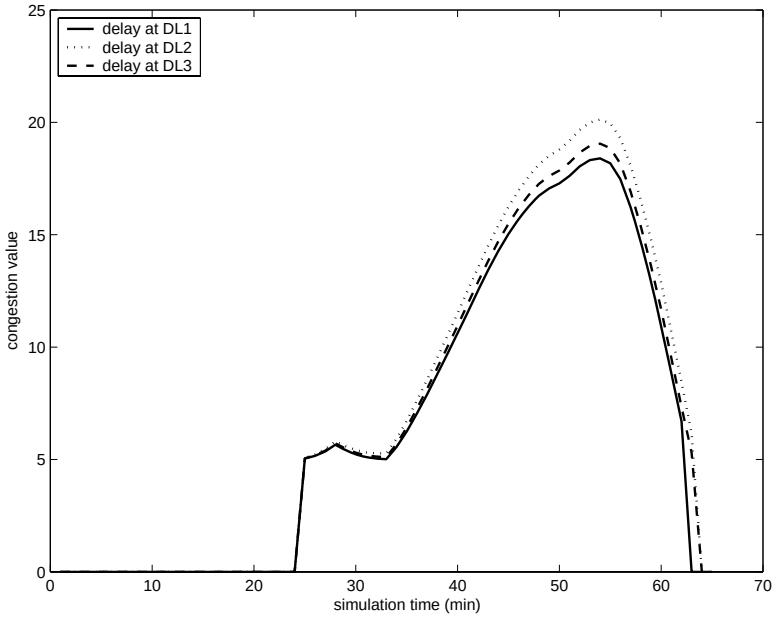

Figure 5.34: Delays on Diverging Links in Fourth Configuration

5.4.2. Comparison and Evaluation of Dynamic Node Model under Different Configurations

In this section, the results and the performance evaluations of the proposed DNM are given with respect to different node configurations under varying flow patterns, which are theoretically set out to simulate over-saturation phenomenon.

Four varying types of a sample node configuration are studied to evalute the performance of the proposed DNM. The proposed DNM showed the best performance under the fourth configuration. Despite the state of capacity had been simulated for the merging links, it is seen that the flows, calculated with the predefined under-saturation condition splitting rates (see Table 5.4), requiring to enter diverging links are over-saturated, as given in Table 5.17.

Table 5.17: Flow Rate/Capacity Values Valid under Different Link and Flow Conditions

	ML1	ML2	ML3	ML4	DL1	DL2	DL3
Configuration 1	1.20	1.26	1.22	1.23	2.18	1.46	1.81
Configuration 2	1.20	1.03	1.02	1.08	1.91	1.28	1.58
Configuration 3	1.20	0.99	0.83	1.23	1.51	0.93	1.12
Configuration 4	1.00	1.00	1.00	1.00	1.25	1.26	1.25

The maximum and the minimum simulation times for computing the merging link outflows, the total simulation times and the required total CPU times of DNM had after trials for different configurations are given in Table 5.18.

Table 5.18: Simulation Times of Proposed DNM under Different Configurations

	Total simulation time (min)	Maximum simulation time for ML (min)	Minimum simulation time for ML (min)	Total CPU time (sec)
Configuration 1	97	85	68	17.502
Configuration 2	72	68	63	4.625
Configuration 3	78	76	63	3.047
Configuration 4	66	64	64	1.672

The performance evaluation of the link model component of the proposed DNM had simultaneously been obtained in the whole simulation process as well, as explained in section 5.1.3. For example; the time to discharge total flows from the third merging link under the third configuration takes 63 minutes where the under-saturated (maximum flow rate/capacity<1) dynamic loading to this link takes 60 minutes.

6. EXTENSION OF PROPOSED DYNAMIC NODE MODEL IN DYNAMIC NETWORK LOADING

In this section, the theoretical basis of the proposed DNM is extended to a DNL formulation for network application. Following, the performance of the proposed DNM in flow propagation modelling is tested on a sample network.

6.1. Theoretical Considerations

In this section, a DNL model is set out to evaluate the performance of proposed DNM in modelling traffic flow propagation on a transportation network. For this purpose, the mathematical formulation of the DNM is improved for extending the model to network scale. The previously set notations are also updated to make the model represent a network scheme as given in the following.

N : set of nodes;

I : set of all possible links belonging to network;

Ω : a transportation network composed of a set of nodes and a set of directed links;

k : a node ($k \in N$);

I_k^+ : set of links diverging from node "k" ($I_k^+ \in I$);

I_k^- : set of links merging to node "k" ($I_k^- \in I$);

i : a merging link ($i \in I_k^-$);

j : a diverging link ($j \in I_k^+$);

O : set of origins ($O \subset N$);

D : set of destinations ($D \subset N$);

o : an origin ($o \in O$);

d : a destination ($d \in D$);

R : set of o-d pairs ($R \subset (O*D)$);

rs : an o-d pair ($rs \in R$);

P : set of paths;

P_{rs} : set of paths between "rs" o-d pair;

p : a path ($p \in P$);

$f_p^{rs}(t)$: the path flow on "p" between "rs" o-d pair departing at time "t";

$D_{rs}(t)$: the time-varying demand flow rate at time "t" on all paths between "rs" o-d pair;

$u^{i,rs}(t)$: the inflow to link "i" of "rs" o-d pair at time "t";

$w^{i,rs}(t)$: the outflow from link "i" of "rs" o-d pair at time "t";

$n^{i,rs}(t)$: the number of vehicles on link "i" of "rs" o-d pair at time "t";

$u^{i}(t)$: the total inflows at time "t" on link "i";

$w^{i}(t)$: the total outflows at time "t" on link "i";

$n^{i}(t)$: the total number of vehicles at time "t" on link "i";

$\xi_p^{\ i}$: dummy variable, equal to 1 if link "i" is on path "p", and 0 otherwise;

$u_p^{\ i}(t)$: the inflow entering to link "i" of path "p" at time "t";

$w_p^{\ i}(t)$: the outflow exiting from link "i" of path "p" at time "t";

$n_p^{\ i}(t)$: the number of vehicles on link "i" of path "p" at time "t";

$w_p^{\ i-}(t)$: the outflow of the link preceding link "i" on path "p" at time "t";

$\delta^{i}(t)$: the total traffic demand ready to exit link "i" at time "t";

$\delta^{ij}(t)$: the partial demand from link "i" to "j" at time "t";

$\sigma^{j}(t)$: the total capacity of link "j" at time "t";

$\sigma^{ij}(t)$: the flow corresponding to the partial capacity of link "j", and allocated on link "i" at time "t";

$\delta_p^{\ i}(t)$: the partial demand from link "i" on path "p" at time "t";

$w^{ij}(t)$: the partial outflow of link "i" directed to link "j" at time "t";

$u^{ij}(t)$: the partial inflow of link "j" entering from link "i" at time "t";

λ^{ij} : the proportion of partial demand relative to the total demand;

$PQ^{j}(t)$: the point-queue at the entrance of link "j" at time "t";

$G^{j}(t)$: the delay on link "j" at time "t".

6.1.1. Network Modelling Concept

In this section a complete network loading model is formulated. Once the set of paths P_{rs} between each o-d pair rs and $f_p^{rs}(t)$ are known, $D_{rs}(t)$ can be calculated as follows:

$$D_{rs}(t) = \sum_{p \in P_{rs}} f_p^{rs}(t) \qquad \textbf{(6.1)}$$

The idea of local flow as the minimum between local supply and demand is generalized in this model. It is possible to reproduce the movements of the users on the network, according to a set of analytical rules as well as the prior knowledge of path flows. Link flows are computed through the proposed mesoscopic link model as explained in details in section 5.1. In terms of input values and output values, the link model has the general structure indicated below in Figure 6.1. It establishes partial supply and demand flow rates at time t* as a function of the inflow patterns at time $t \leq t^*$.

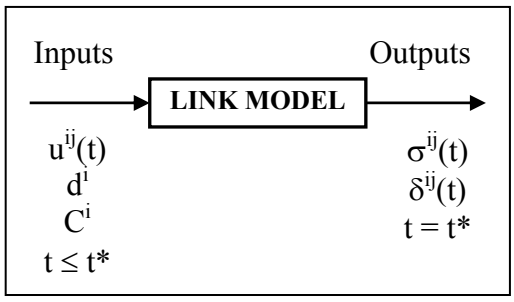

Figure 6.1: General Structure of Proposed Link Model

Flows at each node at time "t" satisfy the flow conservation condition, as in all network models, except that flows at nodes are constrained by the interactions between demand of entering links and supplies of exiting links. A link based DNL model has to solve the problem of calculating flows according to prevailing demands

and supplies at each node of the network, at each instant of time. This task may be reduced to solving the node model for "n" time intervals, assuming that supply and demand flow rates are constant during each time interval. The node model described in detail in section 5.2 has the structure shown below in Figure 6.2. It establishes the flows at time "t", once supply and demand flow rates at time t are known.

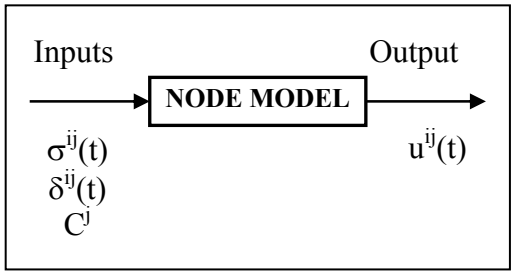

Figure 6.2: General Structure of Proposed Node Model

Since the proposed DNM is set out with point-queuing assumption, the use of a DNL model to deal with the congestion propagation is evaluated with an adapted congestion function, explained in section 5.2.2. The delay modelling component of the proposed DNM, having the congestion function as its argument, is shown in Figure 6.3.

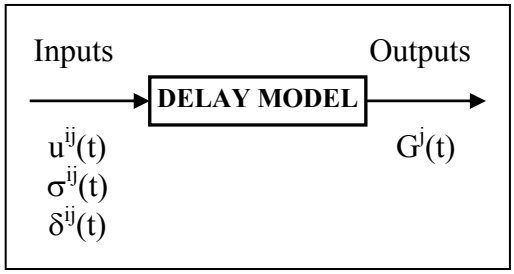

Figure 6.3: Structure of Delay Modelling Component for Proposed Node Model

By giving to the first link of each path an infinite link storage space, the model is able to deal with delay occurrence. A connector link (from a centroid to the network) is used for this purpose. The attributes of connector links (shown in Figure 6.4) are the same as that of other links of the networks.

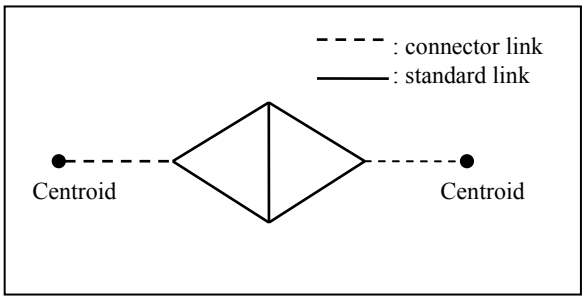

Figure 6.4: A Sample Network

6.1.2. Model Variables and Algorithm for Network Extension

We consider a transportation network Ω = (N, I) composed of a set of nodes "k", $k \in N$ and a set of directed links "i", $i \in I$ ($I = \{i_1, i_2, i_3, ..., i_n\}$). In the following, the backward star set BW_k and the forward star set FW_k, mentioned in section 5.2, are united. Hence, the set of directed links is unique, and noted as "I". Traffic originates at nodes o ($o \in O$, $O \subset N$) and is destined to nodes d ($d \in D$, $D \subset N$). An origin-destination (o-d) pair is designated "rs", $rs \in R \subset (O * D)$. A set of paths "p", $p \in P_{rs}$ connects o-d pairs "rs", and $D_{rs}(t)$ is the time varying demand flow rate that uses these paths. Traffic departs from origins in the interval [0, T] and all traffic arrives at destination within the interval [0, T'] (T' > T). In order to apply the proposed link model algorithm to a general network with multiple o-d pairs, some extensions are required. Notation for the time varying inflow rates, outflow rates and number of vehicles on link "i" for o-d pair "rs" at time "t" are now updated to $u_{rs}^{i}(t)$, $w_{rs}^{i}(t)$ and $n_{rs}^{i}(t)$, respectively. So, the relationships between aggregated and disaggregated variables are calculated as follows:

$$u^{i}(t) = \sum_{rs \in R} \xi_{p}^{i} \cdot u^{i,rs}(t) \qquad \textbf{(6.2)}$$

$$w^{i}(t) = \sum_{rs \in R} \xi_{p}^{i} \cdot w^{i,rs}(t) \qquad \textbf{(6.3)}$$

$$n^{i}(t) = \sum_{rs \in R} \xi_{p}^{i} \cdot n^{i,rs}(t) \qquad \textbf{(6.4)}$$

Here, ξ_{p}^{i} can be determined by the path-link incidence matrix.

Let us update the sets of links I_k^+ and I_k^-, which are the forward and backward stars of node "k". The traffic demand flow rate $\delta^i(t)$ represents the traffic that is ready to exit link "i" to link "i^+", whose capacity is $\sigma^{i^+}(t)$. It is useful to denote $\delta^{ij}(t)$ as the partial demand flow rate from link "i" to "j" and $\sigma^{ij}(t)$ as the partial supply flow rate of link "j" allocated on link "i" at time "t".

The disaggregated outflow for disaggregated variables can be calculated as given in (6.5), while the (6.6) expresses the flow conservation constraint:

$$w_p^i(t) = \frac{n_p^i(t)}{n^i(t)} \cdot W^i\left(n^i(t)\right) \tag{6.5}$$

$$n_p^i(t+\Delta t) - n_p^i(t) = \left(u_p^i(t) - w_p^i(t)\right) \cdot \Delta t \tag{6.6}$$

The path flow notion can be applied to a network scheme as given in (6.7).

$$u_p^i(t) = \begin{cases} w_p^{i^-}(t), & \text{if "}i^-\text{" is the preceeding link along route p} \\ f_p^{rs}(t), & \text{if "i" is the first link of route p} \end{cases} \tag{6.7}$$

Similar to the PQ assumption explained in section 5.2 and given with Eq. (5.31), a PQ at the entrance of link "i" can be determined by assuming that there is no initial queue when t=0, given in (6.8).

$$PQ^i(t) = \begin{cases} 0, & \text{if } (t=0) \vee \left(\left(\sum_{p\in P} \xi_p^i \cdot u_p^i(t)\right) + \frac{PQ^i(t-\Delta t)}{\Delta t} \le \sigma^i\right) \\ \left(\left(\sum_{p\in P} \xi_p^i \cdot u_p^i(t)\right) - \sigma^i\right)\Delta t + PQ^i(t-\Delta t), & \text{if} \left(\sum_{p\in P} \xi_p^i \cdot u_p^i(t)\right) + \frac{PQ^i(t-\Delta t)}{\Delta t} > \sigma^i \end{cases} \tag{6.8}$$

If $u^i(t)$ exceeds the total supply of link "i", the disaggregated path inflows $u^i_p(t)$ in the previous equation are updated with the term given by (6.9):

$$u_p^i(t) = \begin{cases} u_p^i(t), & \text{if } (t=0) \vee \left(\left(\sum_{p\in P} \xi_p^i \cdot u_p^i(t)\right) + \frac{PQ^i(t-\Delta t)}{\Delta t} \le \sigma^i\right) \\ \dfrac{u_p^i(t)}{\left(\sum_{p\in P} \xi_p^i \cdot u_p^i(t) + \frac{PQ^i(t-\Delta t)}{\Delta t}\right)} \cdot \sigma^i, & \text{if } \left(\sum_{p\in P} \xi_p^i \cdot u_p^i(t)\right) + \frac{PQ^i(t-\Delta t)}{\Delta t} > \sigma^i \end{cases} \tag{6.9}$$

The following algorithm summarizes the determination of flows and number of vehicles on all links under exit function approach by using the mesoscopic link model, explained in details in section 5.1, when a network is considered.

1. Set t = (first time interval).
2. Determine the total number of vehicles of each link based on $n^i_p(t)$ with Eq. (6.4).
3. Calculate the aggregated outflow $w^i(t)$ of each link with the mesoscopic link model.
4. Calculate the disaggregated outflow $w^i_p(t)$ with (6.5).
5. Obtain inflow $u^i_p(t)$ with (6.7).
6. Determine a possible point-queue with (6.8). If a PQ exists, update the disaggregated path inflow $u^i_p(t)$ with (6.9), else process to step 7.
7. Determine $n^i_p(t+\Delta t)$ with (6.6).
8. If the time-varying demand is completely discharged from all the paths, which means that the value of (6.1) is equal to zero, stop. Otherwise set t = (following time interval)t+1 and go to Step 2.

Once all the inflows and outflows are determined, the link travel times can then be calculated as explained in section 4.2.2 by following (4.17).

6.1.3. Proposed Dynamic Node Model for Dynamic Network Loading

In this section the rules that govern flows at any intersection node are improved and extended for a network concept.

Due to the constraining capacities, in the DNL, rather than just only flow conservation rules, a more complex problem has to be solved that can be expressed as an optimization problem, where the objective function is to maximize the total flow crossing the node and the constraints are the local supplies and demands at the node.

A node stream $stream_{ij,k}$ is defined as the set of all paths merging or diverging at node "k", and containing the links $i \in I_k^-$ and $j \in I_k^+$ (see Figure 6.5).

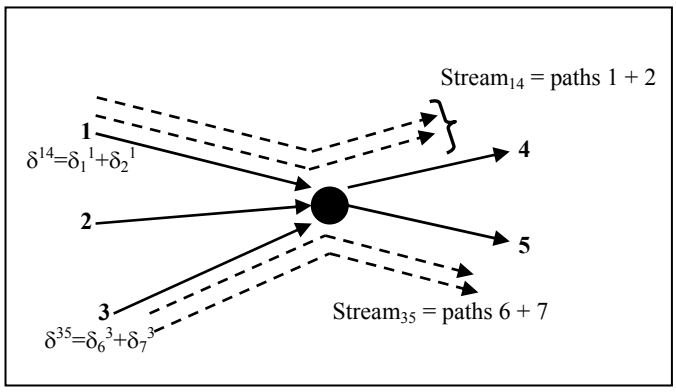

Figure 6.5: Representation of Node Streams with Given Paths

Now, the node problem consists of evaluating the flows for each node stream at each time "t" of the simulation, given the values of partial supplies and partial demands of all the links included in I_k^+ and I_k^-. The outflows $w^{ij}(t)$ of link "i" are equal to the partial inflow rates $u^{ij}(t)$ of link "j". So,we obtain the following set of conservation equations for each pair of entering and exiting links, given in (6.10).

$$w^{ij}(t) = u^{ij}(t); \quad i \in I_k^-,\ j \in I_k^+ \tag{6.10}$$

Stream supply (and demand) flow rates are the inputs to the intersection problem, with the constraints (6.11), (6.12), and (6.13):

$$\delta^{ij}(t) = \sum_{i,j \in p} \delta_p^i(t) \tag{6.11}$$

$$\delta^{i}(t) = \sum_{j \in I_k^+} \delta^{ij}(t) \tag{6.12}$$

$$\sigma^{j}(t) = \sum_{i \in I_k^-} \sigma^{ij}(t) \tag{6.13}$$

where:

- $\delta_p^i(t)$ is the partial demand flow rate of path "p" destined to the link "i",
- "k" is the node connecting link "i" and "j",
- $\sigma^{ij}(t)$ is the flow rate corresponding to the partial supply of link "i" allocated to the link "j".

The computation of the node flow rates uses a model described below. This formulation represents the simplest way of solving the node problem while respecting the FIFO rule. It can be written as a problem of maximizing the total flow that pass through node "k", as given by (6.14):

$$\max\left\{\sum_{t\in T}\sum_{i\in I_k^-}\sum_{j\in I_k^+} w^{ij}(t)\right\} \qquad \textbf{(6.14)}$$

subject to the following constraints:

1. Non-negativity of flow rates, given by (6.15):

$$w^{ij}(t)\geq 0; \qquad i\in I_k^-,\ j\in I_k^+ \qquad \textbf{(6.15)}$$

2. Constraint relevant to demand, given by (6.16):

$$w^{ij}(t)\leq \delta^{ij}(t); \qquad i\in I_k^-,\ j\in I_k^+ \qquad \textbf{(6.16)}$$

3. Constraint relevant to supply, given by (6.17):

$$\sigma^{j}(t)\geq \sum_{i\in I_k^-} w^{ij}(t); \qquad j\in I_k^+ \qquad \textbf{(6.17)}$$

4. The partial flow rates from link "i" to link "j" at time "t", and relative to the total flow exiting link "i", are represented through the term $w^{ij}(t)$. The proportion of the partial demand flow rates $\delta^{ij}(t)$ with respect to the total demand flow rate of link "i" $\delta^{i}(t)$ is maintained. This guarantees that the FIFO rule is respected on link "i", by ensuring that, if a stream is delayed because of a lack of supply on its destination link, all other streams exiting the same link are delayed as well. λ^{ij} is defined as the proportion of partial demand $\delta^{ij}(t)$ with respect to the total demand $\delta^{i}(t)$, given by (6.18).

$$\lambda^{ij}=\frac{\delta^{ij}(t)}{\sum_{j\in I_k^+}\delta^{ij}(t)}=\frac{\delta^{ij}(t)}{\delta^{i}(t)} \qquad \textbf{(6.18)}$$

So, the constraint relevant to the flow splitting is given in (6.19).

$$w^{ij}(t) = \lambda^{ij} \cdot \sum_{j \in I_k^+} w^{ij}(t) = \lambda^{ij} \cdot w^{i}(t); \qquad i \in I_k^-,\ j \in I_k^+ \tag{6.19}$$

5. Likewise, λ^{ij} can be defined as the ratio of partial supply $\sigma^{ij}(t)$ to the total supply $\sigma^{j}(t)$, as given in (6.20).

$$\sigma^{ij}(t) = \lambda^{ij} \cdot \sigma^{j}(t); \qquad i \in I_k^-,\ j \in I_k^+ \tag{6.20}$$

The flow of $stream_{ij}$ must be less than or equal to the given supply, as given in (6.21).

$$w^{ij}(t) \le \sigma^{ij}(t); \qquad i \in I_k^-,\ j \in I_k^+ \tag{6.21}$$

For each entering link i at node k, the resulting partial outflow rate to the link j, which solves the problem (6.14)-(6.21), is given by (6.22).

$$w^{ij}(t) = \min\left(1, \frac{\sigma^{ij}(t)}{\sigma^{j}(t)}\right) \cdot w^{i}(t) \tag{6.22}$$

The main drawback of this formulation is that the values λ^{ij} are fixed. As a result, excess supply is not re-assigned. If link "j" has a higher supply flow rate $\sigma^{ij}(t)$ than the demand $\delta^{ij}(t)$, so that $\min(\sigma^{ij}(t), \delta^{ij}(t)) = \delta^{ij}(t)$, the remaining supply flow rate $\sigma^{ij}(t)-\delta^{ij}(t)$ cannot be (as would be physically expected) used by the others links. Thus a link will always affect the supply for other links in the same way, regardless of its flow.

6.2. Flow Propagation Model Performance Evaluation on a Sample Network

In this sub-section, the performance evaluation of the resultant DNL model is given considering a hypothetical network.

6.2.1. Sample Network Configuration

The performance of the proposed flow propagation model is tested on a sample network shown in Figure 6.6.

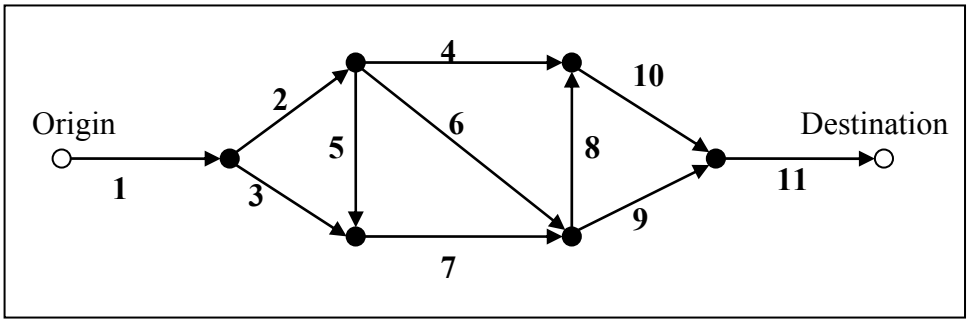

Figure 6.6: Sample Network for Testing Trials

The link and the flow characteristics assigned as network configuration are given in Table 6.1.

Table 6.1: Assigned Link and Flow Characteristics of Sample Network

	Link and flow characteristics										
Link number	1	2	3	4	5	6	7	8	9	10	11
Length (km)	4	4	4	4	4	4	4	4	4	4	4
Capacity (veh/h)	4500	3000	1400	900	900	900	2100	1500	1500	2700	4500
Free-flow speed (km/h)	85	85	85	85	85	85	85	85	85	85	85
Maximum density(veh/km)	210	210	210	210	210	210	210	210	210	210	210
Creeping speed	10	10	10	10	10	10	10	10	10	10	10

Considering the directed links given on the sample network, there are seven paths existing between the given OD pair. Each path is comprised of a series of sequential links, noted in Table 6.1.

Table 6.2: Existing Paths on Given Sample Network

PATH	SEQUENTIAL LINKS
Path 1	1 – 2 – 4 – 10 – 11
Path 2	1 – 2 – 5 – 7 – 8 – 10 – 11
Path 3	1 – 2 – 5 – 7 – 9 – 11
Path 4	1 – 2 – 6 – 8 – 10 – 11
Path 5	1 – 2 – 6 – 9 – 11
Path 6	1 – 3 – 7 – 8 – 10 – 11
Path 7	1 – 3 – 7 – 9 – 11

The path-link incidence matrix that is assigned resultant from the existing paths is given in Table 6.3.

Table 6.3: Path-link Incidence Matrix

	link1	link2	link3	link4	link5	link6	link7	link8	link9	link10	link11
path1	1	1	0	1	0	0	0	0	0	0	1
path2	1	1	0	0	1	0	1	1	0	1	1
path3	1	1	0	0	1	0	1	0	1	0	1
path4	1	1	0	0	0	1	0	1	0	1	1
path5	1	1	0	0	0	1	0	0	0	0	1
path6	1	0	1	0	0	0	1	1	0	1	1
path7	1	0	1	0	0	0	1	0	1	0	1

The time varying demand flow rate at time "t" on all paths between "rs" o-d pair is calculated with Eq. (6.1), since the path flow rates are assumed to be known from a prior assignment process. The total demand between the given OD pair (Figure 6.6) fite a single peak sinusoidal curve as given in Figure 6.7.

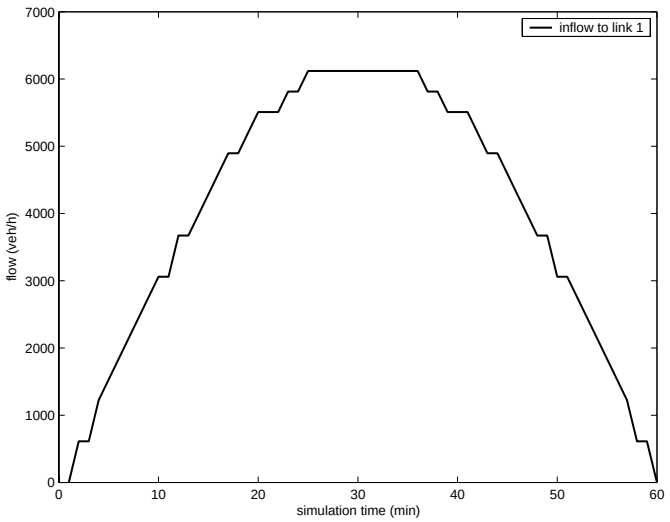

Figure 6.7: Time-varying Demand for Given OD Pair

6.2.2. Network Test Results

The behaviour of the DNL model was evaluated with a number of critical terms from the simulations. The maximum outflow q_{max} and the minimum speed V_{MIN}, computed during the model runs, also allow the calculation of the maximum available density. These values, as well as the rate of capacity used (q_{MAX}/C) and simulation time for each link, are given in Table 6.4.

Table 6.4: Critical Values of Flow Characteristics Calculated with Theoretical Data

	link1	link2	link3	link4	link5	link6	link7	link8	link9	link10	link11
Capacity (veh/h)	4500	3000	1400	900	900	900	2100	1500	1500	2700	4500
V_{MIN} (veh/h)	10	10	10	10	10	10	10	10	10	14.6	15.9
Simulation time (min)	81	85	86	90	90	90	94	91	98	95	98
q_{max}/C	1	1	1	1	1	1	1	1	1	0.89	0.87

The DNL code written in Matlab language was run on a computer with the same the same features as previously defined for link model performance evaluation in section 5.1.3.2. The CPU time needed to simulate the traffic flow propagation on the proposed sample network existed as 17.078 secs. Considering 109.29 minutes as the total time that is needed to discharge all flows from the links of the sample network, it can be said that the integration of DNM to network scale as a DNL model is able to perform efficient computations.

The inflow-outflow diagrams at a selected sample node, node 3, of the sample network (Figure 6.6) is given in Figure 6.8. The inflow-outflow diagrams of flow propagation at the rest of the nodes are given in Appendix D.

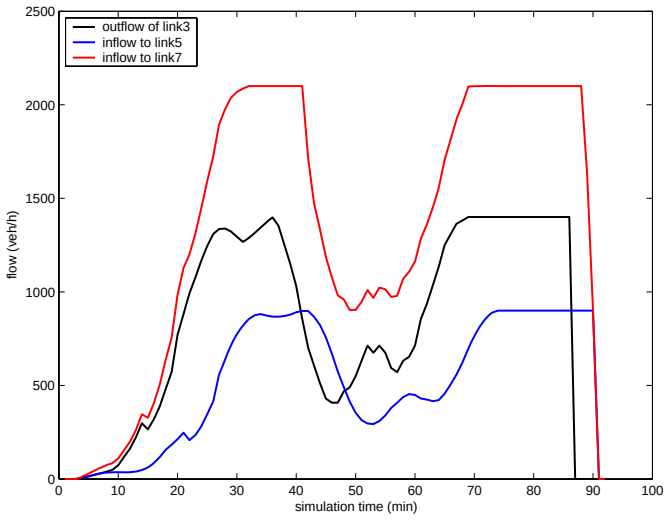

Figure 6.8: Inflows and Outflows at Node 3 in Sample Network

It is seen that the proposed DNM is easy to modify and use in DNL applications, since the run DNL model respected the series of constraints given through (6.15)-(6.21) and simulated appropriate and consistent flow propagation.

7. CONCLUSIONS

In this study, an analytical dynamic node model is proposed by mesoscopic modelling approach. The dynamic network loading problem has been solved by the utilization of the proposed model. Taking into account a set of analytical rules, an algorithm has been derived within an iterative modelling framework. The models for dynamic network loading proposed in the literature are, as in the case of microscopic models, rather difficult to calibrate, or, as in the case of macroscopic models, require explicit expression of capacity and maximum density constraints, as well as congruence and continuity of flows in the nodes.

The new dynamic node model proposed in this study is unique in that it encapsulates a mesoscopic approach in node modelling. The uniqueness of the proposed model is also valid for the node modelling with point-queue assumption. The conclusions derived from the results of this study are summarized in the following.

- Both link and node components of the proposed model consider explicitly the capacity constraints. This property of the model differs it from other models that are also set out within a point-queuing assumption.

- The proposed mesoscopic link model, assuming discrete packets and uniformly accelerated movement, uses the discretisation of time intervals in short durations and therefore does not average, and then does not smooth, all variable speed. Therefore, it provides more realistic results in representing outflow dynamics.

- A link exit function approach is utilized as the performance function, because the links of the simulated configurations throughout this study are not sufficiently short, and the congestion is not treated in the form of physical-queues. Regarding the assumptions made, the link exit function based model provides accurate and consistent approximation of link flow behaviour.

- The link model component computes link flows taking into account the acceleration of packets (vehicles) that validates the consistency of flow propagation with speed. In the presence of step-ups and step-downs on speed, adaptation of flow propagation

is simultaneous, relative to the time lag defined to discretise time dimension. This is the most important difference between the proposed model and other models. The model is easy to calculate at each iteration, although iterative computations are needed. It is obvious that the computing time increases with the precision of the speed value.

- Simulation results have shown that the proposed model performs better than CONTRAM and Friesz models in determining link outflows. It is clearly seen that the proposed model is the only one capable both to fit the real data and to reach the creeping speed in case of over-saturation, in comparison to Friesz, CONTRAM and Merchant-Nemhauser models. Thus, the proposed algorithm yields accurate outputs even in congested traffic conditions.

- By comparing the speed curves obtained by the proposed model and by other considered models, it can be seen that the speed calculated by the proposed model is the lowest one, since other speeds are averaged and then smoothed. Therefore, the proposed model can tackle over-saturation phenomena in a better way than the other compared models.

- Although the fixed-point algorithm is rapidly convergent, the computing time of the model is considerably longer than the other models, due to iterative computation.

- The delays are assumed to be solely dependent to the diverging link capacities. It is assumed that there becomes no delay as a result of flow conflicting. So, the partial flows exiting from merging links are considered to traverse junction area without any loss. This assumption is consistent, since the sample junction is unsignalized and therefore no specific control action is sought. Moreover, the relative increase or decrease on total delays calculated as (Delay due to flow conflict)+(Delay due to flow condition) do not have significant deviations in comparison to the case that delays due to flow conflict are not considered.

- The main drawback of the application of proposed DNM on a network is that the splitting factor values are fixed. As a result, excess supply is not re-assigned. Thus, a link will always affect the supply for other links in the same way, regardless of its flow.

The proposed DNM can easily be integrated with a flow modelling component of a DTA process and can be utilized in a wide range of Intelligent Transportation

Systems (ITS) applications. For example, it can be adopted as an integral part of an Advanced Traffic Management System (ATMS), of which the goal is to predict traffic demand as accurately as possible, as a real world application. This makes an ATMS practice result in providing better guidance. Moreover, the realistic representation of traffic flow dynamics enables the proposed model to be easily utilized in Advanced Traveller Information Systems (ATIS). The predictions on link performances are the basic inputs to ATIS applications, such as variable message signs, in this context. Dynamic signal optimization and ramp-metering are other possible topics that the proposed model's extensions can be studied.

The proposed model's extension to a real network and its validation with field data, possibly integrated with a route choice model, will be a matter of future development, combined with study and analysis of more efficient algorithms.

REFERENCES

[1] **Wardrop, J.**,1952. Some theoretical aspects of road traffic research, *Proceedings of the Institute of Civil Engineers*, Part II, 325-378.

[2] **Ran, B. and Boyce, D.,** 1996. Modeling Dynamic Transport Networks: An Intelligent Transportation System Oriented Aprroach, Second Revised Edition, Springer-Verlag, Heidelberg.

[3] **Nagurney, A.**, 1993. Network Economics: A Variational Inequality Approach, Advances in Computational Economics Series, Kluwer Academic Publishers, Norwell, Massachussets, USA.

[4] **Cascetta, E.,** 2001. Transportation Systems Engineering: Theory and Methods, Applied Optimization Series, Kluwer Academic Publishers.

[5] **Wie, B.W., Tobin, R.L. and Carey, M.,** 2002. The existence, uniqueness and computation of an arc-based dynamic network user equilibrium formulation, *Transportation Research*, **36B**, 10, 897-918.

[6] **Lo, H. and Szeto, W.Y.** 2002. A cell-based variational inequality formulation of the dynamic user optimal assignment problem, *Transportation Research*, **36B**, 5, 421-443.

[7] **Astarita, V.,** 1995. Flow propagation description in dynamic network loading models, *Proceedings of 4th International Conference on Applications of Advanced Technologies in Transportation Engineering*, Capri, 27-30 June, pp. 599-603, ASCE Press.

[8] **Szeto**, **W.Y. and Lo, H**., 2000. A cell-based dynamic simultaneous route and departure time choice model with elastic demand, *Proceedings of the 5th Meeting of Hong Kong Society for Transportation Studies*, Hong Kong, December 2, pp. 147-156.

[9] **Huang, H.J. and Lam, W.H.K.**, 2002. Modeling and solving dynamic user equilibrium route and departure time choice problem in network with queues. *Transportation Research,* **36B**, 3, 253-273.

[10] **Carey, M., Ge, Y.E. and McCartney, M.**, 2003. A whole-link travel time model with desirable properties, *Transportation Science*, **37**, 1, 83-96.

[11] **Friesz, T.L., Bernstein, D.H., Smith, T.E., Tobin, R.L. and Wie, B.W.,** 1993. A variational inequality formulation of the dynamic network user equilibrium problem, *Operations Research*, **41**, 1, 179-191.

[12] **Daganzo, C.F.,** 1994. The cell transmission model: a simple dynamic representation of highway traffic, *Transportation Research*, **28B**, 4, 269-287.

[13] **Daganzo, C.F.,** 1995. The cell transmission model, part II: network traffic, *Transportation Research*, **29B**, 2, 79-93.

[14] **Daganzo, C.F.,** 1998. Queue spillovers in transportation networks with a route choice, *Transportation Science*, **32**, 1, 3-11.

[15] **Lo, H.,** 1999. A dynamic traffic assignment formulation that encapsulates the cell transmission model, *Proceedings of the 14th International*

Symposium on Transportation and Traffic Theory, Jerusalem, Israel, 20-23 July, pp. 327-350.

[16] **Kuwahara, M. and Akamatsu, T.,** 2001. Dynamic user optimal assignment with physical queues for a many-to-many OD pattern, *Transportation Research*, **35B**, 5, 461-479.

[17] **Rubio-Ardanaz, J.M., Wu, J.H., and Florian, M.,** 2001. A numerical analytical model for the continuous dynamic network equilibrium problem with limited capacity and spill back, *IEEE Intelligent Transportation Systems Conference Proceedings*, Oakland, USA, August 25-29, pp. 263-267.

[18] **Merchant, D.K. and Nemhauser, G.L.,** 1978. A model and an algorithm for the dynamic traffic assignment problem, *Transportation Science*, **12**, 3, 183-199.

[19] **Merchant, D.K. and Nemhauser, G.L.,** 1978. Optimality conditions of a dynamic traffic assignment model, *Transportation Science*, **12**, 3, 200-207.

[20] **Ho, J.K.,** 1980. A successive linear optimization approach to the dynamic traffic assignment problem, *Transportation Science*, **14**, 4, 265-305.

[21] **Carey, M.,** 1987. Optimal time-varying flows on congested network, *Operations Research*, **35**, 1, 58-69.

[22] **Janson, B.N.,** 1991. Dynamic traffic assignment for urban road networks, *Transportation Research*, **25B**, 2-3, 143-161.

[23] **Carey, M. and Subrahmanian, E.,** 2000. An approach to modeling time-varying flows on congested networks. *Transportation Research*, **34B**, 3, 157-183.

[24] **Friesz, T.L., Luque, J., Tobin, R.L. and Wie B.W.,** 1989. Dynamic network traffic assignment considered as a continuous time optimal control problem, *Operations Research,* **37**, 6, 893-901.

[25] **Wie, B.W., Friesz, T.L. and Tobin, R.L.,** 1990. Dynamic user optimal traffic assignment on congested multidestination networks, *Transportation Research*, **24B**, 6, 431-442.

[26] **Papageorgiou, M.,** 1990. Dynamic modeling, assignment, and route guidance in traffic networks, *Transportation Research*, **24B**, 6, 471-495.

[27] **Lam, W.H.K. and Huang, H.J.,** 1995. Dynamic user optimal traffic assignment model for many to one travel demand, *Transportation Research*, **29B**, 4, 243-259.

[28] **Yang, H. and Huang, H.J.,** 1997. Analysis of the time-varying pricing of a bottleneck with elastic demand using optimal control theory, *Transportation Research*, **31B**, 6, 425-440.

[29] **Chen, H.K. and Hsueh, C.F.,** 1998. A model and an algorithm for the dynamic user optimal route choice problem, *Transportation Research*, **32B**, 3, 219-234.

[30] **Lo, H. and Szeto, W.Y.,** 2002. A cell-based dynamic traffic assignment model: formulation and properties, *Mathematical and Computer Modelling*, **35**, 7-8, 849-865.

[31] **Lo, H. and Szeto, W.Y.**, 2002. Pradigms of modeling advanced traveler information services, *Proceedings of the IEEE 5th International Conference on Intelligent Transportation Systems* (ITSC'02), National University of Singapore, Singapore, September 3-6, pp. 460-465.

[32] **Addison, J.D. and Heydecker, B.G.,** 1993. A mathematical model for dynamic traffic assignment, *Proceedings of the 12th International Symposium on the Theory of Traffic Flow and Transportation*, Berkeley, CA, 21-23 July, pp. 171-183.

[33] **Heydecker, B.G. and Addison, J.D.,** 1996. An exact expression of dynamic equilibrium, *Proceedings of the 13th International Symposium on Transportation and Traffic Theory (ISTTT)*, Lyon, July 24-26, pp. 359-383.

[34] **Kaufman, D.E., Smith, R.L. and Wunderlich, K.E.,** 1998. User-equilibrium properties of fixed points in dynamic traffic assignment, *Transportation Research*, **6C**, 1-2, 1-16.

[35] **Patriksson, M.,** 1994. The Traffic Assignment Problem: Models and Methods, VSP, The Netherlands.

[36] **Florian, M. and Hearn, D.,** 1995. Network equilibrium models and algorithms, in *Handbooks in Operations Research and Management Science*, *vol. 8: Network Routing*, pp. 485-550, Eds. Ball, M., Magnanti, T.L., Monma, C.L., and Nemhauser, G.L., Elsevier Science, Netherlands.

[37] **Tong, C.O. and Wong, S.C.,** 2000. A predictive dynamic traffic assignment model in congested capacity-constrained road networks, *Transportation Research*, **34B**, 8, 625-644.

[38] **Peeta, S. and Ziliaskopoulos, A.K.,** 2001. Foundations of dynamic traffic assignment: the past, the present and the future, *Networks and Spatial Economics*, **1**, 3-4, 233-265.

[39] **Helbing, D.,** 2001. Traffic and related self-driven many-particle systems, *Reviews of Modern Physics*, **73**, 4, 1067-1141.

[40] **Kühne, R.D.,** 1993. Non-linearity stochastics of unstable traffic flow, *Proceedings of the 12th International Symposium on Transportation and Traffic Theory*, pp. 367, Elsevier, Amsterdam, The Netherlands.

[41] **Gazis, D.C.,** 1974. Traffic Science, John Wiley & Sons.

[42] **Lighthill, M.J. and Whitham, J.B.,** 1955. On kinematic waves. I Flow movement in long rivers. II. A theory of traffic flow on long crowded road, *Proceedings of Royal Society,* A 229, 281-345.

[43] **Richards, P. I.,** 1956. Shockwaves on the highway. *Operations Research*, **4,** 42-51.

[44] **Lebacque, J.P.,** 1996. The Godunov scheme and what it means for first order traffic flow models, *Proceedings of the 13th International Symposium*

on Transportation and Traffic Theory (ISTTT), Lyon, July 24-26, pp. 647-677.

[45] **Greenshields, B.D.,** 1935. A study in highway capacity, *Proceedings*, *Highway Research Board*, **14,** 468-477.

[46] **Smith, M.J. and Wisten, J.B.,** 1996. A distributed algorithm for the dynamic traffic equilibrium assignment problem, Transportation and Traffic Flow Theory. *Proceedings of the 13th International Symposium on Transportation and Traffic Theory (ISTTT).* Lyon, July 1996, pp. 385-408.

[47] **Rothery, R.V.,** 1999. Car Following Models, in *Revised Monograph on Traffic Flow Theory*, Eds. Gartner, N.H., Messer, C.J. and Rathi, A.K.

[48] **Gabard, J.F.,** 1991. Car-Following Models, in *Concise Encyclopedia of Traffic and Transportation Systems*, pp. 337-341, Ed. Papageorgiou, M., Pergamon Elsevier.

[49] **Nagel, K.,** 1996. Particle hopping models and traffic flow theory, *Physical Review E,* **53**, 5, 4655-4672.

[50] **Wu, J.H., Chen, Y. and Florian, M.,** 1998. The continuous dynamic network loading problem: A mathematical formulation and solution method, *Transportation Research*, **32B**, 3, 173-187.

[51] **Xu, Y., Wu, J.H., Florian, M., Marcotte, P. and Zhu, D.L.,** 1999. New advances in the continuous dynamic network loading problem, *Transportation Science*, **33**, 4, 341-353.

[52] **Ben-Akiva, M., Cyna, M. and de Palma, A.,** 1984. Dynamic model of peak period congestion, *Transportation Research*, **18B**, 4, 339-355.

[53] **Carey, M.,** 1992. Nonconvexity of the dynamic traffic assignment problem, *Transportation Research*, **26B**, 2, 127-133.

[54] **Smith, M.J.,** 1993. A new dynamic traffic model and the existence and calculation of dynamic user equilibria on congested capacity-constraint road networks, *Transportation Research*, **27B**, 1, 49-63.

[55] **Ran, B., Boyce D.E. and LeBlanc J.,** 1993. A new class of instantaneous dynamic user-optimal traffic assignment models, *Operations Research,* **41**, 1, 192-202.

[56] **Jayakrishnan, R., Mahmassani H.S. and Hu, T.Y.,** 1994. An evaluation tool for advanced information and management systems in urban networks, *Transportation Research*, **2C**, 3, 129-147.

[57] **Chabini, I. and Y, He.,** 1998. A flow-based approach to the dynamic traffic assignment problem: formulations, algorithms and computer implementations, *TRISTAN III Conference*, San Juan, Puerto Rico, 17-23 June.

[58] **Astarita, V.,** 1996. A continuous time link model for dynamic network loading based on travel time function, *Proceedings of the 13th International Symposium on Transportation and Traffic Theory (ISTTT)*, Lyon, July 24-26, pp. 87-102.

[59] **Chabini, I. And Kachani, S.,** 2006. An analytical model for the dynamic network loading problem: formulation, analysis and solution algorithm, *Transportation Science*, basım aşamasında.

[60] **Astarita, V.,** 2002. Node and link models for network traffic flow simulation, *Mathematical and Computer Modelling*, **35**, 5-6, 643-656.

[61] **Barcelo, J., Ferrer, J.L. and Montero, L.,** 1989. *AIMSUN: Advanced Interactive Microscopic Simulator for Urban Networks. Vol. I: System Description, and Vol. II: Users Manual*, Departamento de Estadistica e Investigacion Operativa, Facultad de Informatica, Universidad Politecnica de Cataluna.

[62] **Barcelo, J.,** 1996. The parallelization of AIMSUN2 microscopic traffic simulator for ITS applications, *The 3rd World Conference on Intelligent Transport Systems*, Orlando, USA, October 14-18.

[63] **Rilett, L., Benedek, C., Rakha, H. and VanAerde, M.,** 1994. Evaluation of IVHS options using CONTRAM and INTEGRATION, *First World Congress on Applications Transport Telematics and Intelligent Vehicle Highway Systems*, Paris, France, November 30 – December 3.

[64] **Van Aerde, M., Yagar, S., Ugge, A. and Case, E.R.,** 1987. A review of candidate freeway arterial corridor traffic models, *Transportation Research Record*, **1132**, 53-65.

[65] **Mahmassani, H.S. and Chen, P.,** 1993. Dynamic interactive simulator for the study of commuter behavior under real-time traffic information supply strategies, *Transportation Research Record*, **1413**, 12-21.

[66] **Gedizlioğlu, E. and Dell'Orco, M.**, 2004. A mesosimulation model of within-day dynamics in transportation systems, *TÜBİTAK-CNR joint research project report*, **İÇTAG-I918-CNR**, İstanbul, Turkey.

[67] **Boyce, D.E., Ran, B. and LeBlanc, L.J.,** 1991. Dynamic user-optimal traffic assignment model: a new model and solution technique, *First Triennal Symposium on Transportation Analysis*, Montreal, Canada, June 6-11.

[68] **Fernandez, J.E. and de Cea, J.,** 1994. Flow propagation description in dynamic network assignment models, *TRISTAN II Triennal International Symposium on Transportation Analysis*, Capri, June 23-28.

[69] **Adamo, V., Astarita, V., Florian, M., Mahut, M. and Wu, J.H.,** 1999. Modelling the spillback of congestion in link based dynamic network loading models: A simulation model with application, *Proceedings of the 14th International Symposium on Transportation Traffic Theory*, Jerusalem, Israel, July 20-23, pp. 555-573.

[70] **Chabini, I. and Kachani, S.,** 1999. Analytical dynamic network loading II: Lebesgue's integrable bounded flow rates, *Optimization Days*, Montreal, May 10-12.

[71] **Wie, B.W., Tobin R.L. and Friesz T.L.,** 1994. The augmented lagrangian method for solving dynamic network traffic assignment models in discrete time, *Transportation Science*, **28**, 3, 204-220.

[72] **Han, S.,** 2003. Dynamic traffic modelling and dynamic stochastic user equilibrium assignment for general road networks, *Transportation Research*, **37B**, 3, 225-249.

[73] **Ran, B., Rouphail, N.M., Tarko, A. and Boyce, D.E.,** 1997. Toward a class of link travel time functions for dynamic assignment models on signalised networks, *Transportation Research*, **31B**, 4, 277-290.

[74] **Daganzo, C.F.**, 1995. Properties of link travel time functions under dynamic loads, *Transportation Research*, **29B**, 2, 93-98.

[75] **Newell, G.F.,** 1993. A simplified theory of kinematic waves in highway traffic. Part I: General theory, *Transportation Research*, **27B**, 4, 281-287.

[76] **Newell, G.F.,** 1993. A simplified theory of kinematic waves in highway traffic, part II: Queuening at freeway bottlenecks, *Transportation Research*, **27B**, 4, 289-303.

[77] **Adamo,V., Astarita, V., Cantarella G.E. and Cascetta, E.** 1999. A doubly dynamic traffic assignment model for planning application, *Proceedings of the 14th International Symposium on Transportation Traffic Theory*, Jerusalem, Israel, July 20-23, pp. 375-395.

[78] **Leonard, D.R., Tough, J.B. and Baguley, P.C.,** 1978. CONTRAM: A traffic assignment model for predicting flows and queues during peak periods, *TRRL Report*, **841**, Crowthorne.

[79] **Yagar, S.,** 1975. CORQ-A model for predicting flows and queues in a road corridor, *Transportation Research Record*, **533**, 77-87.

[80] **Romph, E. de, van Grol, H.J.M. and Hamerslag, R.,** 1992. A dynamic traffic assignment model for short-term predictions, in *Seminar on Urban Traffic Networks*, Capri, July 5-8.

[81] **Di Gangi, M.,** 1992. Continuous flow approach in dynamic network loading, in *Second International Capri Seminar on Urban Traffic Networks*, Capri, July 5-8.

[82] **Di Gangi, M. and Astarita, V.,** 1994. Structure of a dynamic loading model for the evaluation of control strategies, in *TRISTAN Second Triennial International Symposium on Transportation Analysis*, Capri, June 23-28.

[83] **Smith, M.J. and Wisten, M.B.,** 1993. Parallel dynamic traffic equilibrium assignment, *Traffic Engineering & Control*, **34**, 12, 593-597.

[84] **Di Gangi, M., Adamo, V. and Astarita, V.,** 1995. Dynamic network loading model and algorithms for explicit simulation of queue-effects and while-trip re-routing, in *7th WCTR World Conference on Transport Research*, Sydney, July.

[85] **Hammerslag, R.,** 1988. A three-dimensional assignment in the time-space, in *UTSG Annual Conference*, University College London, London, January 28-30.

[86] **Janson, B.N.,** 1989. Dynamic traffic assignment for urban road networks, *Transportation Research*, **25B**, 2-3, 143-161.

[87] **Payne, H.J.,** 1979. FREEFLO: A macroscopic simulation model of freeway traffic, *Transportation Research Record*, **722**, 68-77.

[88] **Messmer, A. and Papageorgiou, M.,** 1990. METANET: a macroscopic simulation program for motorway networks, *Traffic Engineering & Control*, **31**, 466-470, and **10,** 549.

[89] **Payne, H.J.,** 1971. Models of Freeway Traffic and Control, in *Mathematical Models of Public Systems*, Simulation Council, La Jolla, CA, 1971, pp. 1-51.

[90] **Daganzo, C.F.,** 1995. Requiem for second-order approximations of traffic flow, *Transportation Research*, **29B**, 4, 277-286.

[91] **Zhang, H.M.,** 1998. A theory of nonequilibrium traffic flow, *Transportation Research*, **32B**, 7, 485-498.

[92] **Janson, B.N.,** 1995. Network design effects of dynamic traffic assignment, *Journal of Transportation Engineering,* **121**, 1, 1-13.

[93] **Carey, M.,** 1986. A constraint qualification for a dynamic traffic assignment model, *Transportation Science*, **20**, 1, 55-58.

[94] **Carey, M.,** 1990. Extending and solving a multi-period congested network flow model, *Computers and Operations Research*, **17**, 5, 495-507.

[95] **Carey, M. and Srinivasan, A.,** 1993. Externalities, average and marginal costs, and tolls on congested networks with time-varying flows, *Operations Research*, **41**, 1, 217-231.

[96] **Lasdon, L.S. and Luo, S.,** 1994. Computational experiments with a system optimal dynamic traffic assignment model, *Transportation Research*, **2C**, 2, 109-127.

[97] **Wie, B.W.,** 1997. A convex control model of dynamic system optimal traffic assignment, *Preprints of the Eighth IFAC/IFIP/IFORS Symposium*, Chania, Greece, June 16-18, pp. 540-545.

[98] **Wie, B.W., Tobin, R.L., Bernstein, D. and Friesz, T.L.,** 1995. A comparison of system optimum and user equilibrium traffic assignments with schedule delay, *Transportation Research*, **3C**, 6, 389-411.

[99] **Wie, B.W., Tobin, R.L., Friesz, T.L. and Bernstein, D.,** 1995. A discrete time, nested cost operator approach to the dynamic network user equilibrium problem, *Transportation Science*, **29**, 79-92.

[100] **Wie, B.W. and Tobin, R.L.,** 1998. Dynamic congestion pricing for general traffic networks, *Transportation Research*, **32B**, 5, 313-327.

[101] **Friesz, T.L. and Bernstein, D.,** 2000. Analytical dynamic traffic assignment models, in *Handbook of transport modelling*, pp.181-195, Eds. Hensher, D.A. and Button, K.J., Elsevier, New York.

[102] **Addison, J.D. and Heydecker, B.G.,** 1995. Traffic models for dynamic traffic assignment, in Urban Traffic Networks: Dynamic Flow Modeling and Control, pp. 213-231, Eds. Gartner, N.H. and Improta, G., London: Spring.

[103] **Carey, M. and McCartney, M.,** 1999. A class of traffic flow models used in dynamic assignment. I: With light traffic, *Research Report*, Faculty of Business and Management, University of Ulster.

[104] **Carey, M. and McCartney, M.,** 1999. A class of traffic flow models used in dynamic assignment. II: With congested traffic, *Research Report*, Faculty of Business and Management, University of Ulster.

[105] **Boyce, D.E., Ran, B. and LeBlanc, L.J.,** 1995. Solving an instantaneous dynamic user optimal route choice model, *Transportation Science*, **29**, 2, 128-142.

[106] **Ran, B., Lo, H. and Boyce, D.,** 1996. A formulation and a solution algorithm for a multi-class dynamic traffic assignment problem, *Proceedings of the 13th International Symposium on Transportation and Traffic Theory (ISTTT)*, Lyon, July 24-26, pp. 195-216.

[107] **Chen, H.K. and Hsueh, C.F.,** 2000. Dynamic user-optimal departure time/route choice with hard time-windows, *Journal of Transportation Engineering*, **126**, 5, 413-418.

[108] **Zhu, D. and Marcotte, P.,** 2000. On existence of solutions to the dynamic user equilibrium problem, *Transportation Science*, **34**, 4, 402-414.

[109] **Carey, M. and McCartney, M.,** 2002. Behaviour of a whole-link travel time model used in dynamic traffic assignment, *Transportation Research*, **36B**, 1-2, 83-95.

[110] **Rubio-Ardanaz, J.M., Wu, J.H., and Florian, M.,** 2003. Two improved numerical algorithms for the dynamic network loading problems, *Transportation Research* **B 37,** 171-190.

[111] **Bernstein, D., Friesz, T.L., Tobin, R.L. and Wie, B.W.,** 1993. A variational control formulation of the simultaneous route and departure time choice equilibrium problem, *Proceedings of the 12th International Symposium on the Theory of Traffic Flow and Transportation*, Berkeley, CA, 21-23 July, pp. 107-126.

[112] **Kuwahara, M. and Akamatsu, T.,** 1993. Dynamic equilibrium assignment with queues for a many-to-many OD pattern, *Proceedings of the 12th International Symposium on the Theory of Traffic Flow and Transportation*, Berkeley, CA, 21-23 July, pp. 185-204.

[113] **Kuwahara, M. and Akamatsu, T.,** 1997. Decomposition of the reactive dynamic assignments with queues for a many-to-many origin-destination pattern, *Transportation Research*, **31B**, 1, 1-10.

[114] **Jayakrishnan, R., Tsai, W.K. and Chen, A.,** 1995. A dynamic traffic assignment model with traffic-flow relationships, *Transportation Research*, **3C**, 1, 51-72.

[115] **Ran, B., Lee, D.H. and Shin, M.S.I.,** 2002. New algorithm for a multiclass dynamic traffic assignment model, *Journal of Transportation Engineering*, **128**, 4, 323-335.

[116] **Carey, M.,** 2004. Link travel times I: desirable properties, *Networks and Spatial Economics*, **4**, 3, 257-268.

[117] **Carey, M.,** 2004. Link travel times II: properties derived from traffic-flow models, *Networks and Spatial Economics*, **4**, 4, 379-402.

[118] **Beskos, D.E., Okutani, I. and Michalopoulos, P.,** 1984. Testing of dynamic models for signal controlled intersections, *Transportation Research*, **8**, 4-5, 397-408.

[119] **Chang, T.H. and Sun, G.Y.,** 2004. Modeling and optimization of an oversaturated signalized network, *Transportation Research*, **38**, 8, 687-707.

[120] **Dell'Orco, M., Gedizlioglu, E. and Celikoglu, H.B.,** 2005. Introduction to a node management model for traffic networks: a mesoscopic approach, *Proceedings of the 10th EWGT Meeting*, Poznan, Poland, September 13-16, pp. 435-440.

[121] **Celikoglu, H.B.,** 2006. A dynamic node model with a quadratic travel time function based link model, *Proceedings of the 11th EWGT Meeting*, Bari, Italy, September 27-29, pp. 658-666.

[122] **Celikoglu, H.B., Dell'Orco, M. and Gedizlioglu, E.,** 2006. A dynamic model of point-queue process, *Proceedings of the 11th EWGT Meeting*, Bari, Italy, September 27-29, pp. 647-657.

[123] **Leonard, D.R., Gower, P. and Taylor, N.B.,** 1989. CONTRAM: Structure of the model, *TRRL Research Report*, **178,** Crowthorne.

[124] **Dell'Orco, M.,** 2006. A dynamic network loading model for mesosimulation in transportation systems, *European Journal of Operational Research*, **175**, 3, 1447-1454.

[125] **Taylor, N.B.,** 2003. The CONTRAM dynamic traffic assignment model. *Networks and Spatial Economics*, **3**, 3, 297-322.

[126] **Sahin, I. and Akyildiz, G.,** 2005. Bosporus bridge toll plaza in Istanbul, Turkey: Upstream and downstream traffic features, *Transportation Research Record*, **1910**, 99-107.

[127] **Spiess, H.,** 1990. Conical volume-delay functions, *Transportation Science*, **24**, 2, 153-158.

[128] **Branston, D.,** 1976. Link capacity functions: a review, *Transportation Research*, **10**, 223-236.

[129] **Bureau of Public Roads,** 1964. Traffic Assignment Manual, U.S. Department of Commerce, Urban Planning Division, Washington D.C.

Appendix A

Referring to Eq. (5.22), an arbitrary non-decreasing, continuous, concave function of n, can be written as:

$$W(n) = \gamma \cdot \left(1 - e^{-\frac{n}{\gamma}} \right) \qquad \textbf{(i)}$$

where γ is a positive constant. Calling $N^i_{max} = k^i_{max} \cdot d^i$ the maximum possible number of vehicles on the link i, from eq. (i) it results that the constraint $0 \le W(n) \le n_{max}$ is respected $\forall n$ if:

$$0 \le \gamma \cdot \left(1 - e^{-\frac{n^i_{max}}{\gamma}} \right) \le n^i_{max} \qquad \textbf{(ii)}$$

The left hand side of the inequality given in (ii) can be solved as given in (iii):

$$n = 0 \;\Rightarrow\; 0 \le \gamma \left(1 - e^{-\frac{0}{\gamma}} \right) \;\Rightarrow\; 0 \le 0 \qquad \textbf{(iii)}$$

Developing the term $e^{-\frac{n^i_{max}}{\gamma}}$ by Taylor series, we obtain (iv) for the right hand side of inequality given in (ii):

$$e^{-\frac{n^i_{max}}{\gamma}} = 1 - \frac{n^i_{max}}{\gamma} + \frac{1}{2}\left(\frac{n^i_{max}}{\gamma} \right)^2 - \frac{1}{6}\left(\frac{n^i_{max}}{\gamma} \right)^3 + \dots \qquad \textbf{(iv)}$$

Hence, neglecting the terms after the third degree and substituting Eq. (iv) in the right-hand side of Eq. (ii) gives:

$$\frac{n^i_{max}}{\gamma} + \frac{1}{2}\left(\frac{n^i_{max}}{\gamma} \right)^2 - \frac{1}{6}\left(\frac{n^i_{max}}{\gamma} \right)^3 \le \frac{n^i_{max}}{\gamma} \qquad \textbf{(v)}$$

$$\frac{1}{2}\left(\frac{n^i_{max}}{\gamma} \right)^2 \cdot \left(1 - \frac{1}{3}\frac{n^i_{max}}{\gamma} \right) \le 0 \qquad \textbf{(vi)}$$

$$\gamma \geq \frac{n^{i}_{max}}{3} = \frac{k^{i}_{max} \cdot d^{i}}{3} \qquad \textbf{(vii)}$$

The best value of γ, calibrated with our real data, resulted just $\gamma = \frac{k^{i}_{max} \cdot d^{i}}{3}$. Then, finally, the formula in Eq. (5.22) has been obtained:

$$W(n) = \frac{k^{i}_{max} d^{i}}{3} \cdot \left(1 - e^{-\frac{n}{\frac{k^{i}_{max} \cdot d^{i}}{3}}} \right) \qquad \textbf{(viii)}$$

Appendix B

Let y′ be the estimate of N-dimensional vector y (data set), the performance RMSPE can be expressed as given in (i).

$$\mathrm{RMSPE}(y, y') = \left(\frac{1}{N} \sum_{n=1}^{N} \left(\left(\frac{y'(n) - y(n)}{y'(n)} \right) \cdot 100 \right)^2 \right)^{\frac{1}{2}} \quad \textbf{(i)}$$

Moreover, let μ, μ', σ, and σ' be the mean of vector y, mean of vector y′, standard deviation of vector y, and standard deviation of vector y′ respectively. The coefficient of determination R^2 can be expressed as given in (ii).

$$R^2(y, y') = \left(\frac{\frac{1}{N} \sum_{n=1}^{N} (y - \mu)(y' - \mu')}{\sigma \cdot \sigma'} \right)^2 \quad \textbf{(ii)}$$

Appendix C

Delay functions can be classified by road type and intersection type. Since an unsignalized highway junction is considered in this dissertation, delay functions for unsignalized intersections are presented in the following.

Varying types of flow-rate delay functions have been proposed and applied in the past (Branstone, 1976). Most widely used flow-rate delay functions are the Bureau of Public Roads (BPR) function (Bureau, 1964), as given in (i):

$$t(u) = t_{free-flow} \cdot \left(1 + \left(\frac{u}{C}\right)^{a}\right) \qquad \textbf{(i)}$$

where, t(u) is the average approach delay, $t_{free-flow}$ is the free-flow approach delay, u is the total approach flow and "C" is the approach capacity. Parameter "a" is any number larger than 1 and defines how sudden the congestion effects change when the capacity is reached. The BPR function generally used for estimating delays at major/minor priority intersections have the form given in (ii).

$$t(u) = t_{free-flow} \cdot \left(1 + 0.15\left(\frac{u}{C}\right)^{4}\right) \qquad \textbf{(ii)}$$

As for the delay representation for all-way-stop intersections, the following exponential delay model is used (Meneguzzer, 1995):

$$t(u) = \exp\left(3.802\left(\frac{u}{C}\right)\right) \qquad \textbf{(iii)}$$

The simplicity of BPR function is probably the main reason for its wide spread use. Moreover, the forms given in (ii) and (iii) had been found to be suitable for use in network models since they are defined for any value of u/C (Boyce et al., 1997). However these BPR functions have some drawbacks, which are given below.

- For links that are used far under capacity, the BPR functions, especially when greater values of a are used, always generate free-flow times independent of the current traffic volume.

- Initializing the function with higher values of a makes the congestion effect become more and more sudden.

- While for any realistic set of travel volumes, we can assume that u/C≤1 (or at least not much larger than 1) this is usually not the case during the first few iterations of an equilibrium assignment. Values of u/C may well reach values of 3.5 or even more (To prove this, the link time of a link with a=12 and a u/C ratio of 3 is increased by a factor of $1+3^{12}$ = 531443, which means that every minute free flow time becomes roughly one year of congested time).

Spiess (1990) determined the necessary conditions for a delay function to satisfy as given in the following:

"1. f(x) should be strictly increasing. This is the necessary condition for the assignment to converge to a unique solution.

2. f(0) = 1 and f(1) = 2. These conditions ensure compatibility with the well known BPR type functions. The capacity is thus still defined as the volume at which congested speed is half the free flow speed.

3. f′(x) should exist and be strictly increasing. This ensures convexity of the congestion function (not a necessary, but a most desirable property).

4. f′(1) =a. a is, similar to the exponent in BPR functions, the parameter that defines how sudden the congestion effects change when the capacity is reached.

5. f′ (x) < M·a, where M is a positive constant. The steepness of the congestion curve is limited. This in turn limits also the values of the volume delay function not to get too high when considering u/C ratios higher than 1, avoiding the problems mentioned as the drawbacks of BPR functions.

6. f′(0) > 0. This condition guarantees uniqueness of the link volumes. It also renders the assignment stable regarding small coding errors in travel time and distributes volumes on competing uncongested paths proportional to their capacity.

7. The evaluation of f(x) should not take more computing time than the evaluations of the corresponding BPR functions take."

So, the conical congestion function used in this study to model delays at diverging link entrances have the form given in (5-33), which is proposed by Spiess (1990):

$$f(x) = 2 + \sqrt{a^2(1-x)^2 + b^2} - a(1-x) - b \qquad \textbf{(iv)}$$

where b is given as b=(2a-1)/(2a-2) and a is any number larger than 1.

References of Appendix C

Spiess, H., 1990. Conical volume-delay functions, *Transportation Science*, **24**, 2, 153-158.

Branston, D., 1976. Link capacity functions: a review, *Transportation Research*, **10**, 223-236.

Bureau of Public Roads, 1964. Traffic Assignment Manual, U.S. Department of Commerce, Urban Planning Division, Washington D.C.

Meneguzzer, C., 1995. An equilibrium route choice model with explicit treatment of the effect of intersections, *Transportation Research*, **29B**, 5, 329-356.

Boyce, D.E., Lee, D.H., Janson, B.N. and Berka, S., 1997. Dynamic route choice model of large-scale traffic network, *Journal of Transportation Engineering*, **123**, 4, 276-282.

Appendix D

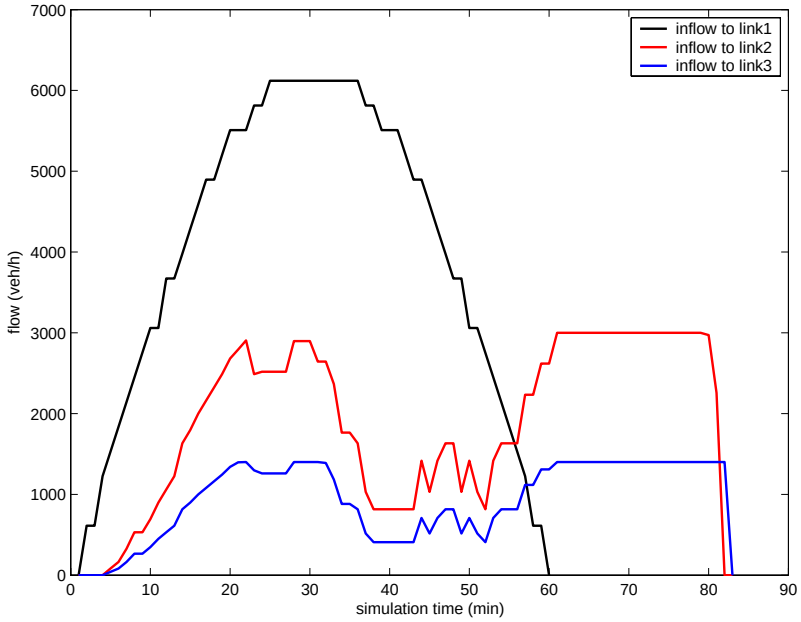

Figure D.1: Inflows and Outflows at Node 1 in Sample Network

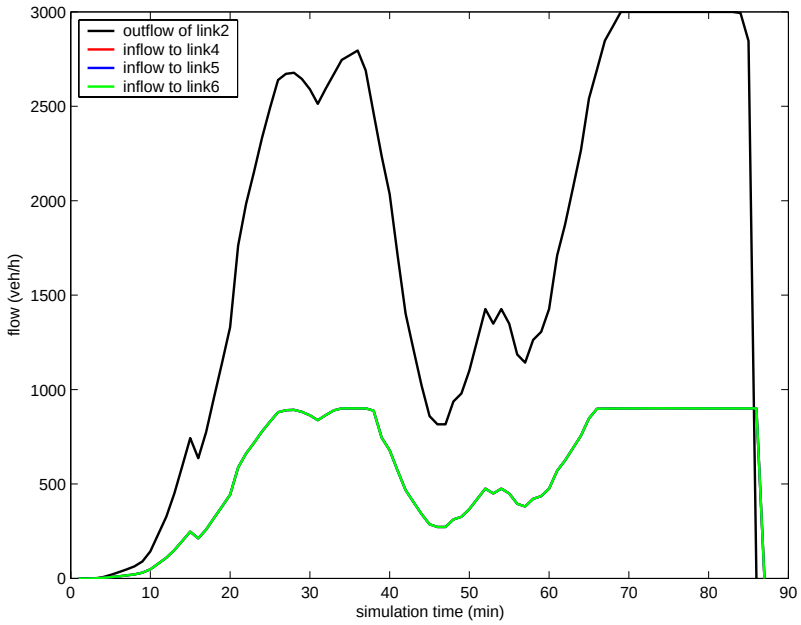

Figure D.2: Inflows and Outflows at Node 2 in Sample Network

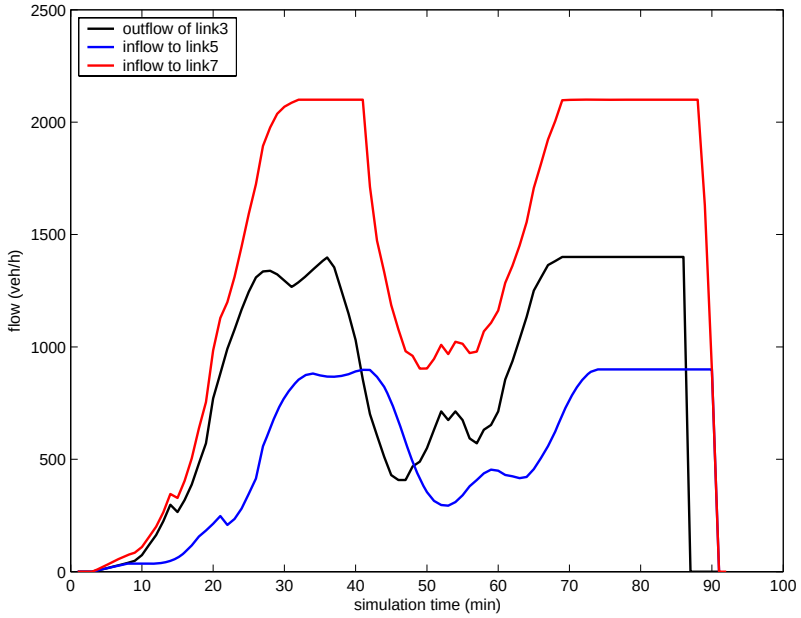

Figure D.3: Inflows and Outflows at Node 3 in Sample Network

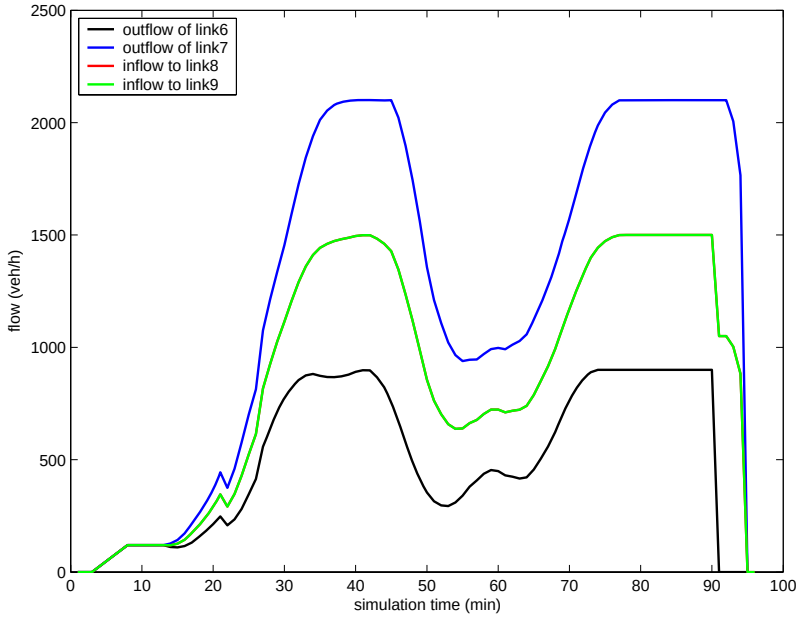

Figure D.4: Inflows and Outflows at Node 4 in Sample Network

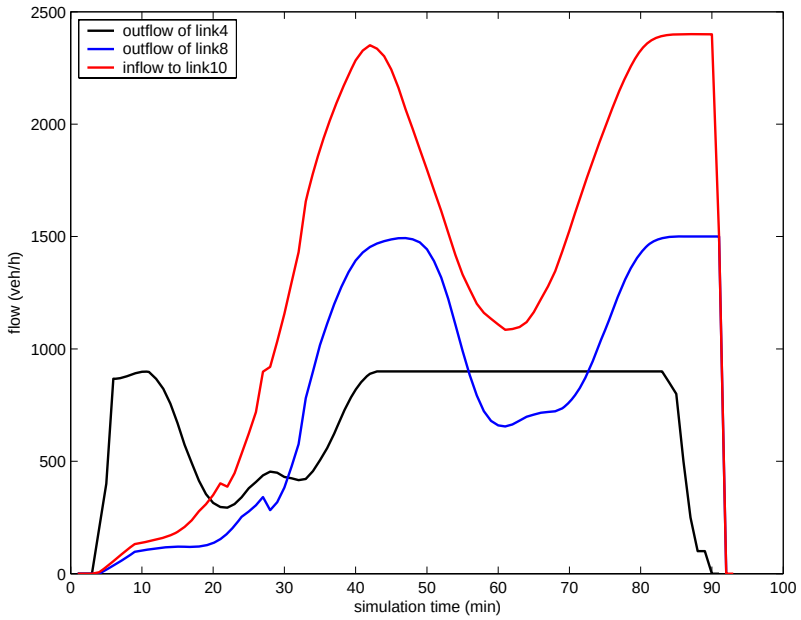

Figure D.5: Inflows and Outflows at Node 5 in Sample Network

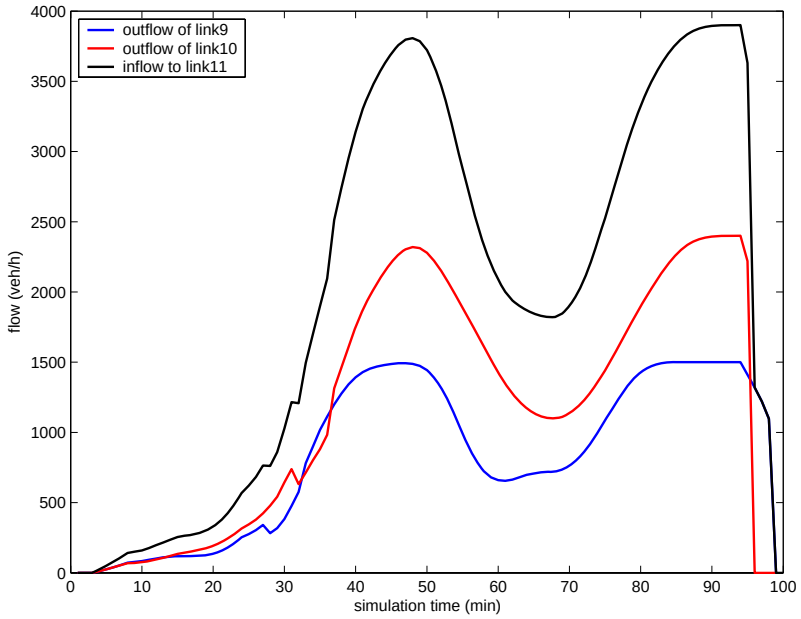

Figure D.6: Inflows and Outflows at Node 6 in Sample Network

BIOGRAPHY

Hilmi Berk ÇELİKOĞLU was born in 1976 in İstanbul. He completed Kütahya Dumlupınar Anadolu High School in 1994 and graduated from Technical University of İstanbul with B.Sc degree in Urban and Regional Planning in 2000. He accomplished his M.Sc degree in Transportation Engineering by 2002, with the thesis entitled "Logit modal-split model calibration: an evaluation for İstanbul" at Technical University of İstanbul, Institute of Science and Technology. He started his Ph.D studies in 2002 at the same institute and continued a part of his doctoral work in Italy, at Technical University of Bari, between September 2005 and September 2006. He has been working as a research and teaching assistant at Technical University of İstanbul, Faculty of Civil Engineering, Civil Engineering Department since 2002. He has been involved in several national and international scientific and technical projects, besides his ongoing research in the fields of traffic engineering and transportation planning.